

**JULIANA NALDONI**

**MYXOZOA PARASITOS DE *Pseudoplatystoma corruscans* (PINTADO), *Salminus franciscanus* (DOURADO) E *Brycon orthotaenia* (MATRINXÃ) ORIUNDOS DA  
BACIA DO RIO SÃO FRANCISCO, MG**

Campinas, SP

2014





**UNIVERSIDADE ESTADUAL DE CAMPINAS**

**INSTITUTO DE BIOLOGIA**

**JULIANA NALDONI**

**“MYXOZOA PARASITOS DE *Pseudoplatystoma corruscans* (PINTADO),  
*Salminus franciscanus* (DOURADO) E *Brycon orthotaenia* (MATRINXÃ)  
ORIUNDOS DA BACIA DO RIO SÃO FRANCISCO, MG”**

Orientador: Prof. Dr. Edson Aparecido Adriano

Tese apresentada ao Instituto de Biologia da  
UNICAMP para obtenção do Título de  
DOUTORA em Parasitologia.

ESTE EXEMPLAR CORRESPONDE A VERSÃO FINAL  
TESE DEFENDIDA PELA ALUNA  
JULIANA NALDONI, E ORIENTADA PELO  
PROF. DR. EDSON APARECIDO ADRIANO

---

CAMPINAS,  
2014

Ficha catalográfica  
Universidade Estadual de Campinas  
Biblioteca do Instituto de Biologia  
Mara Janaina de Oliveira - CRB 8/6972

Naldoni, Juliana, 1986-  
N146m      Myxozoa parasitos de *Pseudoplatystoma corruscans* (pintado), *Salminus franciscanus* (dourado) e *Brycon orthotaenia* (matrinxã) oriundos da bacia do rio São Francisco, MG / Juliana Naldoni. – Campinas, SP : [s.n.], 2014.

Orientador: Edson Aparecido Adriano.  
Tese (doutorado) – Universidade Estadual de Campinas, Instituto de Biologia.

1. Myxozoa. 2. Relação hospedeiro-parasito. 3. Biologia molecular. 4. Filogenia. 5. Peixe de água doce. I. Adriano, Edson Aparecido. II. Universidade Estadual de Campinas. Instituto de Biologia. III. Título.

Informações para Biblioteca Digital

**Título em outro idioma:** Myxozoa parasites of *Pseudoplatystoma corruscans* (pintado), *Salminus franciscanus* (dourado) and *Brycon orthotaenia* (matrinxã) from the São Francisco river basin, MG

**Palavras-chave em inglês:**

Myxozoa

Host-parasite relationship

Molecular biology

Phylogeny

Freshwater fish

**Área de concentração:** Parasitologia

**Titulação:** Doutora em Parasitologia

**Banca examinadora:**

Edson Aparecido Adriano [Orientador]

Maurício Laterça Martins

Maria José Tavares Ranzani de Paiva

Edilson Rodrigues Matos

Marlene Tiduko Ueta

**Data de defesa:** 10-12-2014

**Programa de Pós-Graduação:** Parasitologia

Campinas, 10 de dezembro de 2014.

**BANCA EXAMINADORA**

Prof. Dr. Edson Aparecido Adriano (orientador)



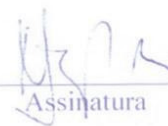
Assinatura

Prof. Dr. Maurício Laterça Martins



Assinatura

Profª. Dra. Maria José Tavares Razani de Paiva



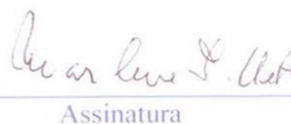
Assinatura

Prof. Dr. Edilson Rodrigues Matos



Assinatura

Profª. Dra. Marlene Tiduko Ueta



Assinatura

Prof. Dr. George Shigueki Yasui



Assinatura

Profª. Dra. Silmara Marques Allegretti



Assinatura

Prof. Dr. Eduardo Makoto Onaka



Assinatura



## RESUMO

Mixosporídeos são cosmopolitas e infectam peixes em diversas regiões do mundo. Atualmente são conhecidas cerca de 2.400 espécies, das quais a grande maioria é parasito de peixes, tanto de ambiente natural como de sistemas de criação, sendo algumas espécies responsáveis por altas taxas de mortalidade em várias partes do mundo. Este trabalho teve como objetivo o estudo da diversidade de mixosporídeos parasitos de *Pseudoplatystoma corruscans* (pintado), *Salminus franciscanus* (dourado) e *Brycon orthotaenia* (matrinxã) da bacia do rio São Francisco, município de Pirapora, MG, Brasil. Foram realizados estudos morfológicos, ultraestruturais, histotológicos e moleculares de cinco novas espécies de mixosporídeos, sendo uma do gênero *Henneguya* em pintado, duas do gênero *Myxobolus* infectando dourado e duas infectando matrinxã. *Henneguya* sp. n. 1 apresentou plasmódios brancos e alongados no tecido conjuntivo das brânquias de pintado. A análise ultraestrutural revelou a parede plasmodial com delicadas projeções em direção aos tecidos do hospedeiro e a presença de uma fina camada de material finamente granular isolando o parasito do contato com o tecido do hospedeiro. A análise histológica revelou que o desenvolvimento do plasmódio causou a compressão no tecido conjuntivo e epitelial, deformação dos filamentos e a fusão lamelar. A análise filogenética, baseada no gene 18S rDNA e utilizando somente espécies dos gêneros *Henneguya* e *Myxobolus* parasitos de siluriformes, revelou o agrupamento de acordo com a família dos peixes hospedeiros. *Myxobolus* sp. n. 1 apresentou plasmódios brancos e arredondados entre os raios da nadadeira de dourado. A análise ultraestrutural revelou uma camada de fibroblastos circundando o plasmódio, impedindo o contato com as células do hospedeiro. *Myxobolus* sp. n. 2 apresentou plasmódios brancos e arredondados no fígado de dourado. *Myxobolus* sp. n. 3 e *Myxobolus* sp. n. 4 apresentaram plasmódios brancos e arredondados, sendo que a primeira ocorreu no baço e a segunda no rim de matrinxã. A análise ultraestrutural de *Myxobolus* sp. n. 2, *Myxobolus* sp. n. 3 e *Myxobolus* sp. n. 4 revelou o contato direto entre a parede do plasmódio do parasito e o tecido dos hospedeiros. As paredes dos plasmódios das cinco espécies aqui estudadas foram compostas por membrana simples. O processo de esporogênese das cinco espécies foi assíncronico, com células germinativas e jovens estágios de desenvolvimento dos esporos ocorrendo na periferia do plasmódio e esporos

imaturos e maduros foram observados na região central. A análise filogenética, baseado no gene 18S rDNA e usando somente espécies dos gêneros *Henneguya* e *Myxobolus* parasitos de peixes da América do Sul mais as quatro novas espécies de *Myxobolus* parasitas de briconídeos, mostrou a especificidade de hospedeiro e a afinidade de órgão/tecido, como um importante sinal evolutivo para *Myxobolus/Henneguya*.

**Palavras-chaves:** Myxozoa, relação hospedeiro-parasito, biologia molecular, filogenia, peixes de água doce.



## ABSTRACT

Myxosporeans are cosmopolitan parasites and infect fish in various regions of the world. So far, are known about 2,400 species, of which the vast majority are parasites of fishes, from natural environment and fish farms, and some species responsible for high mortality rates in various parts of the world. This work aimed to study the diversity of myxosporeans of *Pseudoplatystoma corruscans* (pintado), *Salminus franciscanus* (dourado) and *Brycon orthotaenia* (matrinxã) from the São Francisco River, municipality of Pirapora, MG, Brazil. Morphological, ultrastructural, histological and molecular studies of five new species of myxosporeans were performed, being one species of the genus *Henneguya* infecting pintado, two of the genus *Myxobolus* infecting dourado and two infecting matrinxã. *Henneguya* sp. n. 1 had white and elongated plasmodia in the connective tissue of the gill filaments. The ultrastructural analysis revealed the plasmodial wall with delicate projections towards the tissues of the host, and the presence of a thin layer of fibrous material isolating the parasite of the contact with the host tissue. Histological analysis revealed that the development of the plasmodium caused compression of the connective and epithelial tissue, deformation of the filament and lamellar fusion. Phylogenetic analysis, based on 18S rDNA gene, and using only *Henneguya* and *Myxobolus* parasites of siluriformes revealed clustering according to the family of the host fish. *Myxobolus* sp. n. 1 had white and rounded plasmodia that developed between the fin rays of dourado. The ultrastructural analysis showed a fibroblast layer surrounding the plasmodium, preventing contact of the parasite with the host tissues. *Myxobolus* sp. n. 2 had white and rounded plasmodia that developed in the liver also of dourado. *Myxobolus* sp. n. 3 and *Myxobolus* sp. n. 4 infected matrinxã, being that the first had white and rounded plasmodia in the spleen and the second in the kidney. The ultrastructural analyses of *Myxobolus* sp. n. 2, *Myxobolus* sp. n. 3 and *Myxobolus* sp. n. 4 revealed direct contact between the plasmodial wall and the host tissue. The plasmodial wall of the five myxosporeans species subject of this study was composed by single membrane. The process of sporogenesis in these five species was asynchronous, with germ cells and young development stages of spores occurring in the periphery of the plasmodia and immature and mature spores in the central region. Phylogenetic analysis based on 18S rDNA gene and using only *Henneguya* and

*Myxobolus* parasites of fish from South America plus the four new *Myxobolus* species parasites of bryconids, shows host specificity and organs/tissue affinity as important evolutionary signs to *Myxobolus/Henneguya*.

**Key words:** Myxozoa, parasite-host relationship, molecular biology, phylogeny, freshwater fish.

## SUMÁRIO

|  |     |
|--|-----|
| LISTA DE FIGURAS E TABELAS.....  | xix |
| 1. INTRODUÇÃO.....   | 1   |
| 2. JUSTIFICATIVA.....  | 7   |
| 3. OBJETIVOS.....  | 8   |
| 3.1 Objetivo Geral.....  | 8   |
| 3.2 Objetivos Específicos.....   | 8   |
| 4. MATERIAL E MÉTODOS.....   | 9   |
| 5. REFERÊNCIAS BIBLIOGRÁFICAS.....   | 14  |
| 6. RESULTADOS.....   | 23  |
| Capítulo 1: <i>Henneguya</i> sp. n. 1 (Myxozoa), a parasite of <i>Pseudoplatystoma corruscans</i> in the São Francisco basin, Brazil.....              | 23  |
| Capítulo 2: Four new <i>Myxobolus</i> species parasites of characiforms fishes of the family bryconidae; host-parasite relationship and phylogeny..... | 47  |
| 7. CONSIDERAÇÕES GERAIS.....   | 83  |
| 8. ANEXOS.....   | 85  |
| 8.1 - Certificado da Comissão de Ética no uso de Animais CEUA/Unicamp.....   | 85  |
| 8.2 - Declaração da Comissão de Ética no uso de Animais CEUA/Unicamp.....  | 86  |



## **DEDICATÓRIA**

Dedico este trabalho a pessoa mais importante da minha vida, meu alicerce e minha força para seguir em frente, minha mãe, Clotilde Aparecida Honor. A quem devo o que sou e o que conquistei. Obrigado por sempre acreditar em mim, mesmo nos momentos em que até eu mesma deixei de acreditar.



## AGRADECIMENTOS

- Em primeiro lugar ao meu Deus por toda a formação que ele me abençoou, da graduação até aqui, o que parecia impossível ele criou oportunidades e me capacitou.
- Ao meu orientador Dr. Edson Aparecido Adriano, pela oportunidade de participar do seu grupo de pesquisa desde o mestrado, pelas orientações, acompanhamento nas atividades de pesquisa e paciência.
- Ao Prof. Dr. Antônio Augusto Mendes Maia, professor do Departamento de Medicina Veterinária da Faculdade de Zootecnia e engenharia de Alimentos da USP, pela co-orientação, acompanhamento nas atividades laboratoriais e os valiosos conselhos.
- À minha família que sempre me apoiou e incentivou e faz parte de todas as minhas conquistas, sempre.
- À segunda família que esse doutorado me concedeu:
  - Dr. Márcia Ramos Monteiro, técnica do Laboratório de Parasitologia do Departamento de Medicina Veterinária da Faculdade de Zootecnia e engenharia de Alimentos da USP, pela orientação principalmente na área de biologia molecular e por ter sido como uma mãe para mim e para todos os alunos do grupo.
  - Aos mais que companheiros de pesquisa e amigos, considero irmãos pela convivência e apoio em todos os momentos e nas mais diversas situações relacionadas a pesquisa ou não: Tiago Milanin, Kassia Roberta Hygino Capodifoglio, Suellen Zatti, Gabriel Sassarão Alves Moreira, Mateus Maldonado Carreiro, Elayna Cristina Maciel e Josi Margarete Ponzeto.
- Aos professores da Unicamp pelo conhecimento transmitido nas disciplinas.
- À Dra. Silmara Marques Alegretti, coordenadora do curso de Parasitologia da Unicamp, pelo apoio.
- À FAPESP pelo apoio financeiro na forma de bolsa de doutorado processo 2011/10738-1.





*“Talvez não tenha conseguido fazer o melhor, mas lutei para que o melhor fosse feito. Não sou o que deveria ser, mas Graças a Deus, não sou o que era antes”.*

(Marthin Luther King)

*“O sucesso nasce do querer, da determinação e persistência em se chegar a um objetivo. Mesmo não atingindo o alvo, quem busca e vence obstáculos, no mínimo fará coisas admiráveis.”* (José de Alencar)



## LISTA DE FIGURAS E TABELAS

### MATERIAL E MÉTODOS

|   |    |
|---|----|
| <b>Figura 1</b> – Mapa do Brasil (A), mostrando a localização da bacia do rio São.....    | 11 |
| <b>Figura 2</b> – Coleta de campo. A – Foto mostrando o entardecer no rio São.....        | 12 |
| <b>Figura 3</b> – Foto do laboratório de campo. A – Necrópsia.....                        | 13 |
| <b>Figura 4</b> – Foto das espécies de peixe coletadas. A – <i>Pseudoplatystoma</i> ..... | 13 |

### RESULTADOS

#### Capítulo 1

##### *Henneguya* sp. n. 1 a parasite of *Pseudoplatystoma corruscans* in the São Francisco Basin, Brazil

|   |    |
|---|----|
| <b>Figure 1</b> – <i>Henneguya</i> sp. n. 1 infecting <i>Pseudoplatystoma corruscans</i> .....            | 29 |
| <b>Figure 2</b> – <i>Pseudoplatystoma corruscans</i> infected by <i>Henneguya</i> sp. n. 1. Light.....    | 30 |
| <b>Figure 3</b> – <i>Pseudoplatystoma corruscans</i> infected by <i>Henneguya</i> sp. n. 1. Light.....    | 31 |
| <b>Figure 4</b> – <i>Pseudoplatystoma corruscans</i> infected by <i>Henneguya</i> sp. n. 1. Electron..... | 32 |
| <b>Figure 5</b> – <i>Henneguya</i> sp. n. 1 infecting <i>Pseudoplatystoma corruscans</i> . Electron.....  | 33 |
| <b>Figure 6</b> – <i>Henneguya</i> sp. n. 1. Schematic representation of the mature spore of.....         | 34 |
| <b>Figure 7</b> – <i>Henneguya</i> spp. and <i>Myxobolus</i> spp. Maximum likelihood tree showing.....    | 34 |
| <b>Table 1</b> – <i>Henneguya</i> spp. Comparative data of <i>Henneguya</i> sp. n. 1 with other.....      | 35 |
| <b>Table 2</b> – <i>Henneguya</i> spp. Pairwise genetic identity of the 18S rRNA gene of.....             | 38 |

#### Capítulo 2

##### Four new *Myxobolus* species parasites of characiforms fishes of the family Bryconidae: ultrastructure and phylogeny

|  |    |
|--|----|
| <b>Figure 1</b> - <i>Myxobolus</i> sp. n. 1 parasites of fins <i>Salminus franciscanus</i> . A: mature.....  | 55 |
| <b>Figure 2</b> - Electron micrograph of fin of <i>Salminus franciscanus</i> infected by.....                | 56 |
| <b>Figure 3</b> - <i>Myxobolus</i> sp. n. 2 parasites of liver <i>Salminus franciscanus</i> . A: mature..... | 59 |
| <b>Figure 4</b> - Electron micrograph of liver of <i>Salminus franciscanus</i> infected by.....              | 60 |
| <b>Figure 5</b> - <i>Myxobolus</i> sp. n. 3 parasites of spleen <i>Brycon orthotaenia</i> . A: mature.....   | 63 |
| <b>Figure 6</b> - Electron micrograph of spleen of <i>Brycon orthotaenia</i> from São.....                   | 64 |

|   |    |
|---|----|
| <b>Figure 7</b> - <i>Myxobolus</i> sp. n. 4 parasites of kidney <i>Brycon orthotaenia</i> . A: mature.....        | 67 |
| <b>Figure 8</b> - Electron micrograph of kidney of <i>Brycon orthotaenia</i> infected by.....                     | 68 |
| <b>Figure 9</b> - Fig. 9. Maximum-Likelihood tree showing relationship between the four.....                      | 70 |
| <b>Table I</b> - Comparative data of <i>Myxobolus</i> sp. n. 1; <i>Myxobolus</i> sp. n. 2; <i>Myxobolus</i> ..... | 71 |
| <b>Table II</b> - Similarity matrix for the 18S rDNA sequences from <i>Henneguya</i> and.....                     | 74 |

## 1-INTRODUÇÃO

Os peixes se distribuem em cerca de 25.000 espécies, o que representa 50% de todas as espécies de vertebrados (Nelson, 2006), sendo que 58% dessas espécies vivem em água salgada, 41% em água doce e cerca de 1% (250 espécies) migram regularmente entre os dois sistemas (Cohen, 1970; McDowell, 1997; Lundberg et al., 2000).

O Brasil, que possui a maior disponibilidade de água doce do mundo (SEAP, 2007), é também o país com maior diversidade de peixes dulciaquícolas (Buckup et al., 2007), e apresenta assim, grande potencial para que se torne um grande produtor de pescado (Firetti & Sales, 2004; Gregolin, 2010).

O rio São Francisco, o principal rio do estado de Minas Gerais e um dos mais importantes do Brasil, brota nas nascentes da Serra d'Água, com o nome de Rio Samburá, no Sudoeste do estado de Minas Gerais e somente após receber as águas que vertem no Parque Nacional da Serra da Canastra, recebe o nome de São Francisco. Seus principais afluentes são os rios Pará, Paracatu, Paraopeba, das Velhas e Verde Grande. O rio São Francisco forma a terceira maior bacia hidrográfica do Brasil e a única totalmente brasileira, a qual drena áreas dos estados de Minas Gerais, Bahia, Pernambuco, Alagoas, Sergipe e o Distrito Federal, além de cortar três biomas: Cerrado, Caatinga e Mata Atlântica. Com 645 mil km<sup>2</sup>, a bacia de drenagem cobre 7,6% do território Nacional. Na classificação mundial é o 34º rio de maior vazão, com média anual de 2800 m<sup>3</sup>s<sup>-1</sup> e o 31º em extensão, com 2900 km (Welcomme, 1985).

A fauna de peixes do Rio São Francisco conta com cerca de 160 espécies (Sato & Godinho, 1999), mas novas espécies têm sido descritas com frequência (Lima & Britski 2007; Bichuette & Rizzato, 2012). Três espécies se destacam com relação à pesca: surubim (*Pseudoplatystoma corruscans* Agassiz, 1829); dourado (*Salminus franciscanus* Lima & Britski, 2007) e matrinxã (*Brycon orthotaenia* Günther, 1864).

A alta qualidade da proteína da carne de peixes e os benefícios que este alimento representa para a saúde humana estão fazendo com que o consumo de pescado tenha

aumentado nas últimas décadas, principalmente em países em desenvolvimento (Woo, 2006).

No Brasil, no período de cinco anos (2006 a 2010), a produção brasileira de pescado passou de 1.050.808 para 1.264.765 toneladas (Ibama, 2009; MPA, 2012). A pesca marinha e continental, no entanto, mantiveram seus níveis de produção praticamente inalterados neste período, com cerca de 530 mil toneladas/ano para a pesca marinha e cerca de 250 mil toneladas/ano para a pesca continental, ao passo que a aquicultura continental (piscicultura), saltou de 271.695 toneladas em 2006 para 394.340 em 2010 (Ibama, 2009; MPA, 2012).

Peixes, tanto em ambientes naturais quanto em pisciculturas, estão expostos a vários patógenos, que podem produzir danos importantes (Eiras, 2004; Woo, 2006). Vírus, bactérias, fungos, protozoários, mixozoários (mixosporídeos) e metazoários (Monogenea, Digenea, Nematoda, crustáceos e anelídeos) podem ser agentes etiológicos de doenças em peixes, afetando negativamente o desenvolvimento dos mesmos (Eiras, 1994; Woo, 2006).

Mixosporídeos estão entre os mais abundantes parasitos na natureza (Gómez et al., 2014) e dentre os patógenos de peixes, devido à grande diversidade encontrada neste grupo de hospedeiro e ao grande potencial patogênico que algumas espécies apresentam, tem cada vez mais recebido a atenção dos pesquisadores (Feist & Longshaw, 2006; Gómez et al., 2014).

Atualmente são conhecidas mais de 2400 espécies de mixosporídeos, que parasitam principalmente peixes, tanto em ambiente natural como em sistemas de criação, e algumas espécies infectam répteis, anfíbios, aves e mamíferos (Bartošova-Sojkova et al., 2014; Bartholomew et al., 2008; Prunescu et al., 2007).

*Myxobolus cerebralis* Hofer, 1903, que é o agente etiológico da “doença do rodopio” em salmonídeos, é a espécie mais conhecida, e a enfermidade causa alta mortalidade em várias partes do mundo (Elwell et al., 2009). *Myxobolus cerebralis* é originário da Europa e se espalhou por todo o mundo por meio de atividades antrópicas (Hallett & Bartholomew, 2012). A doença manifesta-se nos espécimes jovens e o parasito se aloja nas cartilagens, causando deformações na cabeça e na coluna vertebral. Na região das Montanhas Rochosas, nos Estados Unidos, a espécie é apontada como responsável pelo

declínio da população de truta arco-íris em ambiente natural (Allen & Bergersen, 2002; Elwell et al., 2009, Hallett & Bartholomew, 2012).

Várias outras espécies de mixosporídeos, pertencentes a diferentes gêneros, foram registradas causando importantes danos a diversas espécies de peixes em todo o mundo: *Kudoa thyrsites* Gilchrist, 1924, foi registrado causando liquefação muscular em *Coryphaena hippurus* na Austrália (Langdon, 1991) e em *Paralichthys adspersus* no Chile (Castro & Burgos, 1996); *Ceratomyxa shasta* Noble, 1950, é considerado um dos mais virulentos mixosporídeos (Hallett & Bartholomew, 2012). O parasito infecta o trato digestório de salmonídeos da América do Norte, causando sérios danos em populações em criações e selvagens (Lom & Dyková, 1995). *Henneguya ictaluri* Pote et al. 2000, produz a doença proliferativa das brânquias, uma das mais importantes doenças do bagre do canal (*Ictaluris punctatus*), causando alta mortalidade em sistemas de criação (Feist & Longshaw, 2006). *Enteromyxum leei* Diamant, Lom, & Dyková, 1994, é responsável por altas taxas de morbidade e mortalidade do perciforme *Sparus aurata* em sistemas de criação no Mediterrâneo (Rigo & Katharios, 2010). Este parasito invade o epitélio intestinal do hospedeiro e causa severa enterite crônica (Estenoro et al., 2011). O déficit de absorção de nutrientes provoca anorexia, conduzindo a uma menor performance no crescimento, seguido de caquexia e morte dos peixes infectados (Sitjà-Bobadilla et al., 2008; Estensoro et al., 2010).

No Brasil, os estudos sobre mixosporídeos parasitos de peixes tem se intensificado nos últimos 10 anos (Adriano et al., 2005a; 2005b; 2005c; 2006; 2009; 2012; Azevedo et al., 2008; 2009; 2010; 2011; 2012; Azevedo et al., 2014; Naldoni et al, 2009; 2011; Eiras et al., 2010; Milanin et al., 2010; Carrierio et al., 2013; Moreira et al., 2014a; 2014b; Azevedo et al., 2014) e algumas espécies tem se mostrado importantes patógenos para seus hospedeiros tanto em ambiente natural como em sistemas de criação. Segundo Adriano et al. 2005a, *Henneguya piaractus* Martins & Souza, 1997, produziu alterações das estruturas branquiais, com hiperplasia do epitélio das lamelas e compressão dos capilares e tecidos adjacentes, em pacus mantidos em sistemas de criação. *Myxobolus cuneus* Adriano, Arana et Cordeiro, 2006, foi descrito parasitando vesícula biliar, bexiga urinária, brânquias, baço, nadadeiras, superfície da cabeça, fígado e coração de pacus oriundos de criação. Dos órgãos

infectados por *M. cuneus*, os maiores danos refletiram-se nas brânquias, visto que o desenvolvimento dos cistos reduziu o lúmen dos vasos, e em alguns casos, obstruiu totalmente as arteríolas dos filamentos branquiais (Adriano et al., 2006). *Henneguya pseudoplatystoma* Naldoni, Maia, Ceccarelli, Tavares, Borges, Pozo et Adriano, 2009, produz importante diminuição da área de epitélio respiratório de pintado híbrido (*Pseudoplatystoma corruscans* x *Pseudoplatystoma fasciatum*) criado no estado de São Paulo e do Mato Grosso do Sul (Naldoni et al., 2009). *Henneguya chydadea* Barassa, Arana et Cordeiro, 2003, produziu compressão dos capilares e do epitélio lamelar de lambari (*Astyanax altiparanae*) oriundos de ambiente natural (Barassa et al., 2003). *Myxobolus salminus* Adriano, Carriero, Naldoni, Ceccarelli et Maia, 2009, se desenvolve nas paredes dos vasos dos filamentos branquiais, onde atuam como importantes barreiras físicas para o fluxo do sangue (Adriano et al., 2009).

Estudos ultra-estruturais e histológicos de mixosporídeos parasitos de peixes sul americanos têm contribuído fortemente para ampliar o conhecimento sobre a interface parasito-hospedeiro (Azevedo & Matos, 2002; Azevedo et al., 2005; 2010; Adriano et al., 2005a; 2005b; 2005c; 2006; 2009; 2012; Casal et al., 2006; Naldoni et al., 2009, 2011; Moreira et al., 2014a; 2014b; Müller et al., 2013). *Henneguya curimata* Azevedo & Matos, 2002, descrito infectando o rim de *Curimata inornata* na Amazônia, apresenta numerosos canais de pinocitose na região periférica dos plasmódios, os quais ligam a membrana do parasito ao seu citoplasma. A análise ultra-estrutural mostrou ainda, uma camada de fibras colagênicas entre a parede dos plasmódios e as células do hospedeiro, prevenindo o contato direto com o parasito (Azevedo & Matos, 2002). Já nas infecções de brânquias de pacu por *H. piaractus*, a parede dos plasmódios encontra-se em contato direto com as células do hospedeiro, e, além de canais de pinocitose, foram observados pontos da parede do plasmódio com partes de tecido hospedeiro, sugerindo fagocitose (Adriano et al., 2005a). Em hospedeiros pimelodídeos, algumas espécies de mixosporídeos têm sido registradas causando importantes alterações nos tecidos dos hospedeiros: *H. pseudoplatystoma*, parasito das brânquias de pintado híbrido de sistema de cultivo, tem seu desenvolvimento no tecido conjuntivo dos filamentos branquiais e causa fusão lamelar e redução da área funcional do epitélio (Naldoni et al., 2009). A parede do plasmódio esteve em contato



direto com o tecido do hospedeiro e apresentou projeções que aumentam a superfície de contato e a capacidade de absorção de nutrientes pelos numerosos canais de pinocitose também observado conectando a parede do plasmódio ao ectoplasma (Naldoni et al., 2009). Um material elétron denso, semelhante a actina, foi observado no ectoplasma periférico do plasmódio e parece funcionar como suporte para as várias projeções emitidas pela parede do plasmódio (Naldoni et al., 2009). Em *Henneguya eirasi* Naldoni, Arana, Maia, Silva, Carriero, Ceccarelli, Tavares et Adriano, 2011, um parasito de filamentos branquiais de *P. corruscans* do Pantanal, o desenvolvimento do plasmódio no tecido conjuntivo sub epitelial do filamento da brânquia causou compressão dos tecidos adjacentes (Naldoni et al., 2011). No ectoplasma periférico foi observado material elétron denso, semelhante ao observado em *H. pseudoplatystoma*, formando uma linha logo abaixo a parede do plasmódio que apresentou projeções e reentrâncias, aumentando a superfície de contato com o tecido hospedeiro (Naldoni et al., 2011). O plasmódio foi isolado do contato direto com o tecido do hospedeiro por uma cápsula de colágeno (Naldoni et al., 2011). *Henneguya multiplasmodialis* Adriano, Carriero, Maia, Silva, Naldoni, Ceccarelli et Arana, 2012, descrito infectando as brânquias de *P. corruscans* e *P. reticulatum* do Pantanal, tem o desenvolvimento dos plasmódios na superfície das brânquias, sobre os filamentos. O parasito apresentou a parede do plasmódio envolvida por um epitélio estratificado que foi composto por vários tipos de células com predominância para as células mucosas e *club cells*, estas últimas relacionadas a resposta imune (Adriano et al., 2012). Internamente o plasmódio apresentou organização peculiar, com a presença de septos dividindo o plasmódio em vários compartimentos, os quais foram compostos por tecido conjuntivo e epitélio estratificado contendo células mucosas e infiltrado inflamatório (Adriano et al., 2012). Em hospedeiros bryconídeos, algumas espécies de mixosporídeos têm também sido descritas com detalhes no contexto da interação parasito-hospedeiro: *Myxobolus macroplasmodialis* Molnár, Ranzani-Paiva, Eiras et Rodrigues, 1998, foi encontrado na cavidade abdominal de *S. brasiliensis*, o grande plasmódio, com aproximadamente 1 cm, foi envolvido por tecido de origem hospedeira; *M. salminus*, desenvolve numerosos plasmódios no endotélio dos vasos sanguíneos dos filamentos branquiais de *S. brasiliensis*, causando obstrução dos vasos sanguíneos, congestão e edema perivascular (Adriano et al.,

2009). A parede do plasmódio esteve em contato direto com o tecido do hospedeiro e vários canais de pinocitose foram observados conectando a parede do plasmódio ao ectoplasma (Adriano et al., 2009). *Myxobolus oliveirai* Milanin, Eiras, Arana, Maia, Alves, Silva Carriero, Ceccarelli et Adriano, 2010, parasita a porção distal dos filamentos braquiais de *Brycon hilarii* do Pantanal mato-grossense, induzindo hipertrofia dos filamentos infectados, com compressão e afinamento do tecido da extremidade distal, que apresentou somente uma delicada camada de células (Milanin et al., 2010). O plasmódio foi isolado do contato direto com o tecido hospedeiro por uma cápsula de colágeno e numerosos canais de pinocitose foram observados conectando a parede do plasmódio ao ectoplasma (Milanin et al., 2010). Em *Henneguya rotunda* Moreira, Adriano, Silva, Ceccarelli et Maia, 2014, um parasito de *Salminus brasiliensis* do rio Mogi Guaçu, os plasmódios se desenvolveram na membrana do arco das brânquias e na membrana entre os raios das nadadeiras, e em ambos sítios de infecção foram observados inúmeros canais de pinocitose conectando a parede do plasmódio ao ectoplasma e no ectoplasma foram observadas vesículas que continham em seu interior material elétron denso e amorfo e foram hipoteticamente considerados vacúolos digestivos (Moreira et al., 2014b).

Métodos de biologia molecular tem sido usados na diferenciação de espécies de mixosporídeos morfologicamente semelhantes (Bahri et al., 2003, Zhao et al., 2008), no estudo da especificidade de hospedeiro e de órgão (Molnár et al., 2002), na elucidação do ciclo de vida (Bartholomew et al., 1997) e no estudo filogenético destes parasitos (Fiala 2006; Fiala & Bartošová, 2010; Evans et al., 2010; Carriero et al., 2013).

Molnár et al. (2002), já em no início da primeira década do século XXI, mostraram que, com o uso exclusivo de métodos zoológicos clássicos, era muito difícil validar espécies de mixosporídeos morfologicamente similares, com idêntica afinidade tecidual e desenvolvendo-se em espécies de hospedeiros taxonomicamente muito próximas. Sugeriram então, que nestes casos o uso de técnicas de biologia molecular era de suma importância. Já no ano seguinte, Bahri et al. (2003), sugeriram que nas descrições de espécies de *Myxobolus* spp. fossem utilizados, além da cuidadosa descrição das características dos esporos, dados do sequenciamento do gene 18S rDNA. Atualmente, a

utilização de dados morfológicos, moleculares e de informações biológicas correlatas (localização geográfica, espécie hospedeira, órgão e/ou tecidos) permitem estudos taxonômicos mais precisos em nível de espécie (Gleeson & Adlard, 2012).

Várias espécies de peixes da bacia do Rio São Francisco têm grande importância para a pesca extrativista e esportiva, sendo que nos últimos anos, algumas espécies têm sido também utilizadas com sucesso na piscicultura (Campeche et al., 2011). Contudo, até aqui os relatos de mixosporídeos infectando peixes deste rio estão restritos à *Henneguya* sp., encontrado parasitando *Myleus micans* (Lütken, 1875), e *Myxobolus franciscoi* Eiras, Monteiro et Brasil-Sato, 2010, infectando *Prochilodus argenteus* (Brasil-Sato, 2003; Eiras et al., 2010).

Diante do exposto, o objetivo deste estudo foi conhecer as espécies de mixosporídeos parasitos de três espécies de peixes de grande importância econômica da bacia do rio São Francisco. Para tanto, foram utilizadas técnicas de biologia molecular, histologia e ultraestrutura na descrição taxonômica das espécies, para análise da relação parasito-hospedeiro, verificação das alterações histológicas e o posicionamento filogenético.

## 2-JUSTIFICATIVA

Na pesca e piscicultura continental, espécies do gênero *Pseudoplatystoma*, *Salminus* e *Brycon* ocupam lugar de destaque, tanto do ponto de vista da produção quanto da aceitação pelo mercado consumidor, o que faz destes peixes, independentemente da bacia onde ocorrem, de grande importância econômica.

O conhecimento dos aspectos sanitários relacionado aos peixes é importante porque microrganismos podem estar envolvidos na mortalidade de peixes até mesmo em ambientes naturais.

O rio São Francisco foi escolhido devido a sua importância para o País, sendo o rio de grande extensão e que atravessa quase todo o estado de Minas Gerais e grande parte dos

estados do Nordeste. O rio tem grande diversidade de peixes e a pesca representa uma atividade importante para a população de várias cidades localizadas às margens do rio São Francisco. Para este estudo foram escolhidas as espécies *P. corruscans*, *S. franciscanus* e *B. orthotaenia*, que estão entre os peixes mais importantes para a pesca da região e que apresentam grande potencial para a piscicultura. Com a crescente tendência da utilização de espécies nativas na criação em sistemas confinados, é inadiável o avanço no conhecimento da diversidade de patógenos que infectam estes peixes. Pois em sistemas de criação as condições intrínsecas da atividade causam estresse aos peixes, aumentando a suscetibilidade às infecções por microrganismos. Este fato é preocupante do ponto de vista sanitário, visto que nestas condições os agentes infecciosos podem ser disseminados com maior facilidade entre os hospedeiros. A escolha da cidade de Pirapora é justificada por se tratar de uma das cidades mineiras com o maior número de colônias de pescadores nas margens do rio São Francisco.

### **3-OBJETIVOS**

#### **3.1- Objetivo Geral**

Estudo taxonômico e da relação parasito-hospedeiro de espécies de mixosporídeos parasitos de pintado (*P. corruscans*), dourado (*S. franciscanus*) e matrinxã (*B. orthotaenia*) procedentes da bacia do Rio São Francisco, Minas Gerais, Brasil.

#### **3.2- Objetivos Específicos**

- 1) Realizar estudo taxonômico de mixosporídeos utilizando técnicas de análises morfológicas através da microscopia de luz e de biologia molecular (sequenciamento do gene 18S rDNA).
- 2) Identificar e/ou descrever espécies de mixosporídeos parasitos de pintado, dourado e matrinxã, baseando-se em dados morfológicos (microscopia de luz, microscopia eletrônica de transmissão e análise molecular).

- 3) Avaliar aspectos da interação parasito-hospedeiro com base em análises histopatológicas e/ou ultra estruturais.
- 4) Propor uma hipótese filogenética para as espécies de mixosporídeos encontrados infectando as espécies alvo do estudo, com base no sequenciamento do gene 18S rDNA.

#### **4- MATERIAL E MÉTODOS**

Este projeto foi desenvolvido no Departamento de Biologia Animal do Instituto de Biologia da UNICAMP, em parceria com o Departamento de Ciências Biológicas do Instituto de Ciências Ambientais, Químicas e Farmacêuticas da Universidade Federal de São Paulo-UNIFESP, Campus Diadema e o Departamento de Medicina Veterinária da Universidade de São Paulo-USP/FZEA, Campus de Pirassununga.

Durante os anos de 2010 a 2013, foram realizadas 5 coletas no rio São Francisco, região do município de Pirapora, estado de Minas Gerais (Fig. 1). Os peixes foram coletados com auxílio de redes de espera, rede de arrasto, tarrafas e anzol, dependendo das características da espécie a ser capturada e do ambiente de pesca de coleta. Após a captura, os peixes foram transportados vivos para o laboratório de campo montado nas proximidades do local de captura (Fig. 2), onde foram eutanasiados mediante a overdose por benzocaína. Este procedimento foi aprovado pela Comissão de Ética no Uso de Animais CEUA/Unicamp e está de acordo com a Lei Federal Nº 11.794 de 8 de outubro de 2008 e o Decreto Federal Nº 6899 de 15 de julho de 2009.

Após a eutanásia, os peixes foram pesados e medidos, sendo em seguida realizada a análise externa, em busca de lesões e/ou cistos de parasitos. Posteriormente foi realizada a necropsia, com exposição das brânquias e da cavidade visceral, com a finalidade de detectar eventuais alterações nas características dos órgãos e a presença de parasitos (Fig. 3). O material coletado foi preparado e/ou fixado de acordo com as técnicas de estudo que seriam realizadas posteriormente, como análise em preparações a fresco e fixação em formol 10% diluído em tampão fosfato para análises morfológicas em microscopia óptica, glutaraldeído 2,5% diluído em tampão cacodilato de sódio 0,2 M (pH 7,2) para microscopia eletrônica e etanol absoluto para análise molecular). Foram fixadas e analisadas amostras obtidas em

coletas realizadas durante o período de 12 a 17 de julho de 2010, 27 de junho a 01 de julho de 2011, 05 a 09 de dezembro de 2011, 04 a 07 de dezembro de 2012 e 18 a 22 de novembro de 2013. No total, foram capturados 91 peixes, sendo 10 *P. corruscans*, 42 *S. franciscanus* e 39 *B. orthotaenia* (Fig. 4).

Este trabalho está dividido em dois capítulos, os quais reportam estudos taxonômicos, filogenéticos e da interação parasito-hospedeiro de espécies de mixosporídeos parasitos de *P. corruscans*, *S. franciscanus* e *B. orthotaenia*. Metodologia detalhada referente às técnicas de estudo encontra-se em cada um dos dois capítulos.

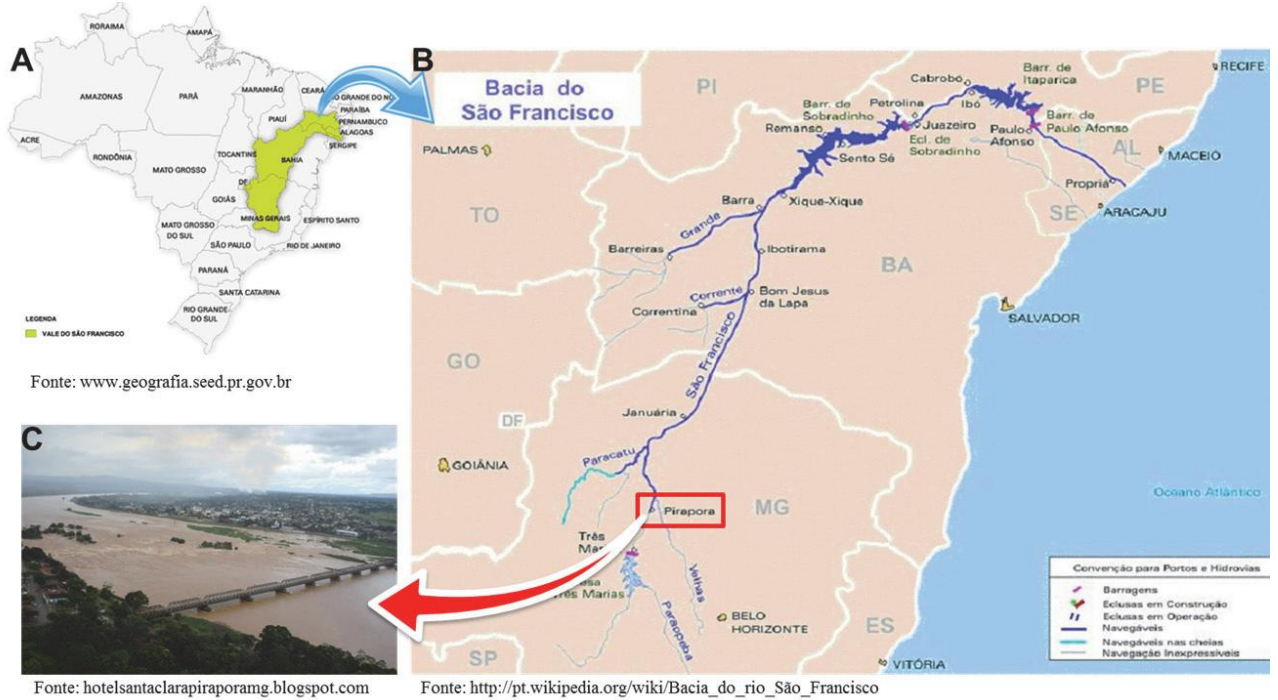


Fig. 1. Mapa do Brasil (A), mostrando a localização da bacia do rio São Francisco (B) e o ponto de coleta no município de Pirapora, MG (C).

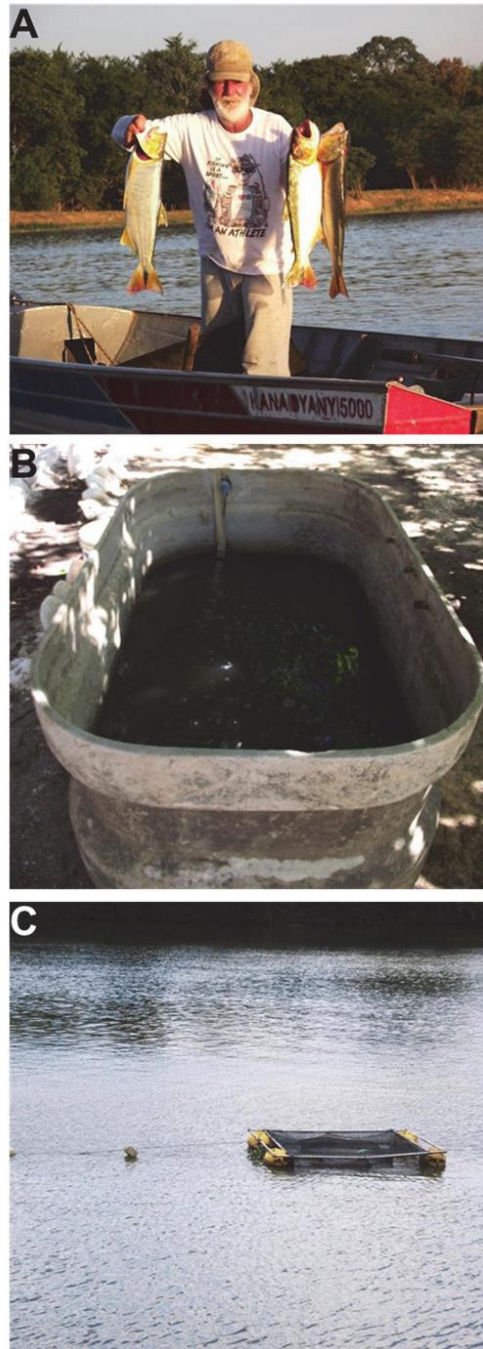


Fig. 2: Coleta de campo. A – Pescador com três espécimes de *Salminus franciscanus*. B – Tanque em rede onde os peixes capturados eram mantidos até o momento da necropsia. C – Caixa d'água com aeração usada no laboratório de campo para manter os peixes vivos até o momento de necropsia. Fonte: arquivo pessoal.





Fig. 3: Foto do laboratório de campo. A – Necropsia. B – Análise das amostras. Fonte: arquivo pessoal.

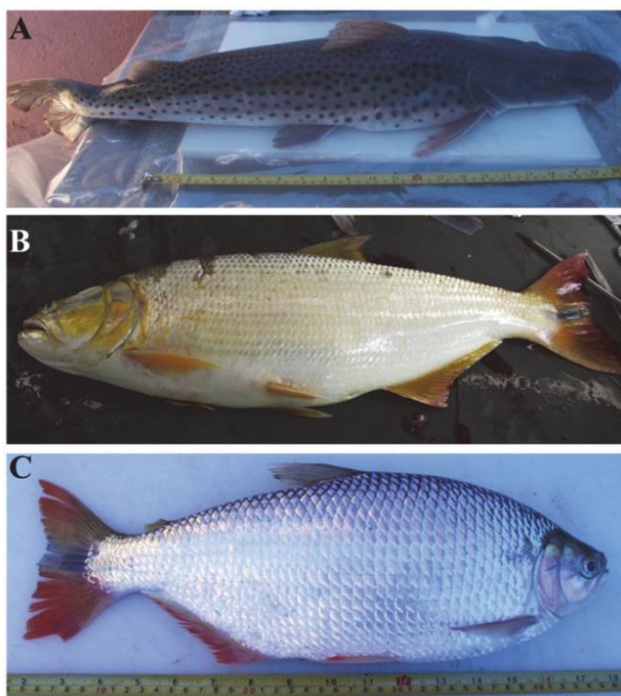


Fig. 4: Foto das espécies de peixe coletadas. A – *Pseudoplatystoma corruscans* (Pintado) B – *Salminus franciscanus* (Dourado). C – *Brycon orthotaenia* (matrinxã). Fonte: arquivo pessoal.

## 5-REFERÊNCIAS BIBLIOGRÁFICAS

- Adriano E.A., Arana S., Cordeiro N.S. 2005a. Histology, ultrastructure and prevalence of *Henneguya piaractus* (Myxosporea) infecting the gills of *Piaractus mesopotamicus* (Characidae) cultivated in Brazil. *Dis Aquat Org*, 64: 229-235.
- Adriano E.A., Arana S., Cordeiro N.S. 2005b. An ultrastructural and histopathological study of *Henneguya pellucida* n. sp. (Myxosporea: Myxobolidae) infecting *Piaractus mesopotamicus* (Characidae) cultivated in Brazil. *Parasitology*, 12: 221-227.
- Adriano E.A., Arana S., Cordeiro N.S. 2005c. Histopathology and ultrastructure of *Henneguya caudalongula* sp. n. infecting *Prochilodus lineatus* (Pisces: Prochilodontidae) cultivated in the state of São Paulo, Brazil. *Mem Inst Oswaldo Cruz*, 100: 177-181.
- Adriano E.A., Arana S., Cordeiro N.S. 2006. *Myxobolus cuneus* n. sp. (Myxosporea) infecting the connective tissue of *Piaractus mesopotamicus* (Pisces: Characidae) in Brazil: histopathology and ultrastructural. *Parasitology*, 13: 137-142.
- Adriano E.A., Arana S., Carriero M.M., Naldoni J., Ceccarelli P.S., Maia A.A.M. 2009. Light, electron microscopy and histopathology of *Myxobolus salminus* n. sp., a parasite of *Salminus brasiliensis* from the Brazilian Pantanal. *Vet Parasitol*, 165: 25-29.
- Adriano E.A., Carriero M.M., Maia A.A.M., Silva M.R.M., Naldoni J., Ceccarelli P.S., Arana S. 2012. Phylogenetic and host-parasite relationship analysis of *Henneguya multiplasmodialis* n. sp. infecting *Pseudoplatystoma* spp. in Brazilian Pantanal wetland. *Vet Parasitol*, 185: 110-120.
- Allen M.B., Bergersen, E.P. 2002. Factors influencing the distribution of *Myxobolus cerebralis*, the causative agent of whirling disease, in the Cache la Poudre River, Colorado. *Dis Aquat Org*, 49: 51-60.
- Azevedo C., Matos E. 2002. Fine structure of the myxosporean, *Henneguya curimata* n. sp., parasite of the Amazonian fish, *Curimata inornata* (Teleostei, Curimatidae). *J Euk Microbiol*, 49: 197-200.

- Azevedo C., Corral L., Matos E. 2005. Ultrastructure of *Triangulamyxa amazônica* n. gen. and n sp. (Myxozoa, Myxosporea), a parasite of the Amazonian freshwater fish, *Sphoeroides tetudineus* (Teleostei, Tetrodontidae). *Europ Protistol*, 41: 57-63.
- Azevedo C., Casal G., Matos P., Matos E. 2008. A new species of Myxozoa, *Henneguya rondoni* n. sp. (Myxozoa), from the peripheral nervous system of the Amazonian fish, *Gymnorhamphichthys rondoni* (Teleostei). *J Eukaryot Microbiol*, 55:229–34.
- Azevedo C., Casal G., Mendonca I., Matos E. 2009. Fine structure of *Henneguya hemiodopsis* sp. n. (Myxozoa), a parasite of the gills of the Brazilian teleostean fish *Hemiodopsis microlepes* (Hemiodontidae). *Mem Inst Oswaldo Cruz*, 104(7): 975–979.
- Azevedo C., Marques D.K.S., Casal G., Amaral C.M.C., Silva E.V., Matos P., Matos E. 2010. Ultrastructural re-description of *Henneguya piaractus* (Myxozoa), a parasite of the freshwater fish *Piaractus mesopotamicus* (Teleostei, Characidae) from the Paraguai River, Brazil. *Acta Protozool*, 49: 115-120
- Azevedo C., Casal G., Matos P., Alves A., Matos E. 2011. *Henneguya torpedo* sp. nov. (Myxozoa), a parasite from the nervous system of the Amazonian teleost *Brachyhypopomus pinnicaudatus* (Hypopomidae). *Dis Aquat Org*, 93: 235–242.
- Azevedo C., São Clemente S.C., Casal G., Matos P., Alves A., Al-Quraishy S. et al. 2012. *Myxobolus myleus* n. sp. infecting the bile of the Amazonian freshwater fish *Myleus rubripinnis* (Teleostei: Serrasalminidae): Morphology and pathology. *Syst Parasitol*, 82:241–7.
- Azevedo R.K., Vieira D.H.M.D., Vieira G.H., Silva R.J., Matos E., Abdallah V.D. 2014. Phylogeny, ultrastructure and histopathology of *Myxobolus lomi* sp. nov., a parasite of *Prochilodus lineatus* (Valenciennes, 1836) (Characiformes: Prochilodontidae) from the Peixes River, São Paulo State, Brazil. *Parasitol Int*, 63:303–307.
- Bahri S., Andree K.B., Hedrick R.P. 2003. Morphological and phylogenetic studies of marine *Myxobolus* spp. from mullet in Ichkeul Lake, Tunisia. *J Eukaryot Microbiol*, 50: 463-470.

- Barassa B., Arana S., Cordeiro N.C. 2003. A new species of *Henneguya*, a gill parasite of *Astyanax altiparanae* (Pisces: characidae) from Brazil, with comments on histopathology and seasonality. Mem Inst Oswaldo Cruz, 98: 761-765.
- Bartholomew J.L., Atkinson S.D., Hallett S.L., Lowenstine L.J., Garner M.M., Gardiner C.H.; Keel M.K.; Brown J.D. 2008. Myxozoan parasitism in waterfowl. Int J Parasitol, 38: 1199–120.
- Bartholomew J.L., Whipple M.J., Stevens D.G., Fryer, J.L. 1997. The life cycle of *Ceratomyxa shasta* a myxosporean parasite of salmonids, requires a freshwater polychaeta as an alternate host. J Parasitol, 83 (5): 859-868.
- Bartošová-Sojtková P., Hrabcová M., Pecková H., Patraa S., Kodádková A., Jurajda P., Týmł T., Sibylle Holzer A. 2014. Hidden diversity and evolutionary trends in malacosporean parasites (Cnidaria: Myxozoa) identified using molecular phylogenetics. Int Parasitol, 44: 565–577.
- Bichuette M.E. & Rizzato P.P. 2012. A new species of cave catfish from Brazil, *Trichomycterus rubbioli* sp.n., from Serra do Ramalho karstic area, São Francisco River basin, Bahia State (Siluriformes: Trichomycteridae) Zootaxa, 3480: 48–66
- Brasil-Sato M.C. 2003. Parasitos de Peixes da Bacia do São Francisco In: Godinho, H.P.; Godinho A.L. (Ed.). Águas, Peixes e Pescadores do São Francisco das Minas Gerais. Belo Horizonte: Puc minas, p. 149-165
- Buckup P.A., Menezes N.A., Ghazzi M.S. (eds.) 2007. Catálogo das espécies de peixes de água doce do Brasil. Rio de Janeiro, Museu Nacional. 195p.
- Campeche D.F.B., Balzana L., Figueire do R.C.R., Barbalho M.R.S., Reis F.J.S., Melo J.F.B. 2011. Peixes Nativos do Rio São Francisco Adaptados para Cultivo *Embrapa*.
- Carriero M.M., Adriano E.A., Silva M.R., Ceccarelli P.S., Maia A.A. 2013. Molecular phylogeny of the *Myxobolus* and *Henneguya* genera with several new South American species. PLoS One, 8:e73713.

- Casal G., Matos E., Azevedo C. 2006: A new myxozoan parasite from the amazonian fish *Metynnis argenteus* (Teleostei, Characidae): light and electron microscope observations. J Parasitol, 92: 817–821.
- Castro R.R., Burgos R. 1996. *Kudoa thyrsithes* (Myxozoa, Multivalvuloda) causing “milky condition” in the musculature of *Paralichthys adspersus* (Neopterygii, Pleuronectiformes, (Paralichthyidae) from Chile. Mem Inst Oswaldo Cruz, 91: 163-164.
- Cohen D.M. 1970. How many recent fishes are there? Proceedings of the California Academy of Science, San Francisco, 38(4): 341-345.
- Eiras J.C. 1994. Elementos de Ictioparasitologia. Porto. Fundação Eng. António de Almeida. 339p.
- Eiras J.C., Pavanelli G.C., Takemoto R.M. 2004. *Henneguya paranaensis* sp. n. (Myxozoa, Myxobolidae) a parasite of the teleost fish *Prochilodus lineatus* (Characiformes, Prochilodontidae) from the Paraná River, Brazil. Bull Eur Ass Fish Pathol, 24: 308-311.
- Eiras J.C., Monteiro C.M., Brasil-Sato M.C. 2010. *Myxobolus franciscoi* SP.nov (Myxozoa:Myxosporidia:Myxobolidae), a parasite of *Prochilodus argenteus* (Actinopterygii: Prochilodontidae) from upper São Francisco River, Brazil, with a revision of *Myxobolus* spp. From South America. Zoologia, 27 (1): 131–137.
- Elwell L.C.S., Stromberg K.E., Ryce E.K.N., Bartholomew J.L. 2009. Whirling Disease in the United States. A Summary of Progress in Research and Management. 36 p.
- Estensoro I., Benedito-Palos L., Palenzuela O., Kaushik S., Sitjà-Bobadilla A., Pérez-Sánchez J. 2011. The nutritional background of the host alters the disease course in a fishmyxosporean system. Vet Parasitol, 175: 141–150
- Estensoro I., Redondo M.J., Álvarez-Pellitero P., Sitjà-Bobadilla A. 2010. Novel horizontal transmission route for *Enteromyxum leei* (Myxozoa) by anal intubation of gilthead sea bream *Sparus aurata*. Dis Aquat Org, 92: 51–58

- Evans N.M., Holder M.T., Barbeito M.S., Okamura B., Cartwright P. 2010. The phylogenetic position of Myxozoa: exploring conflicting signals in phylogenomic and ribosomal datasets. *Mol Biol Evol*, 27(12):2733–2746.
- Feist, S. W., Longshaw, M. 2006. Phylum myxozoa. In PTK Woo (ed.), *Fish diseases and disorders. Protozoan and metazoan infections*. Vol. 1, 2nd ed., CAB International, Oxfordshire, p. 230-296.
- Fiala I. 2006. The phylogeny of Myxosporidia (Myxozoa) based on small subunit ribosomal RNA gene analysis. *J Parasitol*, 36: 1521–1534.
- Fiala I., Bartošová P. 2010. History of myxozoan character evolution on the basis of rDNA and EF-2 data. *BMC Evolution Biol*, 10: 228.
- Firetti R., Sales D.S. 2004. O futuro promissor da cadeia produtiva, ANUALPEC. Disponível em:  
<<http://www.agroinova.com.br/artigos/2004%20O%20futuro%20promissor%20da%20cadeia%20produtiva%20da%20piscicultura%20comercial.pdf>>. Acesso em: janeiro de 2011.
- Gleeson R.J., Adlard R.D. 2012. Phylogenetic relationships amongst *Chloromyxum* Mingazzini, 1890 (Myxozoa: Myxosporidia), and the description of six novel species from Australian elasmobranchs. *Parasitol Int*, 61: 267–274.
- Gómez D., Bartholomew J., Sunyer J.O. 2014. Biology and mucosal immunity to myxozoans, *Developmental and Comparative Immunology*, 43: 243–256.
- Gregolin A. 2010. Brasil quer ser o maior produtor mundial de pesca. *Diário de notícia*, 4 de julho de 2010. Disponível em  
<<http://www.dnoticias.pt/imprensa/diario/212392/economia/212479-brasil-quer-ser-o-maior-produtor-mundial-de-pesca>>. Acesso em janeiro de 2011.
- Hallett S.L. & Bartholomew J.L. 2012. *Myxobolus cerebralis* and *Ceratomyxa shasta*. In *Fish Parasites: Pathobiology and Protection*. Editors: P. T. K. Woo and K. Buchmann. CABI, Oxfordshire, UK.

- IBAMA. 2009. Instituto Brasileiro do Meio Ambiente e dos Recursos Naturais Renováveis. Estatística da pesca 2007 Brasil: grandes regiões e unidades da federação. Brasília: Ibama, 175 p.
- Langdon J.S. 1991. Myoliquefaction post-mortem ('milky flesh') due to *Kudoa thyrsites* (Gilchrist) (Myxoporea) in mahi mahi, *Coryphaena hippurus* L. Fish Dis, 14: 45-54.
- Lima, F.C.T.; Britski, H.A. 2007. *Salminus franciscanus*: a new espécie from the rio São Francisco basin, Brazil (Ostariophysi: Characiformes: Characidae). Neotrop Ichthyol, 5: 237-244.
- Lom J., Dyková I. 1995. *Myxosporea* (Phylum Myxozoa) in PTK Woo (ed.), Fish Diseases and Disorders Vol. 1 Protozoan and Metazoan Infections. CAB International UK. p. 97-148
- Lundberg J.G., Kottelat M., Smith G.R., Stiassny M.L.J., Gill A.C. 2000. So many fishes, so little time: an overview of recent ichthyological discovery in continental waters. Annals of the Missouri Botanical Garden, Saint Louis, 87(1): 26-62.
- McDowell R.M. 1997. The evolution of diadromy in fishes (revisited) and its place in phylogenetic analysis. Reviews In fish Biology And Fisheries, 7(4): 443-462.
- Milanin T., Eiras J.C., Arana S., Maia A.A.M., Alves A.L., Silva M.R.M., Carriero M.M., Ceccarelli P.S., Adriano E.A. 2010. Phylogeny, ultrastructure, histopathology and prevalence of *Myxobolus oliverai* n.sp., parasite of *Brycon hilarii* (Characidae) in the Pantanal wetland, Brasil. Mem Inst Oswaldo Cruz, 105(6): 762-769.
- Molnár K., Eszterbauer E., Sczékely C., Benko M., Harrach B. 2002. Morphological and molecular biological studies on intramuscular *Myxobolus* spp. of cyprinid fish. Fish Dis, 25: 643-652.
- Moreira G.S.A., Adriano E.A., Silva M.R.M., Ceccarelli P.S., Maia A.A.M. 2014a. Morphology and 18S rDNA sequencing identifies *Henneguya visibilis* n. sp., a parasite of *Leporinus obtusidens* from Mogi Guaçu River, Brazil Parasitol Res, 113:81–90.

- Moreira G.S.A., Adriano E.A., Silva M.R.M., Ceccarelli P.S., Maia A.A.M. 2014b. The morphological and molecular characterization of *Henneguya rotunda* n. sp., a parasite of the gill arch and fins of *Salminus brasiliensis* from the Mogi Guaçu River, Brazil. *Parasitol Res*, 113: 1703-1711.
- MPA (Ministério da Pesca e Aquicultura). 2012: Peixes esportivos de água doce. MPA, Brasília. (<http://www.mpa.gov.br/index.php/topicos/33-amadora/1285-peixe-matrinxa>).
- Müller M.I., Adriano E.A., Ceccarelli P.S., Silva M. R. M., Maia A.A.M., Ueta M.T. 2013. Prevalence, intensity, and phylogenetic analysis of *Henneguya piaractus* and *Myxobolus* cf. *colossomatis* from farmed *Piaractus mesopotamicus* in Brazil *Dis Aquat Org*, 107: 129–139
- Naldoni J., Arana S., Maia A.A.M., Ceccarelli P.S., Tavares L.E.R., Borges F.A., Pozo C.F., Adriano E.A. 2009. *Henneguya pseudoplatystoma* n. sp. causing reduction in epithelial area of gills in the farmed pintado, a South American catfish: Histopathology and ultrastructure, *Vet Parasitol*, 166: 52–59.
- Naldoni J., Arana S., Maia A.A.M., Silva M.R.M., Carriero M.M., Ceccarelli P.S., Tavares L.E.R., Adriano E.A. 2011. Host–parasite–environment relationship, morphology and molecular analyses of *Henneguya eirasi* n. sp. parasite of two wild *Pseudoplatystoma* spp. in Pantanal Wetland, Brazil. *Vet Parasitol*, 177: 247-255.
- Nelson J.S. 2006. *Fishes of the World*. 4<sup>a</sup> Edition. John Wiley & Sons, Inc. Press Hoboken, New Jersey, USA. 539p.
- Prunescu C.C., Prunescu P., Pucked Z., Lom J. 2007: The first finding of myxosporean development from plasmodia to spores in terrestrial mammals: *Soricimyxum fegati* gen. sp n. (Myxozoa) from *Sorex araneus* (Soricomorpha). *Folia Parasitol*, 54: 159–164.
- Rigos G, Katharios P. 2010 Pathological obstacles of newly introduced fish species in Mediterranean mariculture: a review. *Rev Fish Biol Fish*, 20: 47–70



- SEAP. 2007. Secretaria Especial de Aqüicultura e Pesca. Aqüicultura no Brasil. Presidência da República, Brasília. Disponível em: <[http://www.presidencia.gov.br/estrutura\\_presidencia/seap/aqui/](http://www.presidencia.gov.br/estrutura_presidencia/seap/aqui/)>.
- Sato Y. & Godinho H.P. 1999. Peixes da bacia do rio São Francisco, p. 401-413. In: R. H. Lowe-McConnell. 1999. Estudos ecológicos de comunidades de peixes tropicais. São Paulo: Edusp, 534p.
- Sitjà-Bobadilla A. 2008. Fish immune response to myxozoan parasites. *Parasite*, 15:420–425
- Welcomme R.L. 1985. River fisheries. *FAO Fish Tech Pap*, 262:1-330.
- Woo P.T.K. 2006. Fish Diseases and Disorders. Protozoan and Metazoan Infections. CAB International, 1: 791.
- Zhao Y., Sun C., Kent M.L., Deng J., Whipps C.M. 2008. Description of a new species of *Myxobolus* (Myxozoa: Myxobolidae) based on morphological and molecular data. *J Parasitol*, 94 (3): 737-742.



## 6. RESULTADOS

### Capítulo 1<sup>1</sup>

#### ***Henneguya* sp. n. 1 (Myxozoa), a parasite of *Pseudoplatystoma corruscans* in the São Francisco Basin, Brazil**

Abstract: *Henneguya* sp. n. 1 was found infecting spotted sorubim catfish *Pseudoplatystomacorruscans* from the São Francisco River, Minas Gerais, Brazil. The parasites form elongated plasmodia of up to 1 cm in length in the gill filaments. Mature spores were ellipsoidal from the frontal view, with total length of  $29.4 \pm 2.4$  (mean  $\pm$  SD, range 23.3–32.4)  $\mu\text{m}$ , body length of  $12.1 \pm 1.0$  (10.0–14.7)  $\mu\text{m}$ , width of  $4.8 \pm 0.4$  (4.0–5.9)  $\mu\text{m}$ , and tail length of  $16.7 \pm 2.0$  (12.3–19.4)  $\mu\text{m}$ . From the lateral view, spores were biconvex, with thickness of  $4.2 \pm 0.7$  (3.9–4.9)  $\mu\text{m}$ . The polar capsules were elongated and equal in size,  $6.2 \pm 0.3$  (5.2–6.2)  $\mu\text{m}$  in length, and  $1.8 \pm 0.1$  (1.4–1.9)  $\mu\text{m}$  in width. Ultrastructural analysis showed that the plasmodial wall had delicate projections towards the host tissue and a thin layer that prevented contact between the host cells and the parasite. In the ectoplasm, few mitochondria were observed, while generative cells, early stages of sporogenesis, and advanced spore development occurred in the plasmodial periphery, and more mature spores in internal regions. Histopathological analysis showed that plasmodia developed in the sub-epithelial connective tissue of gill filaments, causing compression of the adjacent tissues, deformation of gill filaments, and lamellar fusion. Phylogenetic analysis, based on 18S rDNA genes and using only *Henneguya*/*Myxobolus* species parasites of siluriform fish, showed grouping according to the fish family.

Key words: Myxosporean - Siluriformes - River - 18S rDNA - Ultrastructure - histopathology

### **Introduction**

---

<sup>1</sup> Formatação de acordo com as normas da revista Diseases of Aquatic Organisms.

The spotted sorubim *Pseudoplatystoma corruscans* (Spix & Agassiz, 1829), popularly known in Brazil as ‘pintado’ or ‘surubim,’ is a catfish siluriform of the family Pimelodidae. It is found in the La Plata and São Francisco Basins of South America (Resende 2003). These carnivorous, migratory fish can reach up to 160 cm in length and 100 kg in weight (Froese & Pauly 2011), and due to the high quality of their meat, they play an important role in the fishing economy of the regions in which they are found (Campos 2005). *P. corruscans* is important for Brazilian aquaculture, as fingerlings created by crossbreeding of this species with *P. reticulatum* Eigenmann & Eigenmann, 1889 are reared in fish farms across the country (Naldoni et al. 2009). This hybrid fish is called ‘pintado,’ and its production in Brazilian fish farms reached 2486 t in 2010 (MPA 2012). It is sold in the Brazilian market, and is also exported to several countries (Mar & Terra 2013).

The first report of a fish of the genus *Pseudoplatystoma* infected with a myxosporean was made by Eiras et al. (2009), who described *Henneguya corruscans* Eiras, Takemoto et Pavanelli, 2009, infecting *P. corruscans* from the Paraná River. Since then, 5 other species have been described: *H. pseudoplatystoma* Naldoni, Arana, Maia, Ceccarelli, Tavares, Borges, Pozo et Adriano, 2009, was found infecting hybrid pintado taken from fish farms in the states of São Paulo and Mato Grosso do Sul, and *H. eirasi* Naldoni, Arana, Maia, Silva, Carriero, Ceccarelli, Tavares et Adriano, 2011, *H. multiplasmodialis* Adriano, Carriero, Maia, Silva, Naldoni, Ceccarelli et Arana, 2012, *H. maculosus* Carriero, Adriano, Silva, Ceccarelli et Maia, 2013, and *Myxobolus flavus* Carriero, Adriano, Silva, Ceccarelli et Maia, 2013, were found infecting both *P. corruscans* and *P. reticulatum* taken from natural environments in the Brazilian Pantanal wetland (Naldoni et al. 2009, 2011, Adriano et al. 2012, Carriero et al. 2013).

All myxozoan species described herein as occurring in *Pseudoplatystoma* spp. are from the La Plata Basin. We used morphologic, histologic, ultrastructural, and 18S rDNA sequencing data to describe a new *Henneguya* species that parasitizes the gill filaments of *Pseudoplatystoma corruscans* from natural environments in the São Francisco Basin.

## Materials and methods

Ten specimens of *Pseudoplatystoma corruscans* (ranging from 56 to 93 cm in length) were collected from the São Francisco River (17° 12' 8'' S, 44° 50' 0''W) in the municipality of Pirapora, Minas Gerais State, Brazil. These samples were collected in July (n = 4) and December 2011 (n = 6). After capture, the fish were transported alive to the laboratory, where they were euthanized by benzocaine overdose (methodology approved by the ethics research committee of the Universidade Estadual de Campinas-proc. no. 2334-1), in accordance with Brazilian law (Federal Law No. 11.794, dated 8 October 2008 and Federal Decree No. 6899, dated 15 July 2009). Fish were then measured and necropsied. Plasmodia with mature spores were examined in fresh mounts with a light microscope and morphological characterization of the spores was based on mature spores obtained from 3 different specimens. Measurements were performed on 30 spores using a computer equipped with Axivision 4.1 image capture software coupled to an Axioplan 2 Zeiss microscope. The dimensions of the spores are expressed as mean  $\pm$  SD, in  $\mu$ m. Smears containing free spores were airdried and stained with Giemsa solution and mounted in a low-viscosity mounting medium (Cytoseal™) on permanent slides.

For histological analysis, fragments of infected organs were fixed in 10% buffered formalin and embedded in paraffin. Serial sections with a thickness of 4  $\mu$ m were stained with hematoxylin-eosin.

For transmission electron microscopy, plasmodia were fixed in 2.5% glutaraldehyde in 0.1 M sodium cacodylate buffer (pH 7.4) for 12 h, washed in a glucose–saline solution for 2 h, and post-fixed in OsO<sub>4</sub>. All of these processes were performed at 4°C. After dehydration using an acetone series, the material was embedded in EMbed 812 resin. Semithin sections were stained with toluidine blue solution and examined by light microscopy. Ultrathin sections, double stained with uranyl acetate and lead citrate, were examined in an LEO 906 electron microscope at 60 kV.

For molecular study, plasmodia were removed from the host tissue and fixed in absolute ethanol. The plasmodium content was collected in a 1.5 ml microcentrifuge tube and the DNA was extracted using the DNeasy® Blood & Tissue kit (Qiagen), following the manufacturer's instructions. The product was quantified in a NanoDrop 2000 spectrophotometer (Thermo Scientific) at 260 nm. PCR was carried out using a final

volume of 25 µl, which contained 10 to 50 ng of extracted DNA, 1× *Taq* DNA polymerase buffer, 0.2 mmol of dNTP, 1.5 mmol of MgCl<sub>2</sub>, 0.2 pmol of each primer, 0.25 µl (1.25 U) of *Taq* DNA polymerase (all reagents from Invitrogen by Life Technologies), and MilliQ (EMD Millipore) purified water in an Eppendorf AG 22331 Hamburg Thermocycler. Fragments of 1000 bp were amplified using the primers ERIB1+ACT1R (Barta et al. 1997), and fragments of 1200 bp were amplified using the primers MYXGEN+ERIB10 (Hallett & Diamant 2001, Diamant et al. 2004). An initial denaturation step at 95°C for 5 min was followed by 35 cycles of denaturation (95°C for 60 s), annealing (62°C for 60 s), and extension (72°C for 120 s); finishing with an extended elongation step at 72°C for 5 min. PCR products were electrophoresed in 1.0% agarose gel, stained with ethidium bromide, and analyzed in an FLA-3000 scanner (Fuji Photo Film). The size of the amplicons was estimated by comparison with the 1 kb DNA Ladder (Invitrogen by Life Technologies). Purified PCR products were sequenced using the same primer pair that was used in the amplification step, and another primer pair MC5-MC3 (Eszterbauer 2004) with the BigDye® Terminator v3.1 Cycle Sequencing kit (Applied Biosystems™) in an ABI 3730 DNA Analyzer (Applied Biosystems™). A standard nucleotide–nucleotide BLAST (blastn) search was conducted to verify the similarity of the sequence obtained in this study with other sequences available in the GenBank database (Altschul et al. 1997).

Phylogenetic analysis was performed using only myxosporean parasites of siluriforms available from GenBank. This included 13 sequences of *Henneguya* species and 2 sequences of *Myxobolus* species. *Ceratomyxa shasta* and *C. seriolae* were used as the outgroup. Nucleotide sequences were aligned using ClustalW inserted in BioEdit version 7.0.9.0 (Hall 1999). The Jmodeltest 0.1 program (Posada 2008) was used to choose the best evolution model of the sequences, and selected the GRT+G model. Nucleotide frequencies were estimated from the data (A = 0.2500, C = 0.2105, G = 0.2879, T = 0.2116). The 6 rates of nucleotide substitution were (AC) = 0.8263, (AG) = 2.2627, (AT) = 1.1733, (CG) = 0.6128, (CT) = 4.2650, (GT) = 1.0000, gamma shape = 0.3450. These parameters were used for maximum likelihood (ML) testing, which was conducted using PhyML 3.0 (Guindon et al. 2010). Bootstrap analysis (100 replicates) was employed to assess the

relative robustness of the tree branches. The resulting tree was visualized with FigTree v1.3.1 (Rambaut 2008). Other alignment, including the species described in the present study and additional myxosporean parasites of pimelodids, was used to produce a pairwise similarity matrix using MEGA 5.0.

## Results

Eight out of 10 (80%) specimens of *P. corruscans* taken from the São Francisco River had plasmodia of an unknown *Henneguya* species in the gill filaments.

### *Henneguya* sp. n. 1

**Description:** The plasmodia were white and elongated, followed the line of the gill filaments, and measured up to 1 cm long (Fig. 1A). Histopathological analysis revealed that the plasmodia developed in the sub-epithelial connective tissue of the gill filaments, and expanded towards the lamellae. Development of the parasite resulted in compression of adjacent tissues, deformation of gill filaments and deformation and fusion of lamellae. Inflammatory infiltrate was not observed in the infection site (Figs. 2, 3).

Mature spores were ellipsoidal from the frontal view, and had a total length of  $29.4 \pm 2.4$  (23.3–32.4)  $\mu\text{m}$ , a body length of  $12.1 \pm 1.0$  (10.0–14.7)  $\mu\text{m}$ , width of  $4.8 \pm 0.4$  (4.0–5.9)  $\mu\text{m}$ , and a caudal process of  $16.7 \pm 2.0$  (12.3–19.4)  $\mu\text{m}$ . From the lateral view, the spores were biconvex and had a thickness of  $4.2 \pm 0.7$  (3.9–4.9)  $\mu\text{m}$ , while the valves were symmetrical. The polar capsules were elongated and equal in size, and had a length of  $6.2 \pm 0.3$  (5.2–6.2)  $\mu\text{m}$  and a width of  $1.8 \pm 0.1$  (1.4–1.9)  $\mu\text{m}$  (Table 1). The polar capsule occupied a little more than half of the body of the spore, and the anterior ends were adjacent (Fig. 1B). The polar filaments had 10 to 11 turns and were arranged perpendicularly to the longitudinal axis of the polar capsule (Figs. 5B, 6).

Ultrastructure analysis revealed that the plasmodial wall was formed by a single membrane, and had numerous and extensive pinocytotic canals connecting the outside of the plasmodia to the ectoplasm zone (Fig. 4B). The plasmodial wall had delicate projections towards the host tissue and a thin layer, composed of fine granular material, which prevented contact between the host cells and the plasmodial wall (Fig. 4). A layer of fibrous

material was observed throughout the periphery of the plasmodia, and in some cases, this layer of fibrous material was projected toward the interior of the plasmodia (Figs. 4A, 5A). Few mitochondria were observed underneath the ectoplasm. Below the ectoplasm, generative cells, early stages of sporogenesis, and advanced spore developmental stages were seen. Immature and mature spores were more prevalent internally (Fig. 4).

Molecular analysis, based on 18S rDNA genes from the spores of *Henneguya* sp. n. 1 obtained from the gills of *Pseudoplatystoma corruscans*, resulted in a 1200 bp sequence that did not match any myxosporean species sequences available in GenBank. Analysis of the genetic divergence of the *Henneguya* species that parasitize *Pseudoplatystoma* spp. showed that the closest species to *Henneguya* sp. n. 1 was *H. multiplasmodialis* (1.7% divergence from that found infecting *P. reticulatum* and 1.8% from that found in *P. corruscans*), and the most distant was *H. maculosus* (13.1%) (Table 2).

Phylogenetic analysis, using only *Henneguya*/*Myxobolus* species parasites of siluriforms, formed 2 distinct strains. Clade A clustered 2 *Henneguya* species that parasitize fish of the Bagridae family. *Myxobolus cordeiroi*, a parasite of the pimelodid *Zungaro jahu*, appeared as a sister branch of the large clade B, which comprised *Henneguya*/*Myxobolus* parasites of pimelodids, ictalurids, and pangasids. Clade B further divided to form a sub-clade composed only of *Henneguya* species parasites of pimelodids of the genus *Pseudoplatystoma* and another composed of *Henneguya* species that parasitize ictalurids. *M. pangasii* and *M. hackyi* clustered together as a basal branch of the clade formed by parasites of ictalurids, and *M. flavus*, the unique *Myxobolus* species parasite of fish of the genus *Pseudoplatystoma*, appears as a basal branch of clade B. (Fig. 7).

**Host type:** *Pseudoplatystoma corruscans*.

**Locality:** São Francisco River, municipality of Pirapora, state of Minas Gerais, Brazil.



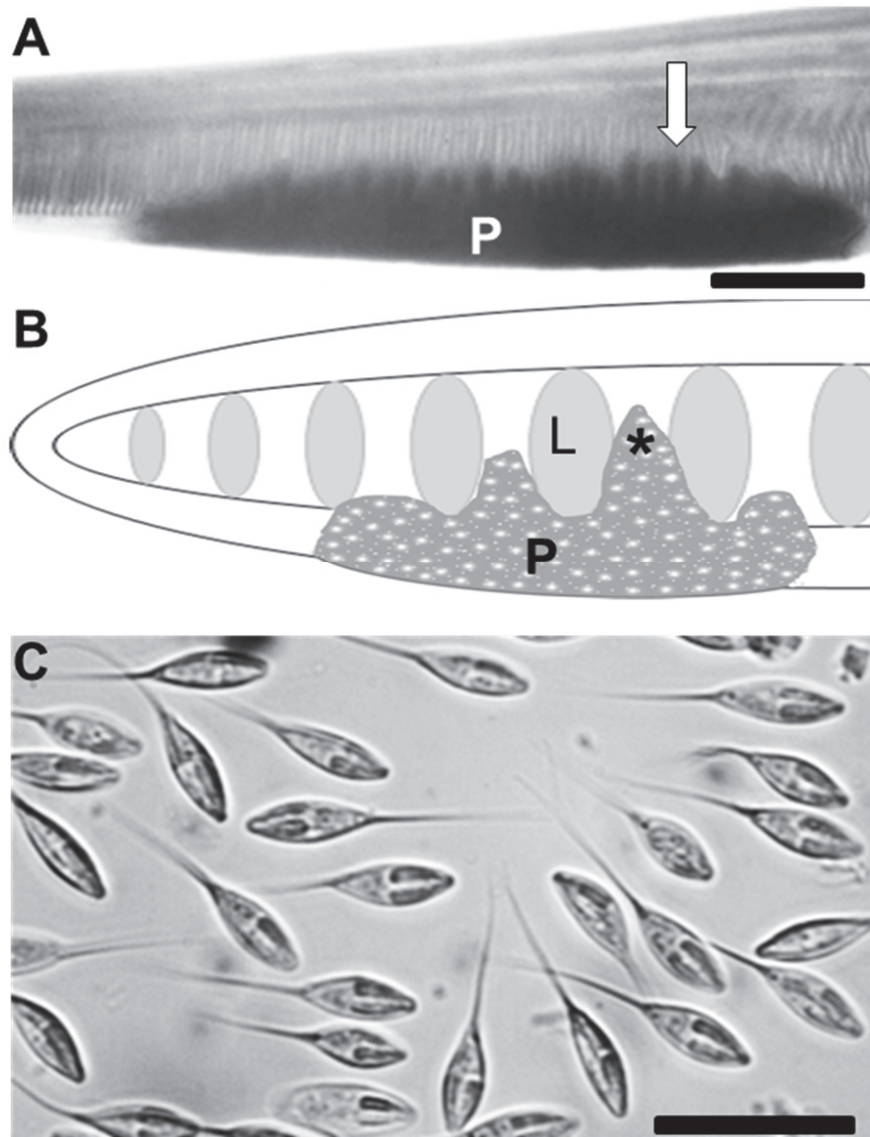


Fig. 1. *Henneguya* sp. n. 1 infecting *Pseudoplatystoma corruscans*. (A) Formalin-fixed gill filament showing intrafilamental-epithelial plasmodium (P) growing towards the interlamellar region (arrow). Scale bar = 1000  $\mu$ m. (B) Schematic drawing of a gill filament in frontal view showing the development of intrafilamental-epithelial plasmodium (P) growing towards the interlamellar region (\*) and causing compression and deformation of the lamellae (L). (C) Photomicrograph of mature fresh spores in frontal view. Scale bar = 20  $\mu$ m

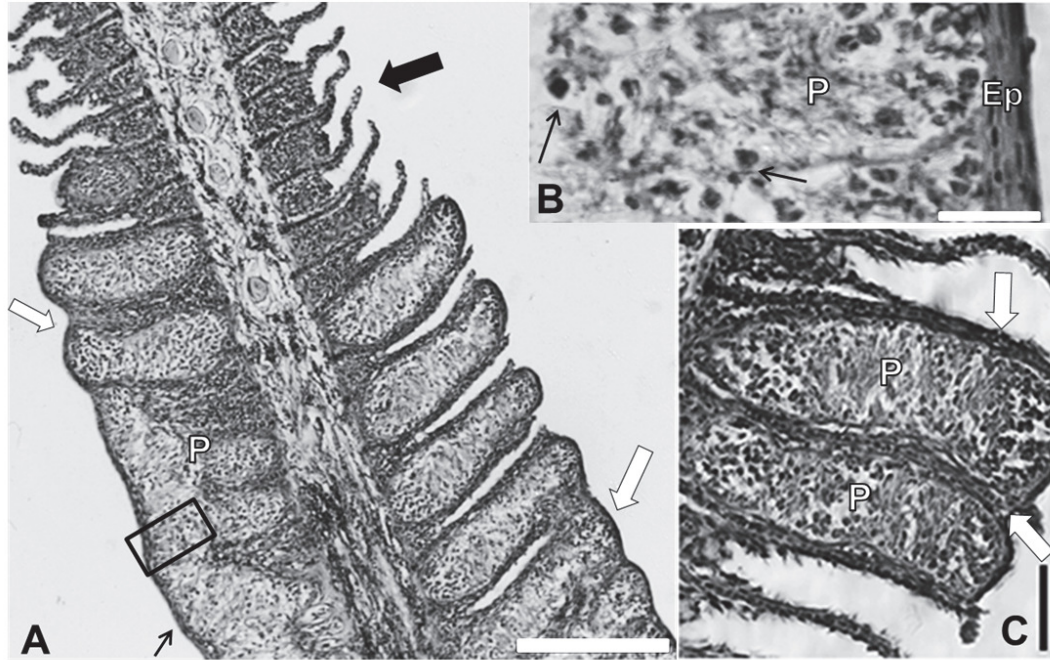


Fig. 2. *Pseudoplatystoma corruscans* infected by *Henneguya* sp. n. 1. Photomicrographs of histological sections of gill filaments. (A) Plasmodium (P) in sub-epithelial connective tissue (thin black arrow) occupying all area of the filament. Note normal lamellae (thick black arrow) and several deformed lamellae and lamellar fusion in areas affected by the growth of the plasmodium (white arrows). Scale bar = 200 µm. (B) Magnified section (rectangle) from (A); note the asynchronous process of sporogony inside of the plasmodium (P), with young developmental stage spores (arrows) spread across all areas of the plasmodium. Ep: epithelium. Scale bar = 40 µm. (C) Detail of the development of plasmodium (P) growing towards the interlamellar regions occupying the entire interlamellar space and causing deformation and compression of the lamellae (white arrows). Stained with hematoxylin-eosin. Scale bar = 50 µm

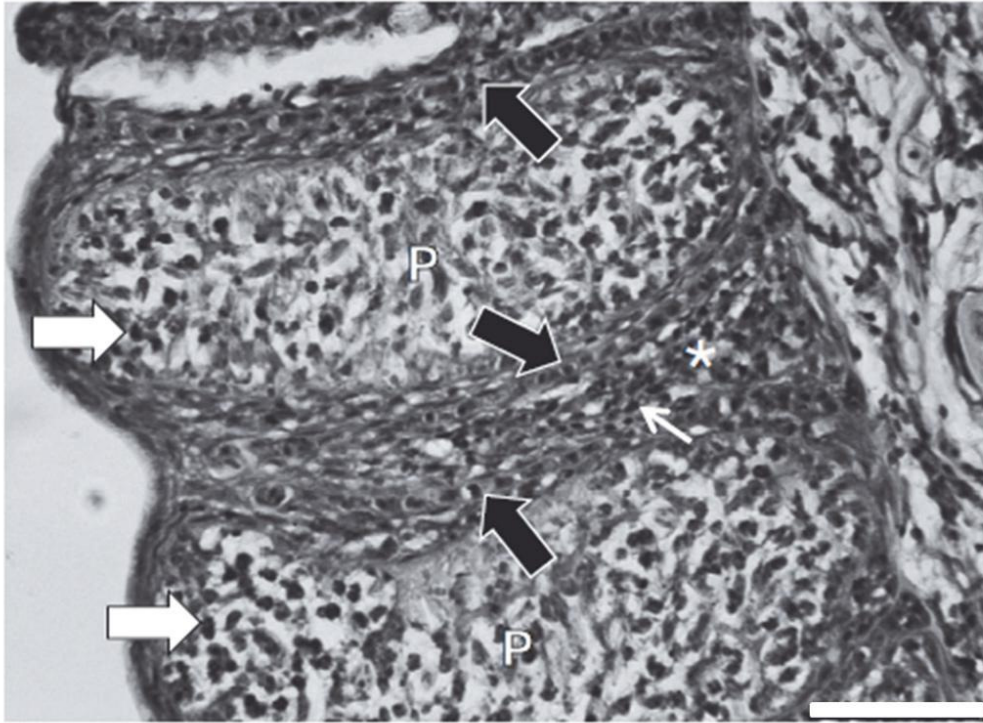


Fig. 3. *Pseudoplatystoma corruscans* infected by *Henneguya* sp. n. 1. Photomicrograph of histological section of gill filaments. Note deformation and compression of the interlamellar epithelium (\*) with agglomerated nuclei of epithelial cells (thin white arrow), deformation of the lamellae (thick black arrows), and young developmental spores (thick white arrows) spread across all areas of the plasmodium (P). Stained with hematoxylin-eosin. Scale bar = 50  $\mu$ m



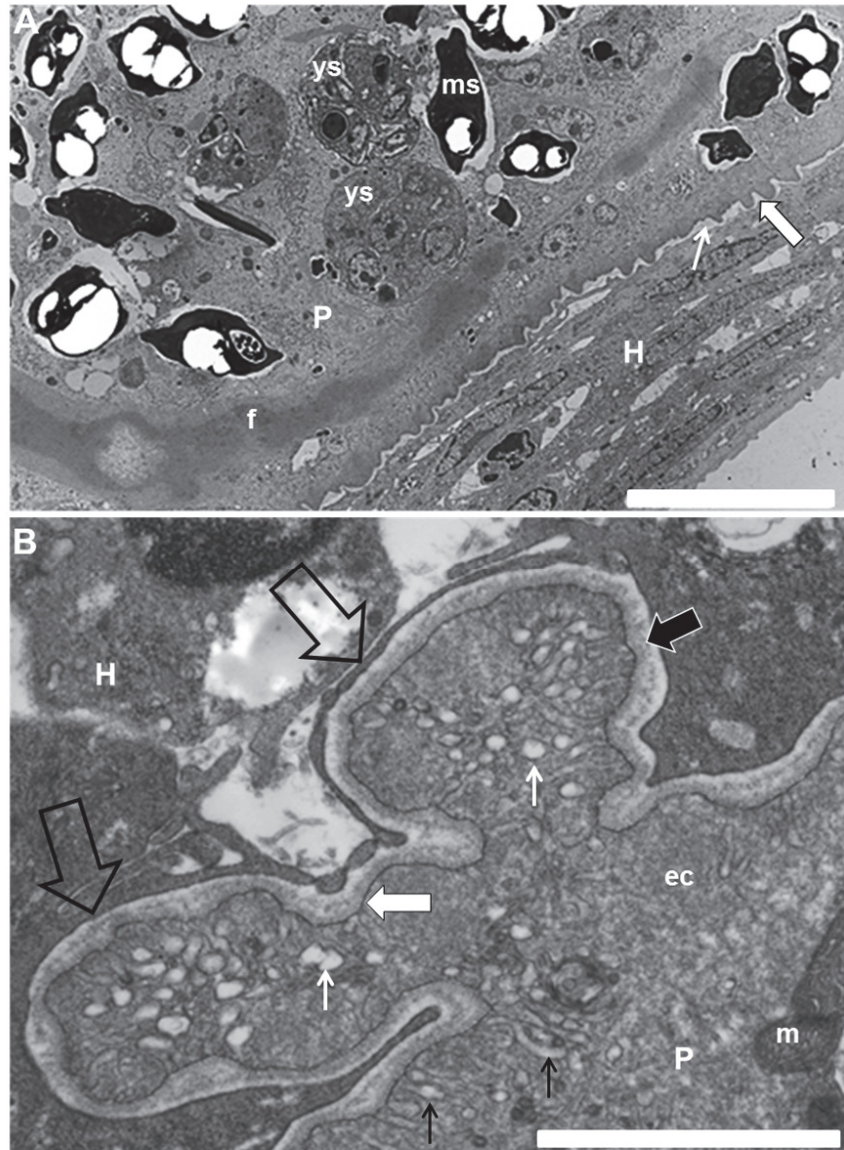


Fig. 4. *Pseudoplatystoma corruscans* infected by *Henneguya* sp. n. 1. Electron micrograph of gill filaments. (A) Host-parasite interface showing host tissue (H) separated from plasmodium by a layer of fine granular material (thin arrow) and delicate projections of the plasmodial wall (thick arrow). Note the presence of a layer of fibrous material (f) in the periphery of the plasmodium, young sporoblasts (ys), and mature spores (ms). Scale bar = 10 μm. (B) Amplified portion of the host-parasite interface showing the projection of plasmodial expansion (empty arrows) toward the host tissue (H) and a layer of granular material (thick black arrow) separating the plasmodial (P) from the host cells. Note the single plasmodial membrane (thick white arrow) with numerous pinocytotic channels (thin black arrows) toward the ectoplasm zone (ec) and ending in pinocytotic vesicles (thin white arrows). Scale bar = 2 μm

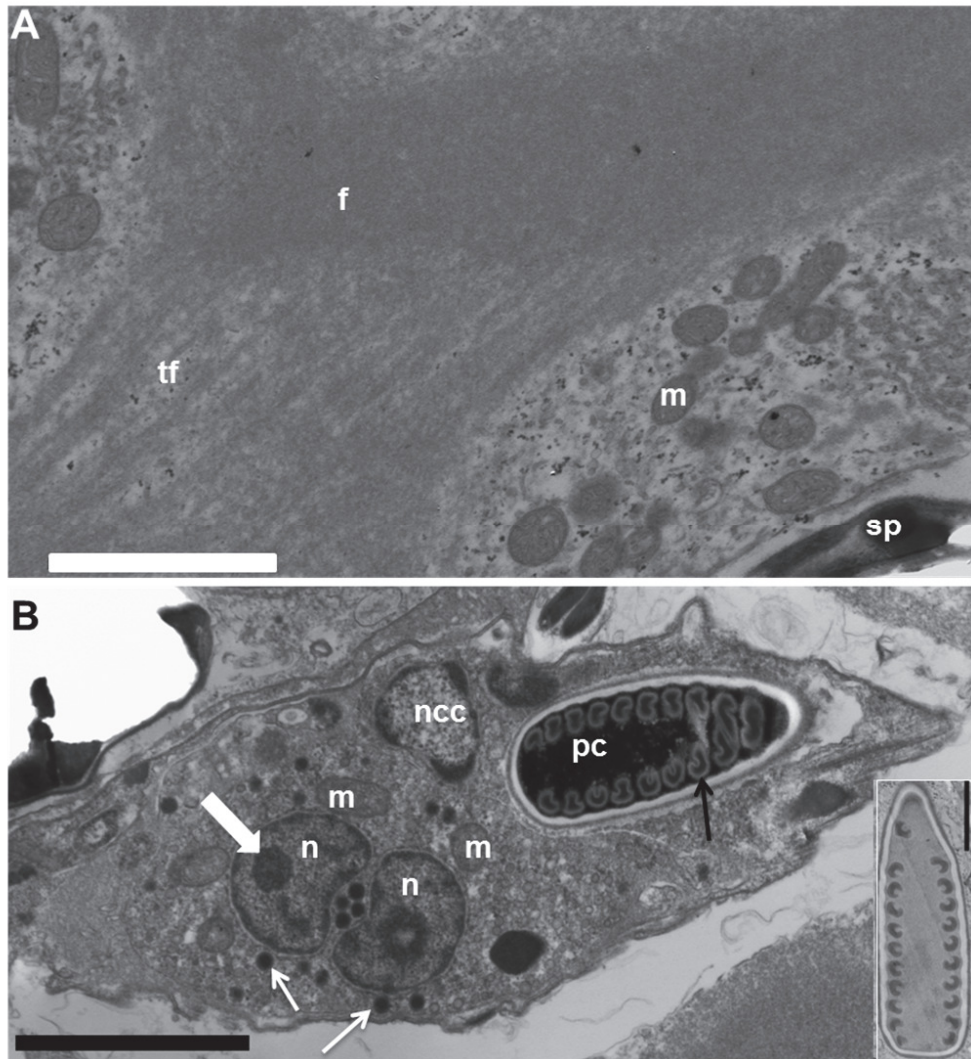


Fig. 5. *Henneguya* sp. n. 1 infecting *Pseudoplatystoma corruscans*. Electron micrograph of plasmodium of *Henneguya* sp. n. 1 parasitizing gill filaments of *P. corruscans*. (A) Details of layer of fibrous material (f) of the periphery of the plasmodia showing thin fibriles (tf), mitochondria (m), and part of a spore (sp). Scale bar = 5 µm. (B) Longitudinal section of a young spore showing sporoplasm binucleate (n) with nucleoli (thick white arrow), sporoplasmosomes (white arrows), and several mitochondria (m); polar capsule (pc) with polar filaments (black arrow) and nucleus of the capsulogenic cell (ncc). Scale bar = 2.5 µm. On the right is a longitudinal section of a whole polar capsule showing the number of turns of the polar filament. Scale bar = 1 µm

The phylogenetic tree illustrates the evolutionary relationships among various species of the genera *Ceratomyxa*, *Henneguya*, and *Myxobolus*. The tree is rooted at the bottom left and branches upwards. Bootstrap values are indicated at the nodes. The species are grouped into five main categories based on their fish hosts, as indicated by vertical bars on the right side of the tree:

- Bagridae:** Includes *Ceratomyxa seriola* AB530265 and *Ceratomyxa shasta* AF001579.
- Pimelodidae:** Includes *Henneguya mystusia* EU732603, *Henneguya basifilamentalis* EU732604, and several species of *Henneguya* and *Myxobolus*.
- Ictaluridae:** Includes *Henneguya gurlei* DQ673465, *Henneguya pellis* FJ468488, *Henneguya sutherlandi* EF191200, *Henneguya ictaluri* AF195510, and *Henneguya exilis* AF021881.
- Pangasidae:** Includes *Myxobolus pangasii* FJ816270 and *Myxobolus hackyi* FJ816260.
- Pimelodidae (continued):** Includes *Henneguya corruscans* KF296356, *Henneguya corruscans* JQ654971, *Henneguya multiplasmodialis* KF296354, *Henneguya multiplasmodialis* JQ654969, and *Henneguya sp. 1*.

A scale bar representing 0.3 substitutions per site is shown at the bottom center of the tree.

Table 1. *Henneguya* spp. Comparative data of *Henneguya* sp. n. 1 with other *Henneguya* species that are parasites of siluriform fishes. Spore dimensions, infection sites, and collection sites are given. LPC: length of polar capsules; WPC: width of polar capsules; NCF: number of coils of polar filaments; –: no data. All measurements are means  $\pm$  SD and/or range, in  $\mu\text{m}$ .

| Species                     | Total length                 | Spore length                   | Spore width                  | Thickness                     | LPC                           | WPC                          | Tail length                  | NCF   | Site of infection and host                                     | Locality  |
|-----------------------------|------------------------------|--------------------------------|------------------------------|-------------------------------|-------------------------------|------------------------------|------------------------------|-------|--|---|
| <i>Henneguya</i> sp. n. 1.  | 29.4 $\pm$ 1.9 $\mu\text{m}$ | 12.13 $\pm$ 0.69 $\mu\text{m}$ | 4.8 $\pm$ 0.29 $\mu\text{m}$ | 4.23 $\pm$ 0.15 $\mu\text{m}$ | 6.18 $\pm$ 0.28 $\mu\text{m}$ | 1.8 $\pm$ 0.12 $\mu\text{m}$ | 16.7 $\pm$ 1.9 $\mu\text{m}$ | 10-11 | Gill filaments of <i>P. corruscans</i>                         | São Francisco River, Brazil                                 |
| <i>H. multiplasmodialis</i> | 30.8 $\pm$ 1.3 $\mu\text{m}$ | 14.7 $\pm$ 0.5 $\mu\text{m}$   | 5.2 $\pm$ 0.3 $\mu\text{m}$  | 4.4 $\pm$ 0.1 $\mu\text{m}$   | 6.1 $\pm$ 0.1 $\mu\text{m}$   | 1.4 $\pm$ 0.1 $\mu\text{m}$  | 15.4 $\pm$ 1.3 $\mu\text{m}$ | 6-7   | Large cysts in the gills of <i>P. corruscans</i>               | Brazilian Pantanal wetland, Brazil                          |
| <i>H. multiplasmodialis</i> | 30.6 $\pm$ 1.2 $\mu\text{m}$ | 14.5 $\pm$ 0.4 $\mu\text{m}$   | 5.2 $\pm$ 0.2 $\mu\text{m}$  | 4.2 $\pm$ 0.3 $\mu\text{m}$   | 6.2 $\pm$ 0.2 $\mu\text{m}$   | 1.5 $\pm$ 0.2 $\mu\text{m}$  | 14.8 $\pm$ 1.4 $\mu\text{m}$ | 6-7   | Large cysts in the gills of <i>P. fasciatum</i>                | Brazilian Pantanal wetland, Brazil                          |
| <i>H. pseudoplatystoma</i>  | 33.2 $\pm$ 1.9               | 10.4 $\pm$ 0.6                 | 3.4 $\pm$ 0.4                | –                             | 3.3 $\pm$ 0.4                 | 1.0 $\pm$ 0.4                | 22.7 $\pm$ 1.7               | 6-7   | Gills of hybrid pintado  | Fish farms: São Paulo and Mato Grosso do Sul states, Brazil |
| <i>H. corruscans</i>        | 27.6 (25-29)                 | 14.3 (13-15)                   | 5.0                          | –                             | 6.8 (6-7)                     | 2.0                          | 13.7 (12-15)                 | 5-6   | Gills of <i>P. corruscans</i>                                  | Paraná River, Brazil  |
| <i>H. eirasi</i>            | 37.1 $\pm$ 1.8               | 12.9 $\pm$ 0.8                 | 3.4 $\pm$ 0.3                | 3.1 $\pm$ 0.1                 | 5.4 $\pm$ 0.5                 | 0.7 $\pm$ 0.1                | 24.6 $\pm$ 2.2               | 12–13 | Gill filaments of <i>P. corruscans</i> and <i>P. fasciatum</i> | Brazilian Pantanal wetland, Brazil                          |
| <i>H. maculosus</i>         | 31.2                         | 13.7 $\pm$ 0.6                 | 4.1 $\pm$ 0.2                | 3.0 $\pm$ 0.3                 | 5.6 $\pm$ 0.5                 | 1.6 $\pm$ 0.2                | 17.5 $\pm$ 0.5               |       | Gill filaments of <i>P. corruscans</i>                         | Brazilian Pantanal wetland, Brazil                          |
| <i>H. maculosus</i>         | 33.0                         | 13.3 $\pm$ 0.7                 | 4.4 $\pm$ 0.4                | 3.5 $\pm$ 0.4                 | 5.2 $\pm$ 0.6                 | 1.6 $\pm$ 0.2                | 19.7 $\pm$ 0.6               |       | Gill filaments of <i>P. reticulatum</i>                        | Brazilian Pantanal wetland, Brazil                          |
| <i>H. mystusia</i>          | 32.2 (27.0-40.0)             | 13.0 (12.0-15.0)               | 3.7 (3.0-4.0)                | 2.8 (2.5-3.0)                 | 5.04 (5.0-6.0)                | 1.2 (1.0-1.3)                | 19.3 (17.0-25.0)             | –     | Gills of <i>Mystus</i> sp.                                     | India   |
| <i>H. basifilamentalis</i>  |                              | 14.0 (13–15)                   | 6.9 (6–7.5)                  | 2.8 (4–5)                     | 6.5 (5–7)<br>5.0 (4–5.6)      | 2.8 (2–3)<br>2.6 (1.3–       | 26–38                        | 7     | Basal crypts of Hemibranchs of <i>Hemibagrus nemurus</i>       | Malaysia  |

2)

|                          |                         |                         |                   |                   |                   |                   |                      |       |   |       |
|--------------------------|-------------------------|-------------------------|-------------------|-------------------|-------------------|-------------------|----------------------|-------|---|-------|
| <i>H. gurlei</i>         | 60.9<br>(48.7–<br>68.5) | 18.2<br>(15.7–<br>20.3) | 5.4 (3.8–<br>6.1) | 3.2 (2.8–<br>3.5) | 5.9 (4.8–<br>7.1) | 1.2 (1.0–<br>1.5) | 41.1 (34.0–<br>49.9) | –     | Dorsal, pectoral, and anal<br>fins of <i>Ameiurus<br/>nebulosus</i>                               | USA   |
| <i>H. pellis</i>         | 100.4<br>(79–124)       | 13.0<br>(11.0–<br>14.5) | 5.0<br>(4.5–5.2)  | –                 | 6.9<br>(5.5–8.5)  | 1.8<br>(1.5–2.0)  | 87.8<br>(66–112)     | –     | Skin of <i>Ictalurus furcatus</i>   | USA   |
| <i>H. sutherlandi</i>    | 65.9<br>(48.2–90)       | 15.4<br>(12.2–<br>19.3) | 5.5 (4.5–<br>6.8) | –                 | 6.1<br>(4.0–7.9)  | 1.7 (1.0–<br>2.2) | 50.5 (34.8–<br>71.4) | 6     | Skin nodules of <i>Ictalurus<br/>punctatus</i>  | USA   |
| <i>H. ictaluri</i>       | –                       | 23.9<br>(20.8–<br>26.1) | 6.0<br>(4.5–6.4)  | –                 | 8.1<br>(7.6–9.6)  | 2.5<br>(2.0–3.2)  | 63<br>(48.1–80.2)    | –     | Gills of <i>Ictalurus<br/>punctatus</i>   | USA   |
| <i>H. adiposa</i>        | 55.6<br>(40.7–<br>65.8) | 17.1<br>(14.7–<br>20.5) | 4.1<br>(3.4–4.6)  | –                 | 7.2<br>(5.8–8.3)  | 1.3<br>(0.9–1.9)  | 38.0<br>(23.2–48.8)  | –     | Adipose of fin <i>Ictalurus<br/>punctatus</i>   | USA   |
| <i>H. suprabranchiae</i> | –                       | 13 (11–<br>14)          | 3 (2–5)           | –                 | 3 (2.5–<br>5)     | 1 (1.5–4)         | 29 (27–30)           | 10-11 | suprabranchial organ of<br><i>Clarias gariepinus</i>  | Egypt |
| <i>H. branchialis</i>    | (28–41)                 | 12.5-17.5               | 4.5-6.5           | –                 | 1.5-3             | –                 | 15.5-23.5            | –     | gills, intestine of <i>Clarias<br/>lazera</i>   | Egypt |
| <i>H. longicauda</i>     | 108.3<br>(91–127)       | 16.2<br>(14–17.5)       | 4.0<br>(3.4–4.5)  | –                 | 7.7<br>(7.0–8.5)  | 1.8<br>(1.5–2.0)  | 90.5<br>(75–110)     | –     | Gills of <i>Ictalurus<br/>punctatus</i>   | USA   |
| <i>H. nilótica</i>       | 35.02–45.<br>6          | 12.6–17.4               | –                 | –                 | 7.2–8.4           | 1.5–2.7           | 22–30                | –     | Secondary respiratory<br>organ of <i>Clarias<br/>gariepinus (lazera)</i>                          | Egypt |
| <i>H. exilis</i>         | (60–70)                 | (18–20)                 | (4–5)             | –                 | (8–9)             | (1.0–1.5)         | (15 – 41.5)          | –     | Gills of <i>Ictalurus<br/>punctatus</i> ,<br><i>Ameiurus melas</i> ,<br><i>Ameiurus nebulosus</i> | USA   |
| <i>H. postexilis</i>     | 52<br>(42–62)           | 15<br>(13.5–17)         | 3.4<br>(3.5–4.0)  | 3.0 (3.5–<br>4.0) | 6.6<br>(5.9–7.2)  | 1.5<br>(1.0–2.0)  | 37.0<br>(28–49)      | –     | Gills of <i>Ictalurus<br/>punctatus</i>   | USA   |



|                           |                  |                  |               |               |               |               |                |      |  |          |
|---------------------------|------------------|------------------|---------------|---------------|---------------|---------------|----------------|------|--|----------|
| <i>H. diversis</i>        | 49.5 (40–62)     | 14.8 (13.5–16.5) | 4.0 (3.2–5.0) | 3.9 (3.0–4.5) | 6.2 (6.0–7.5) | 1.5 (1.0–2.0) | 34.6 (25–47)   | –    | Base of barbels, pectoral fins and along isthmus, liver and kidney of <i>Ictalurus punctatus</i> | USA      |
| <i>H. ameiurensis</i>     | –                | 23.3             | 4.1           | 3.0           | 5.4           | 1.6           | (15–41.5)      | –    | Barbels of <i>Ameiurus nebulosus</i>   | USA      |
| <i>H. fusiformis</i>      | (59–61)          | (29–33)          | (5–7)         | –             | (5–6)         | (3–4)         | (28–31)        | –    | Gills of <i>Clarias angularis</i>  | Chad     |
| <i>H. laterocapsulata</i> | 32.7 (29.0–36.2) | 14.7 (13.8–16)   | 4.3 (3.7–5.3) | 3.8 (3.3–4.3) | 4.8 (4.1–5.3) | 2.6 (2.2–3.0) | 18 (15.2–20.2) | –    | Dermis of <i>Clarias lazera</i> , <i>H. bidorsalis</i> , hybrid                                  | Israel   |
| <i>H. clariae</i>         | (45–107)         | (17.5–28.5)      | (5.5–8.5)     | –             | (5–13.5)      | (2.5–3.5)     | –              | –    | Gills of <i>Clarias lazera</i>   | Nigeria  |
| <i>H. bopeleti</i>        | (41–48)          | (15–19)          | (5.5–7)       | –             | (7–9)         | (1.5–2.5)     | (22.5–32)      | 7-9  | Gills of <i>Chrysichthys nigrodigitatus</i>  | Cameroon |
| <i>H. chrysichthyi</i>    | (27–32)          | (13.5–16)        | (4.5–6.5)     | –             | (4–5.5)       | (1–2)         | (10-15)        | 9-11 | Gills of <i>Chrysichthys nigrodigitatus</i>  | Nigeria  |
| <i>H. assuite</i>         | 45.5             | 12.3             | 5.1           | –             | 6.0           | 1.54          | –              | 9    | Gills of <i>Clarias lazera</i>   | Egypt    |
| <i>H. camerounensis</i>   | (13.5–21.5)      | (9–11)           | (4–5.5)       | –             | (4.5–6.5)     | (1–2)         | –              | –    | Gills of <i>Synodontis batesi</i> , <i>Eutropius multitaeniatus</i>                              | Cameroon |

Table 2. *Henneguya* spp. pairwise genetic identity of the 18S rRNA gene of *Henneguya* sp. n. 1 and related *Henneguya* species that are parasites of fish of the genus *Pseudoplatystoma*. The area above the diagonal shows nucleotide differences in relation to the number of bases compared. The area below the diagonal shows % pairwise distance identity.

| Species  | 1    | 2       | 3       | 4        | 5        | 6        | 7        | 8        |
|--|------|---------|---------|----------|----------|----------|----------|----------|
| 1. <i>Henneguya</i> sp. n. 1                             | —    | 18/1030 | 22/1214 | 53/1215  | 50/1214  | 107/915  | 136/1222 | 156/1206 |
| 2. <i>H. multiplasmodialis</i> ( <i>P. reticulatum</i> ) | 1.7  | —       | 11/1316 | 82/1315  | 85/1315  | 184/1329 | 208/1340 | 213/1330 |
| 3. <i>H. multiplasmodialis</i> ( <i>P. corruscans</i> )  | 1.8  | 0.8     | —       | 109/1559 | 109/1562 | 187/1210 | 241/1592 | 268/1507 |
| 4. <i>H. corruscans</i> ( <i>P. corruscans</i> )         | 4.2  | 6.3     | 7.0     | —        | 44/1895  | 193/1206 | 259/1938 | 273/1504 |
| 5. <i>H. corruscans</i> ( <i>P. reticulatum</i> )        | 4.1  | 6.5     | 7.0     | 2.3      | —        | 202/1203 | 266/1924 | 269/1505 |
| 6. <i>H. eirasi</i> ( <i>P. corruscans</i> )             | 11.8 | 15.6    | 15.9    | 16.4     | 17.1     | —        | 111/1209 | 116/1209 |
| 7. <i>H. maculosus</i> ( <i>P. corruscans</i> )          | 11.3 | 15.9    | 15.5    | 13.7     | 14.1     | 9.2      | —        | 29/1496  |
| 8. <i>H. maculosus</i> ( <i>P. reticulatum</i> )         | 13.1 | 16.4    | 18      | 18.      | 18.1     | 9.7      | 1.9      | —        |

## Discussion

Six myxosporeans have been found to infect the gills of fish of the genus *Pseudoplatystoma*. *Henneguya pseudoplatystoma* was found infecting gill filaments of pintado hybrids from fish farms, causing stretching and deformation of these structures, leading to a reduction of the functional area of the epithelium (Naldoni et al. 2009). *H. eirasi* was found parasitizing gill filaments of *P. corruscans* and *P. reticulatum* from natural environments in the Brazilian Pantanal wetland, and produced only slight compression of the adjacent tissues (Naldoni et al. 2011). *H. corruscans* was described infecting the gill lamellae from *P. corruscans* from natural environments in the Paraná River and caused hypertrophy of the infected lamella (Eiras et al. 2009). *H. multiplasmodialis* was found forming large plasmodia on the surface of the gills of *P.*

*corruscans* and *P. reticulatum* from the Brazilian Pantanal wetland. The plasmodia of this species were arranged unusually, being externally enveloped by a stratified epithelium composed of several cell types, with a predominance of mucus and club cells. Internally, the plasmodia were composed of a network of septa formed by connective tissue, dividing the plasmodium into compartments, with inflammatory infiltrate in the tissue surrounding the plasmodium, as well as in the septa (Adriano et al. 2012). *H. maculosus* was found in the gill filaments and *M. flavus* in the gill arch (Carriero et al. 2013) of fish from the Brazilian Pantanal wetland, but histological analysis was not performed. In the species analyzed in the present study, histological analysis revealed the development of the plasmodia in the sub-epithelial connective tissue of the gill filaments, producing compression of the adjacent tissues, deformation of the gill filaments, and lamellar fusion, leading to the reduction of the functional epithelium area, similar to that observed for *H. pseudoplatystoma* (Naldoni et al. 2009). However, as observed for *H. corruscans*, *H. pseudoplatystoma*, and *H. eirasi*, inflammatory infiltrate was not found at the infection site for *Heneguya* sp. n.1

Ultrastructural analysis of the host-parasite interface of *Heneguya* sp. n. 1 showed a thin layer of fine granular material preventing contact between the plasmodium and the host tissue, while numerous pinocyte canals connected the outside of the plasmodia to the ectoplasm zone, demonstrating the intense nutritional activity of the plasmodium. The plasmodial wall of *Heneguya* sp. n. 1, which was comprised of a single membrane, also presented delicate projections towards the host tissue, seemingly seeking increased surface contact with the host tissue, a mechanism related to nutritional activity, as also observed by Naldoni et al. (2009) and El-Mansy & Bashtar (2002). The sporogenesis process of *Heneguya* sp. n. 1 was similar to those observed in other species of *Heneguya* (Matos et al. 2005, Ali et al. 2007, Abdel-Ghaffar et al. 2008, Azevedo et al. 2008, Naldoni et al. 2009, 2011, Barassa et al. 2012). However, the plasmodia of *Heneguya* sp. n. 1 presented a conspicuous layer of slightly electrondense fibrous material spreading throughout the periphery. This material is similar to that observed in the periphery of *H. pseudoplatystoma* and *H. eirasi* (Naldoni et al. 2009, 2011). According to Naldoni et al. (2009), this electron-

dense fibrous material corresponds to actin filaments and may play a role in the support of the plasmodium. Fibrous material resembling aggregated actin anchoring the mural cells of the presporogonic cells of the malacosporean *Tetracapsuloides bryosalmonae* was also reported by Morris & Adams (2007). The presence of microfilaments in the developmental stages of myxosporeans was also reported by Casal et al. (1997), who identified myosin filaments occupying the space of pericyte cells of *H. striolata* Casal, Matos et Azevedo, 1997.

The morphologic and morphometric characteristics of *Henneguya* sp. n. 1 were compared with those of all *Henneguya* spp. that parasitize siluriform fish (Eiras 2002, Rabie et al. 2009, Eiras & Adriano 2012). Spores of the species *H. multiplasmodialis*, *H. maculosus*, *H. corruscans*, *H. suprabranchiae* Landsberg, 1987, and *H. nilotica* Marwan, 1998 had a higher morphometric and morphologic resemblance to those of *Henneguya* sp. n. 1. Nevertheless, a small number of subtle morphologic differences were observed, such as spore body length (12.1  $\mu\text{m}$  for *Henneguya* sp. n. 1; 13.3 and 13.7  $\mu\text{m}$  for *H. maculosus*, 14.5 and 14.7  $\mu\text{m}$  for *H. multiplasmodialis*, and 14.3  $\mu\text{m}$  for *H. corruscans*) and the number of turns of the polar filaments (10 to 11 turns in *Henneguya* sp. n. 1, 6 to 7 turns in *H. multiplasmodialis* and *H. maculosus*, and 5 to 6 turns in *H. corruscans*). Differences may also be observed in the length of the polar capsules (6.2  $\mu\text{m}$  for *Henneguya* sp. n. 1 and 3  $\mu\text{m}$  for *H. suprabranchiae*) and in tail length (16.7  $\mu\text{m}$  for *Henneguya* sp. n. 1; 13.7  $\mu\text{m}$  for *H. corruscans*; 22 to 30  $\mu\text{m}$  for *H. nilotica*, and 29  $\mu\text{m}$  for *H. suprabranchiae*; detailed morphometric data are displayed in Table 1). Other important differences observed relate to the host, location of infection sites, and appearance of the plasmodia, which were small and in the gill lamellae in case of *H. corruscans* (Eiras et al. 2009) and large and on the gill surface in case of *H. multiplasmodialis* (Adriano et al. 2012), while the plasmodia of *Henneguya* sp. n. 1 were located in the internal areas of the gill filaments. *H. suprabranchiae* infects the hyaline cartilage of the supra branchial organ of *Clarias gariepinus* (El-Mansy & Bashtar 2002) and *H. nilotica* forms spherical plasmodia in the tips of the suprabranchial organ of *C. lazera* Valenciennes, 1840 (junior synonym of *C. gariepinus*) (Rabie et al. 2009).

Geography should also be considered. *Pseudoplatystoma corruscans* is known to inhabit rivers from the La Plata and São Francisco basins (Resende 2003). However, in phylogenetic studies of *Pseudoplatystoma* species, based on analysis of cytochrome *b* mtDNA sequences, Carvalho-Costa et al. (2011) showed the existence of geographically distinct clades for *P. corruscans*, with the samples from the São Francisco and La Plata Basins being clearly separated. According to those authors, *P. corruscans* haplotypes from the São Francisco Basin are on average 1.5% divergent from the populations from the La Plata Basin. The authors also pointed out that these genetic differences suggest a substantial period of evolutionary divergence and speculated that such divergence may be related to reproductive isolation, since these populations have been geographically separated for a considerable time. In this same way, geography may also contribute to the divergence of these parasites, as *Henneguya* sp. n. 1 infects *P. corruscans* from the São Francisco Basin, while *H. multiplasmodialis*, *H. maculosus*, and *H. corruscans* were described in *P. corruscans* and *P. reticulatum* taken from rivers from the La Plata Basin.

There is no exact value that defines at what point a difference in the 18S rDNA genes of a myxozoan species should be considered as intra- or interspecific variation (Gunter & Adlard 2009). However, according to Cech et al. (2012), identity values close to 100% undoubtedly indicate that the 2 species are identical, but a 98–99% sequence identity makes it difficult to decide whether a single or multiple species are being considered. The comparison of the 18S rDNA gene sequences from *Henneguya* sp. n. 1 with *H. multiplasmodialis* in *Pseudoplatystoma* spp. shows genetic divergence of 1.7–1.8% (Table 2). The small genetic divergence observed between *Henneguya* sp. n. 1 and *H. multiplasmodialis* is not robust enough to be defined as an interspecific variation and would not by itself be strong enough to separate these 2 *Henneguya* species. On the other hand, this genetic divergence, when added to other data such as site of parasite development, the histologic appearance of the plasmodia, differences in spore characteristics (smaller spore body length and higher number of polar filaments turns in *Henneguya* sp. n. 1), strongly support the separation of these species. Another important aspect to be considered here is the extended period of geographical isolation of the La Plata and São Francisco Basins,

which can play a decisive role in genetic divergence, as observed by Carvalho-Costa et al. (2011) in the *P. corruscans* populations from these 2 basins. Based on such morphologic, molecular, and geographic arguments, we believe that there is enough evidence to support the creation of new species.

The phylogenetic studies of the sequences of *Henneguya* and *Myxobolus* available in the GenBank database illustrate a general tendency to group according to the taxonomic affinities of the host fish (Ferguson et al. 2008, Naldoni et al. 2011, Adriano et al. 2012, Carriero et al. 2013). Thus, in the present study, phylogenetic analysis was performed only for *Henneguya/Myxobolus* species that are parasites of siluriform fish. The results showed that the grouping of *Henneguya/Myxobolus* exactly followed the family of host fish, corroborating the hypothesis of a notably close relationship between the evolution of *Henneguya/Myxobolus* parasites and their hosts.

#### **Literature cited**

- Abdel-Ghaffar F, Abdel-Baki AS, Bayoumy EM, Bashtar AR, Qurieshy SA, Morsey KS, Alghamdy A, Mehlhorn H (2008) Light and electron microscopic study on *Henneguya suprabranchiae* Landsberg, 1987 (Myxozoa: Myxosporea) infecting *Oreochromis niloticus*, a new host record. *Parasitol Res* 103: 609–617
- Adriano EA, Carriero MM, Maia AAM, Silva MRM, Naldoni J, Ceccarelli OS, Arana S (2012) Phylogenetic and host–parasite relationship analysis of *Henneguya multiplasmodialis* n. sp. infecting *Pseudoplatystoma* spp. in Brazilian Pantanal wetland. *Vet Parasitol* 185: 110–120
- Ali MA, Abdel-Baki AS, Sakran Th, Entzeroth R, Abdel- Ghaffar F (2007) *Myxobolus lubati* n. sp. (Myxosporea: Myxobolidae), a new parasite of haffara seabream *Rhabdosargus haffara* (Forsskal, 1775), Red Sea, Egypt: a light and transmission electron microscopy. *Parasitol Res* 100: 819–827
- Altschul SF, Madden TL, Schaffer AA, Zhang J, Zhang Z, Miller W, Lipman DJ (1997) Gapped BLAST and PSIBLAST: a new generation of protein database search programs. *Nucleic Acids Res* 25: 3389–3402

- Azevedo C, Casal G, Matos P, Matos E (2008) A new species of Myxozoa, *Henneguya rondoni* n. sp. (Myxozoa), from the peripheral nervous system of the Amazonian fish, *Gymnorhamphichthys rondoni* (Teleostei). J Eukaryot Microbiol 55: 229–234
- Barassa B, Adriano EA, Cordeiro NS, Ceccarelli PS (2012) Morphology and host–parasite interaction of *Henneguya azevedoi* n. sp., parasite of gills of *Leporinus obtusidens* from Mogi-Guaçu River, Brazil. Parasitol Res 110: 887–894
- Barta JR, Martin DS, Liberato PA, Dashkevich M, Anderson JW, Feighner SD, Elbrecht A, Perkins-Barrow A, Jenkins MC, Danforth HD, Ruff MD, Profous-Juchelka H (1997) Phylogenetic relationships among eight *Eimeria* species infecting domestic fowl inferred using complete small subunit ribosomal DNA sequences. J Parasitol 83: 262–271
- Campos JL (2005) O cultivo do pintado, *Pseudoplatystoma corruscans* (Spix & Agassiz 1829). In: Baldisserotto B, Gomes LC (eds) Espécies nativas para piscicultura no Brasil. UFSM, Santa Maria, p 327–343
- Carriero MM, Adriano EA, Silva MRM, Ceccarelli PS, Maia AAM (2013) Molecular phylogeny of the *Myxobolus* and *Henneguya* genera with several new South American species. PLoS ONE 8: e73713
- Carvalho-Costa LF, Piorski NM, Willis SC, Galetti PM Jr, Ortí G (2011) Molecular systematics of the neotropical shovelnose catfish genus *Pseudoplatystoma* Bleeker 1862 based on nuclear and mtDNA markers. Mol Phylogenet Evol 59: 177–194
- Casal G, Matos E, Azevedo C (1997) Some ultrastructural aspects of *Henneguya striolata* sp. nov. (Myxozoa, Myxosporea), a parasite of the Amazonian fish *Serrasalmus striolatus*. Parasitol Res 83: 93–95
- Cech G, Molnár K, Székely C (2012) Molecular genetic studies on morphologically indistinguishable *Myxobolus* spp. infecting cyprinid fishes, with the description of three new species, *M. alvarezae* sp. nov., *M. sitjae* sp. nov. and *M. eirasianus* sp. nov. Acta Parasitol 57: 354–366

- Diamant A, Whipps CM, Kent ML (2004) A new species of *Sphaeromyxa* (Myxosporea: Sphaeromyxina: Sphaeromyxidae) in devil firefish, *Pterois miles* (Scorpaenidae), from the northern Red Sea: morphology, ultrastructure, and phylogeny. *J Parasitol* 90: 1434–1442
- Eiras JC (2002) Synopsis of the species of the genus *Henneguya* Thelohan, 1892 (Myxozoa: Myxosporea: Myxobolidae). *Syst Parasitol* 52: 43–54
- Eiras JC, Adriano EA (2012) A checklist of new species of *Henneguya* Thelohán, 1892 (Myxozoa: Myxosporea, Myxobolidae) described between 2002 and 2012. *Syst Parasitol* 83: 95–104
- Eiras JC, Takemoto RM, Pavanelli GC (2009) *Henneguya corruscans* n. sp. (Myxozoa, Myxosporea, Myxobolidae), a parasite of *Pseudoplatystoma corruscans* (Osteich thyes, Pimelodidae) from the Parana River, Brazil: a morphological and morphometric study. *Vet Parasitol* 159: 154–158
- El-Mansy A, Bashtar AR (2002) Histopathological and ultrastructural studies of *Henneguya suprabranchiae* Landsberg 1987 (Myxosporea; Myxobolidae) parasitizing the suprabranchial organ of the freshwater catfish *Clarias gariepinus* Burchell 1822 in Egypt. *Parasitol Res* 88: 617–626
- Ferguson JA, Atkinson SD, Whipps CM, Kent ML (2008) Molecular and morphological analysis of *Myxobolus* spp. of salmonid fishes with the description of a new *Myxobolus* species. *J Parasitol* 94: 1322–1334
- Froese R, Pauly D (2011) FishBase. [www.fishbase.org](http://www.fishbase.org) (accessed on 5 March 2013) Griffin MJ, Pote LM, Wise DJ, Greenway TE, Mauel MJ, Camus AC (2008) A novel *Henneguya* species from channel catfish described by morphological, histological, and molecular characterization. *J Aquat Anim Health* 20: 127–135
- Guindon S, Dufayard JF, Lefort V, Anisimova M, Hordijk W, Gascuel O (2010) New algorithms and methods to estimate maximum-likelihood phylogenies: assessing the performance of PhyML 3.0. *Syst Biol* 59: 307–321



- Gunter NL, Adlard RD (2009) Seven new species of *Ceratomyxa* Thelohan, 1892 (Myxozoa) from the gall-bladders of serranid fishes from the Great Barrier Reef, Australia. *Syst Parasitol* 73: 1–11
- Hall TA (1999) BioEdit: A user-friendly biological sequence alignment editor and analysis program for Windows 95/98/NT. *Nucleic Acids Symp Ser* 41: 95–98
- Hallett SL, Diamant A (2001) Ultrastructure and small subunit ribosomal DNA sequence of *Henneguya lesteri* n. sp. (Myxosporea), a parasite of sand whiting *Sillago analis* (Sillaginidae) from the coast of Queensland, Australia. *Dis Aquat Org* 46: 197–212
- Mar & Terra (2013) Our production process: logistics and transportation. Available at [www.mareterra.com.br/site/2013/empresa.asp?lang=in](http://www.mareterra.com.br/site/2013/empresa.asp?lang=in) (accessed on 5 March 2013)
- Matos E, Tajdari J, Azevedo C (2005) Ultrastructural studies of *Henneguya rhamdia* n. sp. (Myxozoa) a parasite from the Amazon teleost fish, *Rhamdia quelen* (Pimelodidae). *J Eukaryot Microbiol* 52: 532–537
- Morris DJ, Adams A (2007) Sacculogenesis and sporogony of *Tetracapsuloides bryosalmonae* (Myxozoa: Malacosporea) within the bryozoan host *Fredericella sultana* (Bryozoa: Phylactolaemata). *Parasitol Res* 100: 983–992
- MPA (Ministério da Pesca e Aquicultura) (2012) Boletim estatístico da pesca e aquicultura. MPA, Brasília
- MPA (Ministério da Pesca e Aquicultura) (2012) Boletim estatístico da pesca e aquicultura. MPA, Brasília
- Naldoni J, Arana S, Maia AAM, Ceccarelli PS, Tavares LER, Borges FA, Pozo CF, Adriano EA (2009) *Henneguya pseudoplatystoma* n. sp. causing reduction in epithelial area of gills in the farmed pintado, a South American catfish: histopathology and ultrastructure. *Vet Parasitol* 166: 52–59
- Naldoni J, Arana S, Maia AAM, Silva MRM, Carriero MM, Ceccarelli PS, Tavares LER, Adriano EA (2011) Host–parasite–environment relationship, morphology and molecular

- analysis of *Henneguya eirasi* n. sp. parasite of two wild *Pseudoplatystoma* ssp. in Pantanal Wetland, Brazil. *Vet Parasitol* 177: 247–255
- Posada D (2008) JModelTest: phylogenetic model averaging. *Mol Biol Evol* 25: 1253–1256
- Rabie SA, Mohammed NI, Hussein AA, Hussein NM (2009) The infection of freshwater fishes with three species of *Henneguya* in Qena, Upper Egypt. *Egypt Acad J Biol Sci* 1: 11–19
- Rambaut A (2008) FigTree v1.1.1: Tree figure drawing tool. Available from: <http://tree.bio.ed.ac.uk/software/figtree/>
- Resende EK (2003) Migratory fishes of the Paraguay-Paraná Basin excluding the upper Paraná Basin. In: Carolsfeld J, Harvey B, Ross C, Baer A (eds) *Migratory fishes of South America: biology, fisheries and conservation status*. World Fisheries Trust, The World Bank, and International Development Research Center, Ottawa, p 99
- Resende EK (2003) Migratory fishes of the Paraguay-Paraná Basin excluding the upper Paraná Basin. In: Carolsfeld J, Harvey B, Ross C, Baer A (eds) *Migratory fishes of South America: biology, fisheries and conservation status*. World Fisheries Trust, The World Bank, and International Development Research Center, Ottawa, p 99

## Capítulo 2<sup>2</sup>

### Four new *Myxobolus* species parasites of characiforms fishes of the family Bryconidae: ultrastructure and phylogeny

**Abstract:** Four new myxosporeans species are described from South American freshwater fishes. The parasites were described infecting the bryconids *Salminus franciscanus* and *Brycon orthotaenia* from the São Francisco River, Minas Gerais state, Brasil. *Myxobolus* sp. n. 1 and *Myxobolus* sp. n. 2 were found infecting respectively fins and liver of *S. franciscanus* and *Myxobolus* sp. n. 3 and *Myxobolus* sp. n. 4 infecting respectively spleen and kidney of *B. orthotaenia*. Ultrastructural analysis of the four species revealed an asynchronous sporogenesis process, with germinative cells and young developmental stage spores in the periphery of the plasmodia. The walls of the plasmodia of the four *Myxobolus* species were formed by a single membrane. In *Myxobolus* sp. n. 1 a layer of fibroblasts was observed surrounding the plasmodium, in the others species was observed direct contact of the plasmodial wall with the host tissue. Phylogenetic analysis based on 18S rDNA genes and using only *Henneguya/Myxobolus* species parasites of fish from South American, shows the four new species grouping in a subclade together with others *Myxobolus* species parasites of the bryconids hosts.

**Key words:** Myxozoa · *Salminus franciscanus* · *Brycon orthotaenia* - São Francisco River · 18S rDNA · Ultrastructure.

---

<sup>2</sup> Formatação de acordo com as normas da revista Diseases of Aquatic Organisms.

## Introduction

The São Francisco River is the third largest river from Brazil and the 31th of the world, with 2900 km of extension (Welcomme 1985). The fish fauna of this river concerns about 160 fish species known (Sato & Godinho 1999).

*Salminus franciscanus* Lima & Britski 2007, and *Brycon orthotaenia* Günther 1864, are characiforms fishes of the Bryconidae family endemics to the San Francisco river basin and popularly known in Brazil as *dourado* and *matrinxã* respectively. *Salminus franciscanus* is a carnivorous fish, which can reach over 1.4 m in length (Sato et al. 2003), and is important in the fishing economy of the region, valued for its meat and by sports fisherman. *B. orthotaenia* is an omnivorous fish, which can reach over 30 cm in length (Froese & Pauly 2013). Like the other species of genus *Brycon*, *B. orthotaenia* has also large potential for fish farm, as well as is an important species for the regional fishing (Sato et al. 2003).

The expansion of the aquaculture industry in Brazil and around the world has increased the importance of studies of fish diseases, especially in those hosts that have the potential for production and sale (Luque 2004). Among the fish parasites, myxosporeans are between the most common (Feist & Longshaw 2006, Gómez et al. 2014). Approximately 2400 species have been described worldwide (Bartošová-Sojková 2014) and the genus *Myxobolus* is the most specious among myxosporeans and its members are important pathogens of fish in several geographical areas (Eiras et al. 2005, Lom & Dyková 2006). So far, 31 *Myxobolus* species has been described for Brazilian fishes, a very low number if compared with the large number of fresh water fish species found in country (Naldoni et al. 2011, Eiras et al. 2014).

Despite the wide distribution of fish species of the genus *Salminus* and *Brycon* in neotropical region (Froese & Pauly 2013), their economic importance in sports, extractive fishing and fish farming, few studies on the myxosporean infection and on parasite-host relationship has been performed (Adriano et al. 2009, Milanin et al. 2010, Azevedo et al. 2011, Carneiro et al. 2013, Moreira et al. 2014a, 2014b). Among myxosporean species

described in the genus *Salminus* and *Brycon*, some of them have been observed causing significant changes in their hosts, as *Myxobolus salminus* Adriano, Arana, Carriero, Naldoni, Ceccarelli et Maia, 2009, that cause edema and obstruction of the blood vessels of the gills of *Salminus brasiliensis* (Adriano et al. 2009). *Myxobolus brycon* Azevedo, Casal, Marques, Silva et Matos, 2011, was observed causing lamellar fusion and consequently less surface area for gas exchange in the gills of *Brycon hilarii* and *Myxobolus oliveirai* Milanin, Eiras, Arana, Maia, Alves, Silva, Carriero, Ceccarelli et Adriano, 2010, was also observed causing changes in the gill filament, with loss of functional surface of the distal end of the filament. The others species described in these genus are: *Myxobolus macroplasmoidal* Molnár, Ranzani-Paiva, Eiras et Rodrigues, 1998, in abdominal cavity of the *S. brasiliensis*; *Myxobolus paranensis* Bonetto & Pignalberi 1965, in testes and ovary of *S. brasiliensis*; *Myxobolus aureus* Carriero, Adriano, Silva, Ceccarelli et Maia, 2013, in liver of *S. brasiliensis*; *Henneguya rotunda* Moreira, Adriano, Silva, Ceccarelli et Maia, 2014, in gill arch and fins of *S. brasiliensis*; *Myxobolus pantanalis* Carriero, Adriano, Silva, Ceccarelli et Maia, 2013, in gill of *S. brasiliensis*; *Myxobolus umidus* Carriero, Adriano, Silva, Ceccarelli et Maia, 2013, infecting spleen of *B. hilarii*; and *Myxobolus piraputangae* Carriero, Adriano, Silva, Ceccarelli et Maia, 2013, infecting kidney of *B. hilarii*.

In fishes from São Francisco River, only two myxosporean species have been reported: *Henneguya* sp. found infecting *Myelus micans* (Brasil-Sato 2003) and *Myxobolus franciscoi* Eiras et al. 2010, found infecting *Prochilodus argenteus*.

The present study describes, based on morphology, 18S rDNA gene sequencing and ultrastructure, four new *Myxobolus* species parasitizing fishes of the family Bryconidae. Two species infecting *S. franciscanus* and two others in *B. orthotaenia* from the São Francisco River, Brazil.

## **Material and methods**

Forty-two specimens of *S. franciscanus* and thirty-nine specimens of *B. orthotaenia* were collected from the São Francisco River (17°12'8, 44°50'0 W) in the municipality of

Pirapora, state of Minas Gerais, Brazil. Samples were collected between July of the 2010 to November 2013.

After capture, the fish were immediately transported alive to nearby field laboratory, where they were euthanized by benzocaine overdose, measured and examined. Plasmodia with mature spores were examined in fresh mounts with a light microscope. Morphological characterization of the spores was based on mature spores obtained from three different specimens. Measurements were performed on 30 spores using a computer equipped with Axivision 4.1 image capture software coupled to an Axioplan 2 Zeiss Microscope. The dimensions of the spores are expressed as mean $\pm$ standard deviation (SD), in  $\mu$ m. Smears containing free spores were air-dried and stained with Giemsa solution and mounted in a low-viscosity mounting medium (Cytoseal<sup>TM</sup>) on permanent slides for deposit into museum.

For transmission electron microscopy, plasmodia were fixed in 2.5% glutaraldehyde in 0.1M sodium cacodylate buffer (pH 7.4) for 12 h, washed in a glucose-saline solution for 2 h and post-fixed in  $O_3O_4$ . All these processes were performed at 4°C. After dehydration using an acetone series, the material was embedded in EMbed 812 resin. Semithin sections were stained with toluidine blue solution and examined by light microscopy. Ultrathin sections, double stained with uranyl acetate and lead citrate were examined in an LEO 906 electron microscope at 60 kV.

For molecular study, plasmodia were removed from the host tissue and fixed in ethanol PA. The plasmodium content was collected in a 1.5-ml microcentrifuge tube and the DNA was extracted using the DNeasy<sup>®</sup> Blood & Tissue kit (Qiagen, USA), following manufacturer's instructions. The product was quantified in a NanoDrop 2000 spectrophotometer (Thermo Scientific) at 260 nm. The polymerase chain reaction (PCR) was carried out using a final volume of 25 $\mu$ l, which contained 10–50 ng of extracted DNA, 1 $\times$ Taq DNA polymerase buffer, 0.2mmol of dNTP, 1.5mmol of MgCl<sub>2</sub>, 0.2 pmol of each primer, 0.25 $\mu$ l (1.25 U) of Taq DNA polymerase (all reagents from Invitrogen By Life Technologies) and ultrapure (MilliQ) water in an Eppendorf AG 22331 Hamburg Thermocycler. Fragments of ~1000 bp were amplified using the primers ERIB1-ACT1R

(Barta et al. 1997) and fragments of ~1200 bp were amplified using the primers MYXGEN-ERIB10 (Hallett & Diamant 2001, Diamant et al. 2004). An initial denaturation step at 95°C for 5min was followed by 35 denaturation (95° C for 60 s) cycles, an annealing step (62° C for 60 s to species of *Myxobolus* infecting *S. franciscanus* and 58° C for 60 s to species of *Myxobolus* infecting *B. orthotaenia*) and an extension step (72° C for 120 s to species of *Myxobolus* infecting *S. franciscanus* and 72° C for 90 s to species of *Myxobolus* infecting *B. orthotaenia*), finishing with an extended elongation step at 72° C for 5min. PCR products were electrophoresed in 1.0% agarose gel (BioAmerica), stained with ethidium bromide and analyzed in a FLA-3000 (Fugi) scanner. The size of the amplicons was estimated by comparison with the 1 kb DNA Ladder (Invitrogen). Purified PCR products were sequenced using the same primer pair that was used in the amplification step, and another primer pair MC5-MC3 (Eszterbauer 2004) with the BigDye® Terminator v3.1 Cycle Sequencing Kit (Applied Biosystems™) in an ABI 3730 DNA sequencing analyzer (Applied Biosystems™). A standard nucleotide-nucleotide BLAST (blastn) search was conducted to verify the similarity of the sequence obtained in this study with other sequences available in the GenBank database (Altschul et al. 1997).

Phylogenetic analysis was performed using only sequences of myxosporeans parasites of South American fishes available from GenBank. This included 13 sequences of *Henneguya* species and 11 sequences of *Myxobolus* species, plus *Myxobolus* sp. n. 1, *Myxobolus* sp. n. 2, *Myxobolus* sp. n. 3 and *Myxobolus* sp. n. 4 sequences. *Ceratomyxa shasta* and *Ceratomyxa seriolae* were used as outgroup. Nucleotide sequences were aligned using ClustalW inserted in BioEdit version 7.0.9.0 (Hall 1999). The Jmodeltest 0.1 (Posada 2008) program was used to choose the best evolution model of the sequences, and selected the GTR+G model. Nucleotide frequencies were estimated from the data (A= 0.2470, C= 0.2076, G= 0.2908, T= 0.2546). The six rates of nucleotide substitution were (AC) = 0.8643, (AG) = 2.6062, (AT) = 1.4188, (CG) = 0.5639, (CT) = 4.1753, (GT) = 1.0000), gamma shape = 0.3850. These parameters were used for maximum likelihood (ML) testing, which was conducted using PhyML 3.0 (Guindon et al. 2003). Bootstrap analysis (100 replicates) was employed to assess the relative robustness of the tree branches. The

resulting tree was visualized with FigTree v1.3.1 (Rambaut 2008). Other alignment, including the species described in the present study and *Henneguya/Myxobolus* species parasites of South American characiforms fishes, was used to produce a pairwise similarity matrix using MEGA 5.0.

The methodology of the present study was approved by the ethics research committee of the Universidade Estadual de Campinas (proc. n° 2334-1), in accordance with Brazilian law (Federal Law N° 11.794, dated October 8<sup>th</sup> 2008 and Federal Decree N° 6899, dated July 15<sup>th</sup> 2009).

The  $\chi^2$  test, with the level of significance set at  $p < 0.05$ , was used to evaluate if there were differences among the prevalences between the different parasites species.

## Results

From a total of 42 specimens of *S. franciscanus* caught, 100% were infected by myxosporeans, 32 (76.2%) had plasmodia of an unknown *Myxobolus* species in the fins, 22 (52.3%) had plasmodia of another unknown *Myxobolus* species in the liver and 12 (28.6%) had plasmodia of both species. From a total of 39 specimens of *B. orthotaenia* caught, 31 (79.5%) were infected by myxosporeans. Twenty six (66.7%) had plasmodia of an unknown *Myxobolus* species in the spleen and 23 (60%) had plasmodia of another unknown *Myxobolus* species in the kidney. Fifteen specimens (38.5%) were infected by both species.

### *Myxobolus* sp. n. 1.

**Description:** white and spherical plasmodia measuring 0.5 to 1.5 mm in the fins of *S. franciscanus*.

Mature spores were round from the frontal view, with  $10.7 \pm 0.4 \mu\text{m}$  in length and  $8.1 \pm 0.5 \mu\text{m}$  in width (Table I). In lateral view, the spores were biconvex and had  $5.4 \pm 0.1 \mu\text{m}$  in thickness and the valves were symmetrical. The polar capsules were elongated and equal in size, and had  $4.7 \pm 0.3 \mu\text{m}$  in length and  $2.3 \pm 0.3 \mu\text{m}$  in width (Fig. 1A-B). The polar capsule occupied the half of the body of the spore (Fig. 1C). The polar filaments had 9 turns and arranged perpendicularly to the longitudinal axis of the polar capsule (Fig. 1 and 2).



Ultrastructure analysis showed plasmodia surrounded by a single layer of fibroblasts, which presented cellular projections that, in some points, established direct contact to the plasmodial membrane (Fig. 2 A - C). The plasmodial wall had a single membrane, and had few pinocytotic canals connecting the outside of the plasmodia to the ectoplasm zone. In the ectoplasm of the plasmodia, were observed few mitochondria (Fig. 2D). Below of the ectoplasm were seen generative cells and early stages of sporogenesis, while immature and mature spores were found more internally (Fig. 2A and E).

Molecular analysis, based on 18S rDNA genes of *Myxobolus* sp. n. 1, obtained from the fins of *S. franciscanus*, resulted in a 1591 bp sequence that did not match any myxosporean species sequences available in GenBank. Analysis of the genetic similarity of the myxosporean parasites of characiforms fishes showed that the closest species to *Myxobolus* sp. n. 1 was *M. macroplasmodialis*, with 1.3% of distance (Table II).

**Prevalence:** 32 specimens infected of 42 examined (76.2%).

**Site of infection:** fins.

**Host type:** *Salminus franciscanus* Lima & Britski, 2007: Characiformes: Bryconidae.

**Locality:** São Francisco River, municipality of Pirapora, state of Minas Gerais, Brazil.

**Remarks:** Among all the *Myxobolus* species parasites of bryconid fishes, three presented largest resemblance to *Myxobolus* sp. n. 1: *M. macroplasmodialis* resembles in respect to morphology and dimensions of the spores, but differs in the number of coils of the polar filaments (6 to *M. macroplasmodialis* and 9 to *Myxobolus* sp. n. 1), site of infection (abdominal cavity to *M. macroplasmodialis* and fins to *Myxobolus* sp. n. 1) and host (*M. macroplasmodialis* reported to *S. brasiliensis* and *Myxobolus* sp. n. 1 reported to *S. franciscanus*). *Myxobolus salminus* was similar in respect to length and thickness of the spores and length of the polar capsules, but differs in spore shape (oval to *M. salminus* and round to *Myxobolus* sp. n. 1), spore width ( $6.1 \pm 0.4$  to *M. salminus* and  $8.1 \pm 0.5$  to *Myxobolus* sp. n. 1), width of the polar capsules (to  $1.7 \pm 0.1$  *M. salminus* and  $2.3 \pm 0.3$  to *Myxobolus* sp. n. 1), number of coils of the polar filaments (to 7-8 to *M. salminus* and 9 to

*Myxobolus* sp. n. 1), site of infection (gill to *M. salminus* and fins to *Myxobolus* sp. n. 1) and host species (*S. brasiliensis* harbored *M. salminus* and *S. franciscanus* *Myxobolus* sp. n. 1). *M. aureus* was similar to spore width, thickness of the body, width polar capsule and site of infection, but differs in spore shape (oval to *M. aureus* and round to *Myxobolus* sp. n. 1), spore length ( $12.6 \pm 0.5$  to *M. aureus* and  $10.7 \pm 0.4$  to *Myxobolus* sp. n. 1), length of the polar capsule ( $5.7 \pm 0.3$  to *M. aureus* and  $4.7 \pm 0.3$  to *Myxobolus* sp. n. 1), number of coils of the polar filaments (to 7-8 *M. aureus* and 9 to *Myxobolus* sp. n. 1) and host species (*S. brasiliensis* to *M. aureus* and *S. franciscanus* to *Myxobolus* sp. n. 1). The geographic distribution was different in all species compared above (La Plata basin to *M. salminus*, *M. macroplasmodialis* and *M. aureus* and São Francisco basin to *Myxobolus* sp. n. 1).

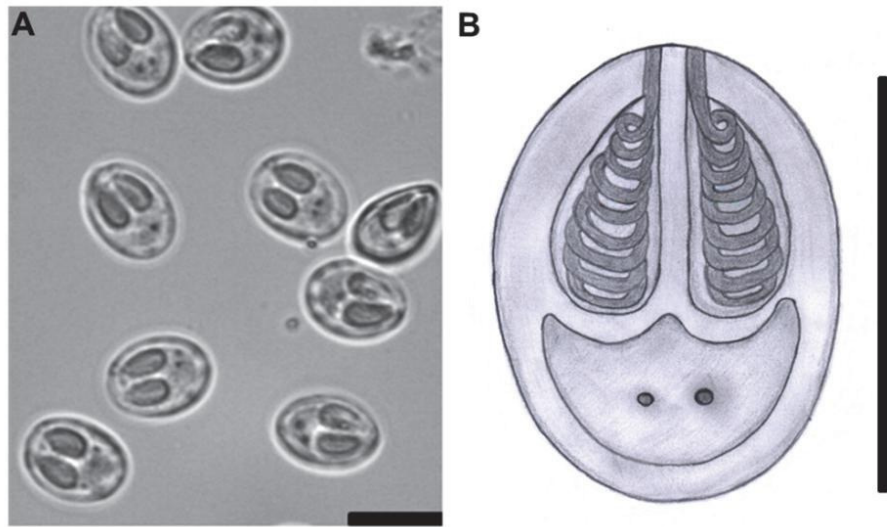


Fig. 1. *Myxobolus* sp. n. 1 parasite of fins of *Salminus franciscanus*. A: photomicrograph of mature spores in frontal view. Scale bar = 10  $\mu$ m. B: schematic representation of mature spore. Scale bar = 10  $\mu$ m

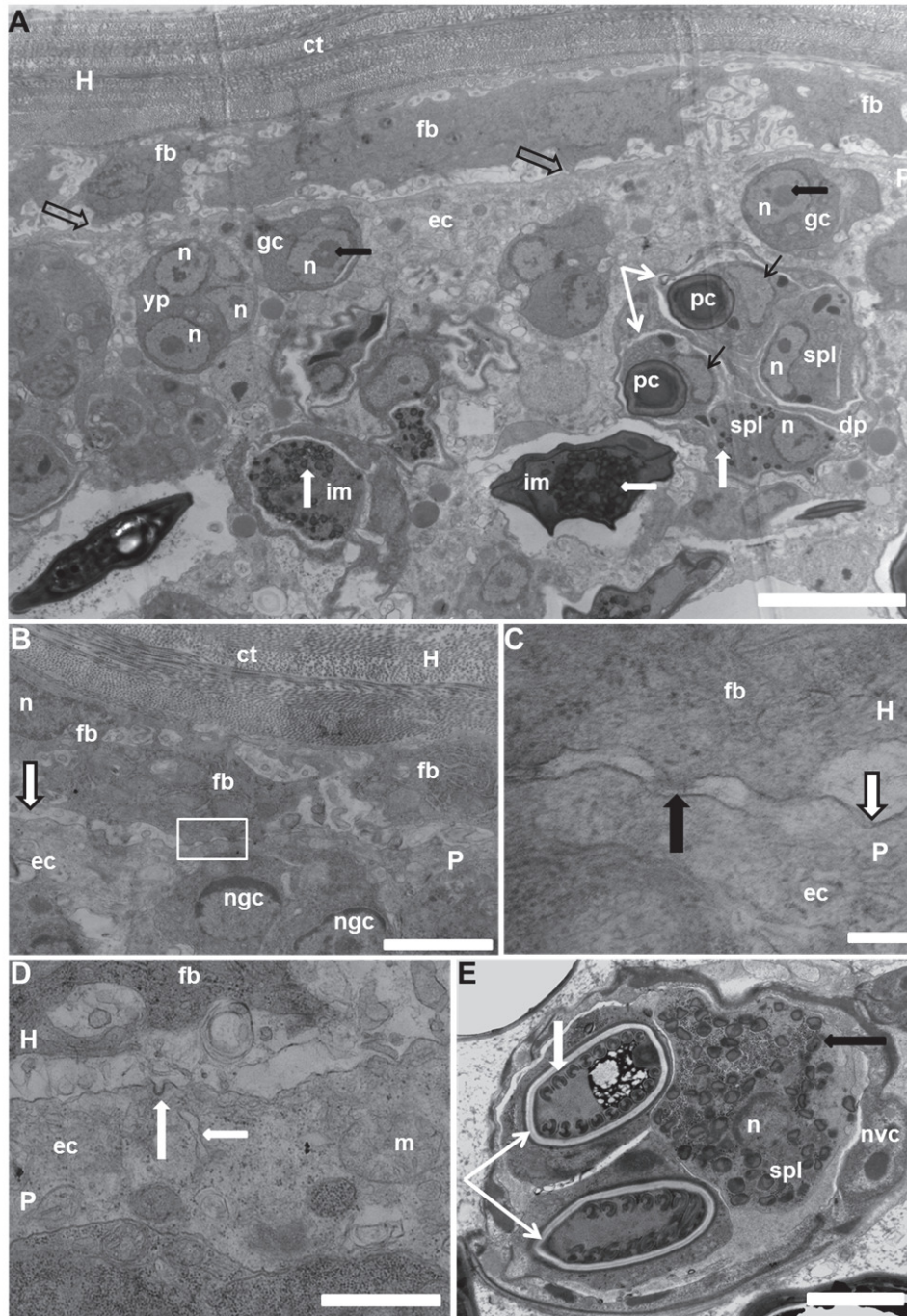


Fig. 2. Electron micrograph of fin of *Salminus franciscanus* infected by *Myxobolus* sp. n. 1. A: host-parasite interface showing a layer single of fibroblasts (fb) surrounding the

plasmodium (P). Note cellular projections of fibroblasts with direct contact to the plasmodial membrane in some points (empty arrows). Inside of the plasmodium observe a thin ectoplasm (ec), generative cells (gc) with its nucleus (n) and nucleoli (black arrow), young pansporoblast (yp) and nuclei (n), disporic pansporoblast (dp) containing immature spores (thin white arrow) with their polar capsules (cp), nuclei of capsulogenic cells (thin black arrows), sporoplasms (spl) with their nuclei (n) and sporoplasmosomes (thick white arrow), and immature spores (im). H: host; ct: connective tissue of fin. Scale bar = 5  $\mu$ m. B: Amplified portion of the host-parasite interface showing connective tissue of the fin (ct), layer of fibroblasts (fb) and their nuclei (n), plasmodial wall (white arrow), ectoplasm (ec) of the plasmodium (P) and nuclei of generative cells (ngc). Scale bar: 2  $\mu$ m. C: insert of B showing area of contact (black arrow) of the fibroblasts (fb) with the single membrane (white arrow) of plasmodia (P). Scale bar: 200 nm. D: Details of the portion of the host-parasite interface showing the plasmodial wall with pinocytic channels (white arrows) in ectoplasm (ec). Note the presence of the mitochondria (m). P: plasmodium; H: host. Scale bar: 1  $\mu$ m. E: Spore in advanced developmental stage showing polar capsule (thin white arrow) with their polar filaments in horseshoe-shaped (white arrow), sporoplasm (spl) showing a nucleus (n) and numerous sporoplasmosomes (black arrows). Note the nucleus of the valvogenic cell (nvc). Scale bar: 2  $\mu$ m.

### ***Myxobolus* sp. n. 2**

**Description:** white and spherical plasmodia measuring around 1.0 mm in the liver of *S. franciscanus*.

Mature spores oval in frontal view, with  $7.6 \pm 0.4 \mu\text{m}$  in length and  $4.8 \pm 0.5 \mu\text{m}$  in width (Table I). In lateral view, spores were biconvex and the valves symmetrical. The polar capsules were elongated and equal in size, with  $3.9 \pm 0.4 \mu\text{m}$  in length and  $1.6 \pm 0.1 \mu\text{m}$  in width. The polar capsule occupied slightly more than half of the body of the spore (Fig. 3A-B). The polar filaments had 9 turns and arranged perpendicularly to the longitudinal axis of the polar capsule (Fig. 4 D).

Ultrastructure analysis show the plasmodial wall formed by a single membrane and had pinocytotic canals connecting the outside of the plasmodia to the ectoplasm zone. The plasmodial wall established direct contact with the host tissue. In the ectoplasm, were observed mitochondrias and vesicles (Fig. 4 B). Below of the ectoplasm were seen generative cells, early stages of sporogenesis and advanced spore developmental stages. Mature spores were more prevalent internally (Fig. 4 A-C).

Molecular analysis, based on 18S rDNA genes from the spores of *Myxobolus* sp. 2 obtained from the liver of *S. franciscanus*, resulted in a 1580 bp sequence that did not match any myxosporean species sequences available in GenBank. Analysis of the genetic similarity of the myxosporean species that parasitize of the Characiform fishes showed that the closest species to *Myxobolus* sp. 2 was *M. aureus* with 2.0% of distance (Table II).

**Prevalence:** 22 specimens infected of 42 examined (52.3%).

**Site of infection:** liver.

**Host type:** *Salminus franciscanus* Lima & Britski, 2007: Characiformes: Bryconidae.

**Locality:** São Francisco River, municipality of Pirapora, state of Minas Gerais, Brazil.

**Remarks:** *Myxobolus* sp. n. 2 showed similarity with *Myxobolus brycon* concerning morphology and dimensions of the spores, differing with respect to the site of infection (gill to *M. brycon* and liver to *Myxobolus* sp. n. 2) and host (*Brycon hilarii* to *M. brycon* and *S. franciscanus* to *Myxobolus* sp. n. 2). *Myxobolus aureus* was similar in shape spore and site of infection, but differs in spore length ( $12.6 \pm 0.5$  to *M. aureus* and  $7.6 \pm 0.4$  to *Myxobolus* sp. n. 2), spore width ( $8.3 \pm 0.3$  to *M. aureus* and  $4.8 \pm 0.5$  to *Myxobolus* sp. n. 2) length of the polar capsule ( $5.7 \pm 0.3$  to *M. aureus* and  $3.9 \pm 0.4$  to *Myxobolus* sp. n. 2), width of the polar capsule ( $2.9 \pm 0.2$  to *M. aureus* and  $1.6 \pm 0.1$  to *Myxobolus* sp. n. 2) number of coils of the polar filaments (to 7-8 *M. aureus* and 9 to *Myxobolus* sp. n. 2) and other host species (*S. brasiliensis* to *M. aureus* and *S. franciscanus* to *Myxobolus* sp. n. 2). *Myxobolus salminus* was similar in spore shape and width of the polar capsules but differs in spore length ( $10.1 \pm 0.4$  to *M. salminus* and  $7.6 \pm 0.4$  to *Myxobolus* sp. n. 2), spore width ( $6.1 \pm 0.4$  to *M. salminus* and  $4.8 \pm 0.5$  to *Myxobolus* sp. n. 2), length of the polar capsule ( $4.6 \pm 0.2$  to *M. salminus* and  $3.9 \pm 0.4$  to *Myxobolus* sp. n. 2), number of coils of the polar filaments (to 7-8 to *M. salminus* and 9 to *Myxobolus* sp. n. 2), site of infection (gill to *M. salminus* and liver to *Myxobolus* sp. n. 2) and other host (*S. brasiliensis* to *M. salminus* and *S. franciscanus* to *Myxobolus* sp. n. 2). The geographic distribution was different in all species compared above (La Plata basin to *M. brycon*, *M. aureus* and *M. salminus* and São Francisco basin to

*Myxobolus* sp. n. 2). *M. franciscoi* was similar to width of the polar capsules and to the locality, but showed distinct morphology, too morphometry and host. The others *Myxobolus* species from South American were more distinct.

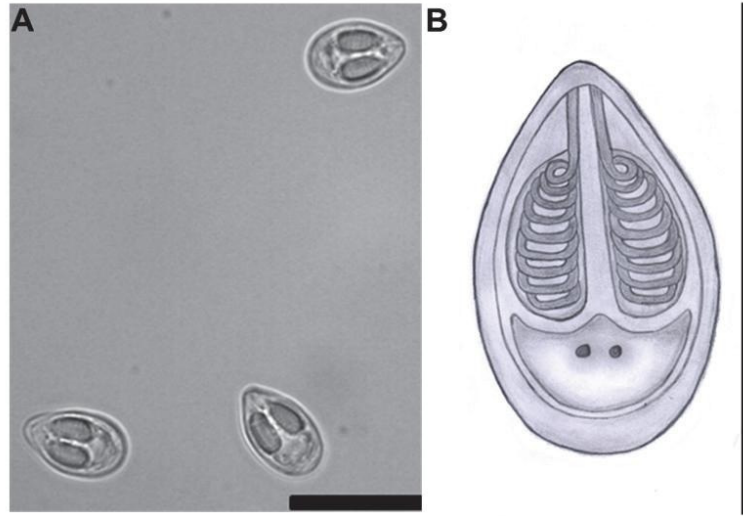


Fig. 3. *Myxobolus* sp. n. 2 parasites of liver of *Salminus franciscanus*. A: photomicrograph of mature spores in frontal view. Scale bar = 10  $\mu$ m. B: schematic representation of mature spore. Scale bar = 10  $\mu$ m



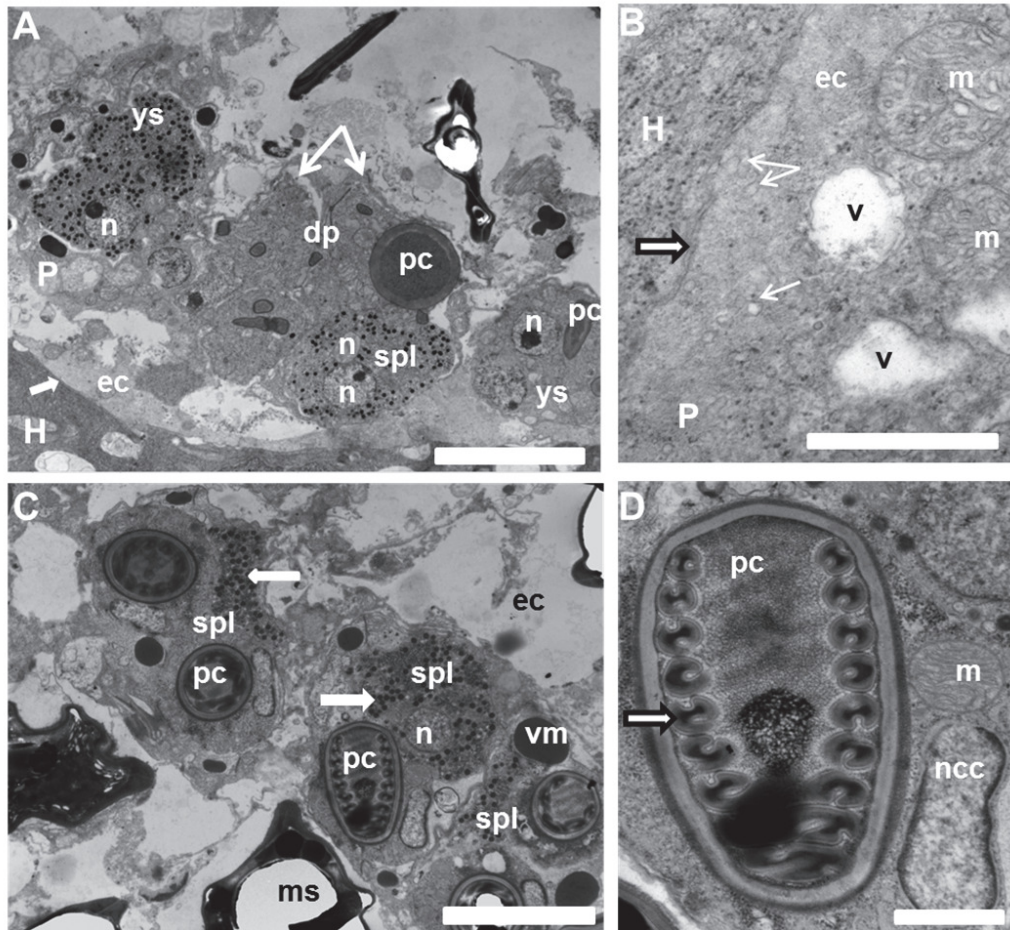


Fig. 4. Electron micrograph of liver of *Salminus franciscanus* infected by *Myxobolus* sp. n. 2. A: host–parasite interface showing the tissue host (H) in direct contact (white arrow) with the plasmodium (P). Note the thin ectoplasm (ec), disporic pansporoblast (dp), containing young spores (thin white arrows), showing polar capsule (cp) and sporoplasm (spl) with their two nuclei (n). Young spores (ys). Scale bar = 5  $\mu$ m. B: Amplified portion of the host-parasite interface showing the plasmodial wall composed by a single membrane (thick white arrow) in direct contact with membrane of the host cells (H), ectoplasm (ec) of the plasmodium (P) with pinocytic channels (thin white arrow) and mitochondria (m). Note several vesicles (v). Scale bar: 1  $\mu$ m. C: Immature spores showing polar capsule (pc), sporoplasm (spl) with numerous small sporoplasmosomes (white arrow) and valve-forming material (vm). Note almost mature spores (ms). Scale bar: 5  $\mu$ m. D: Details of a polar capsule (pc) with its polar filament (arrow). Note nucleus of capsulogenic cells (ncc) and a mitochondria (m). Scale bar: 1  $\mu$ m.



### ***Myxobolus* sp. n. 3**

**Description:** white and spherical plasmodia measuring around 1.0 mm in the spleen of *B. orthotaenia*.

Mature spores rounded from the frontal view, measuring  $12.0 \pm 0.8$   $\mu\text{m}$  in length and  $8.3 \pm 0.6$   $\mu\text{m}$  in width (Table 1). In lateral view, the spores were biconvex and had  $7.0 \pm 0.8$   $\mu\text{m}$  in thickness and the valves were symmetrical. The polar capsule occupied the half of the body of the spore (Fig. 5 A-B). The polar capsules were elongated and equal in size, measuring  $4.6 \pm 0.3$   $\mu\text{m}$  of length and  $2.8 \pm 0.3$   $\mu\text{m}$  of width and occupied the half of the spore body. The polar filaments had 6 turns and were arranged perpendicularly to the longitudinal axis of the polar capsule (Figs. 5 A, 6 C).

Ultrastructure analysis revealed that the plasmodial wall was formed by a single membrane and established direct contact with the host tissue. This membrane had few and calibrous pinocytic channels connecting and delicate projections toward the ectoplasm zone (Fig. 6 A and B). In the ectoplasm were observed few mitochondrias and generative cells and early stages of sporogenesis were seen in the subsequent layer of the plasmodium (Figs. 6 A and C).

Molecular analysis, based on 18S rDNA genes from the spores of *Myxobolus* sp. n. 3 resulted in a sequence with 1886 bp, which did not match any myxosporean species sequences available in GenBank. Analysis of the genetic similarity of the myxosporean species that parasitize of the Characiform fishes showed that the closest species to *Myxobolus* sp. n. 3 was *M. umidus* with 1.5% of distance (Table II).

**Prevalence:** 26 specimens infected of 39 examined (66.7%).

**Site of infection:** spleen.

**Host type:** *Brycon orthotaenia* Günther, 1864 : Characiformes: Bryconidae.

**Locality:** São Francisco River, municipality of Pirapora, state of Minas Gerais, Brazil.

**Remarks:** *Myxobolus* sp. n. 3 showed similarity with *M. aureus* concerning dimensions of the spores, showing differences however, with respect to number of coils of

the polar filaments (7-8 to *M. aureus* and 6 to *Myxobolus* sp. n. 3), site of infection (liver to *M. aureus* and spleen to *Myxobolus* sp. n. 3), host (*S. brasiliensis* to *M. aureus* and *B. orthotaenia* to *Myxobolus* sp. n. 3) and morphology (*M. aureus* has the front end more attuned and *Myxobolus* sp. n. 3 has the front end more rounded). *Myxobolus umidus* was similar relative to morphology, site of infection and genus of the host, but differs in spore length ( $13.5 \pm 0.7$  to *M. umidus* and  $12.0 \pm 0.8$  to *Myxobolus* sp. n. 3) and number of coils of the polar filaments (to 4-5 *M. umidus* and 6 to *Myxobolus* sp. n. 3). *M. paranensis* was similar to spore length, spore width and width of the polar capsules, but differs in spore length of the polar capsules (6-7 to *M. paranensis* and  $4.6 \pm 0.3$  to *Myxobolus* sp. n. 3), in other host species (*Salminus brasiliensis* to *M. paranensis* and *B. orthotania* to *Myxobolus* sp. n. 3) and site of infection (ovary and testis to *M. paranensis* and spleen to *Myxobolus* sp. n. 3). The geographic distribution was different in all species compared above (La Plata basin to *M. aureus*; Pantanal wetland to *M. umidus*; Argentina to *M. paranensis* and São Francisco basin to *Myxobolus* sp. n. 3).

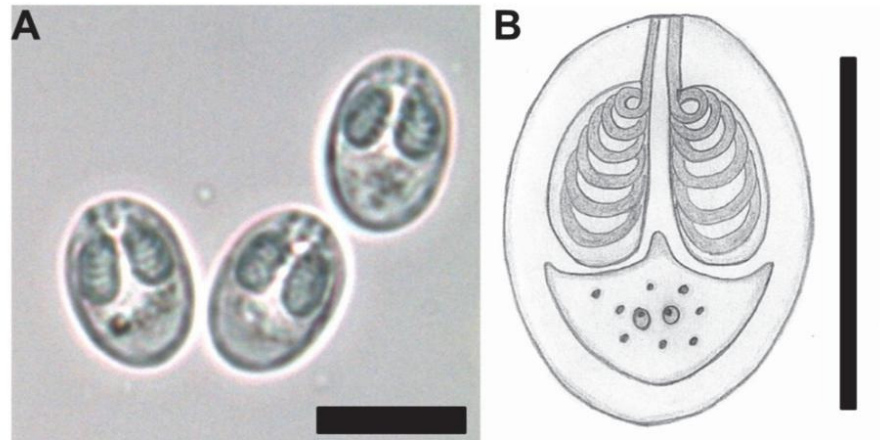


Fig. 5. *Myxobolus* sp. n. 3 parasite of spleen of *Brycon orthotaenia*. A: photomicrograph of mature fresh spores in frontal view. Scale bar = 10  $\mu$ m. B: schematic representation of mature spore. Scale bar = 10  $\mu$ m

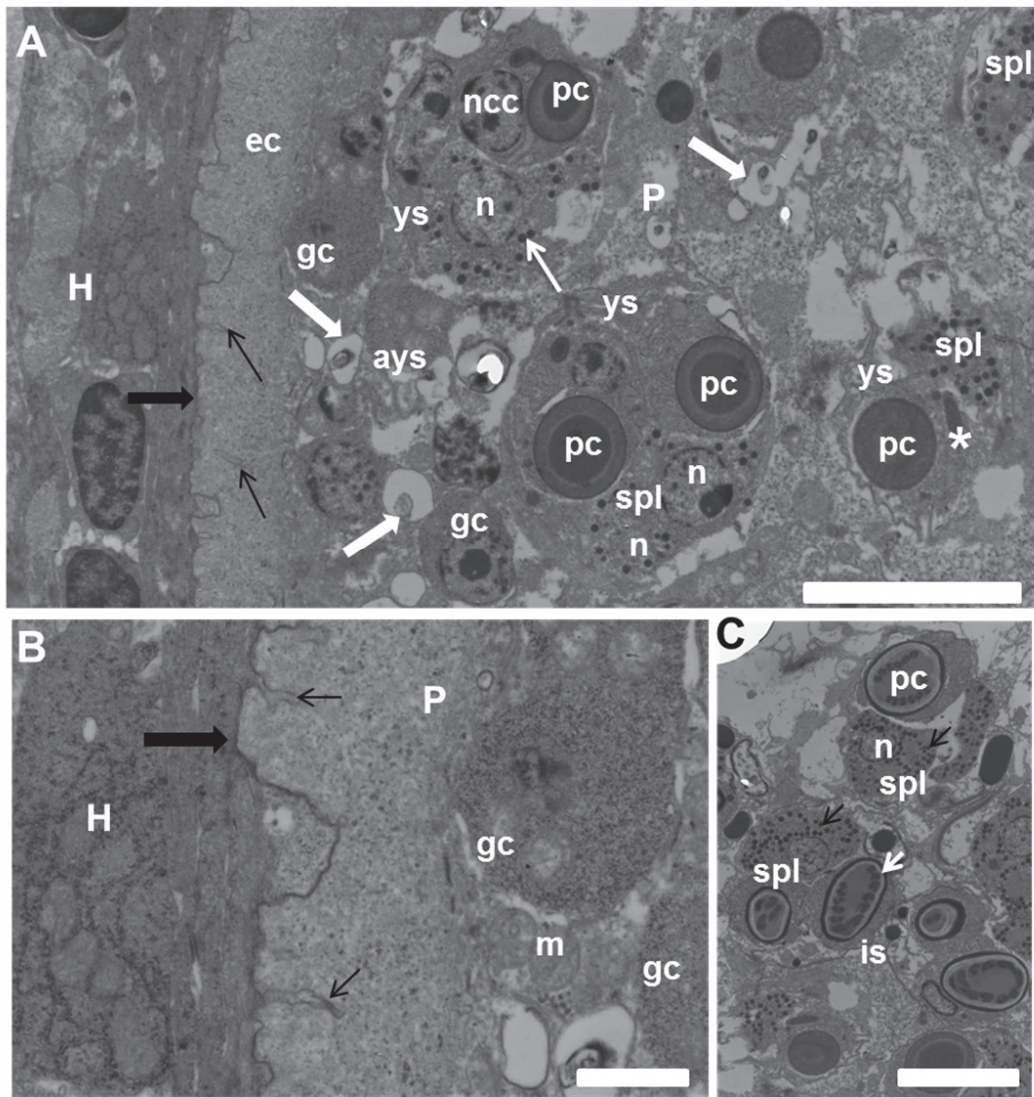


Fig. 6. Electron micrograph of spleen of *Brycon orhtotaenia* from São Francisco River infected by *Myxobolus* sp. n. 3. A: showing the host–parasite interface with plasmodial wall in direct contact (thick black arrow) with the tissue host (H) and pinocytic channels (black thin arrow) in the ectoplasm (ec). Note in innermost layer of the plasmodium (P) the presence of generative cells (gc), young spores (ys) with their polar capsules (pc) still without internalized polar filaments (asterisk), sporoplasms (spl) with two nuclei (n) and numerous sporoplasmosomes (white thin arrows). Observe also the presence of abnormal young spores (ays) with vacuoles containing electron dense structures (white thick arrow). Ncc: nucleus of capsulogenic cells. Scale bar: 5  $\mu$ m. B: Amplified portion of A showing details of the plasmodial wall constituted by a single membrane (black thick arrow) and

with few pinocytic channels (black thin arrows). Inside of the plasmodium (P) note the presence of generative cells (gc) and mitochondria (m). Scale bar: 1  $\mu$ m. C: Sporogenesis process showing various immature spores (is) with their polar capsules (pc) containing polar filaments already internalized (white arrow), spororoplasm (spl) with numerous sporoplasmosomes (black arrow). Scale bar: 5  $\mu$ m.

#### ***Myxobolus* sp. n. 4**

**Description:** white and spherical plasmodia measuring around 1.0 mm in the kidney of *B. orthotaeni*.

Mature spores round in frontal view, measuring,  $10.5 \pm 0.5$   $\mu$ m of length and  $9.2 \pm 0.7$   $\mu$ m of width (Table I). In lateral view, the spores were biconvex and the valves were symmetrical. The polar capsules were elongated and equal in size, measuring  $4.9 \pm 0.4$   $\mu$ m of length and  $2.9 \pm 0.2$   $\mu$ m of width. The polar capsule occupied more than half of the spore body (Fig. 7 A-B). The polar filaments had 7 turns and arranged perpendicularly to the longitudinal axis of the polar capsule (Fig. 8 D).

Ultrastructure analysis shows plasmodial wall composed by a single membrane, which established direct contact with the host tissue and had pinocytic channels connecting the outside of the plasmodium to the ectoplasm zone (Fig. 8 A and B). The ectoplasms were wide and markedly well delimited, containing vesicles (Fig. 8 A). Below ectoplasm area were observed mitochondrias, generative cells, early stages of sporogenesis and spore in advanced developmental stages (Figs 8 A, C).

Molecular analysis, based on 18S rDNA genes from the spores of *Myxobolus* sp. n. 4 obtained from the gills of *B. orthotaenia*, resulted in 1846 bp sequence that did not match any myxosporean species sequences available in GenBank. Analysis of the genetic similarity of the myxosporean species that parasitize of the Characiform fishes showed that the closest species to *Myxobolus* sp. n. 4 were *Myxobolus* sp. 3 with 1.5% of distance and *M. umidus* with 1.9% of distance (Table II).

**Prevalence:** 23 specimens infected of 39 examined (60%).

**Site of infection:** kidney.

**Host type:** *Brycon orthotaenia* Günther, 1864: Characiformes: Bryconidae.

**Locality:** São Francisco River, municipality of Pirapora, state of Minas Gerais, Brazil.

**Remarks:** Compared with others *Myxobolus* species parasites of South American fish, *M. piraputangae* showed similar morphology, spore length, spore width, length of the polar capsules, width of the polar capsules, site of infection and genus of the host, but differ in number of coils of the polar filaments (4-5 to *M. piraputangae* and 7 to *Myxobolus* sp. n. 4) and geographic distribution (Pantanal wetland to *M. piraputangae* and São Francisco basin to *Myxobolus* sp. n. 4). *Myxobolus* sp. n. 2 was similar in morphology, spore length, spore width, length of the polar capsules, width of the polar capsules, and geographic distribution, but differ in number of coils of the polar filaments (9 to *Myxobolus* sp. n. 2 and 7 to *Myxobolus* sp. n. 4), site of infection (fins to *Myxobolus* sp. n. 2 and kidney to *Myxobolus* sp. n. 4) and host (*S. franciscanus* to *Myxobolus* sp. n. 2 and *B. orthotaenia* to *Myxobolus* sp. n. 4). The others *Myxobolus* species from South American were different.

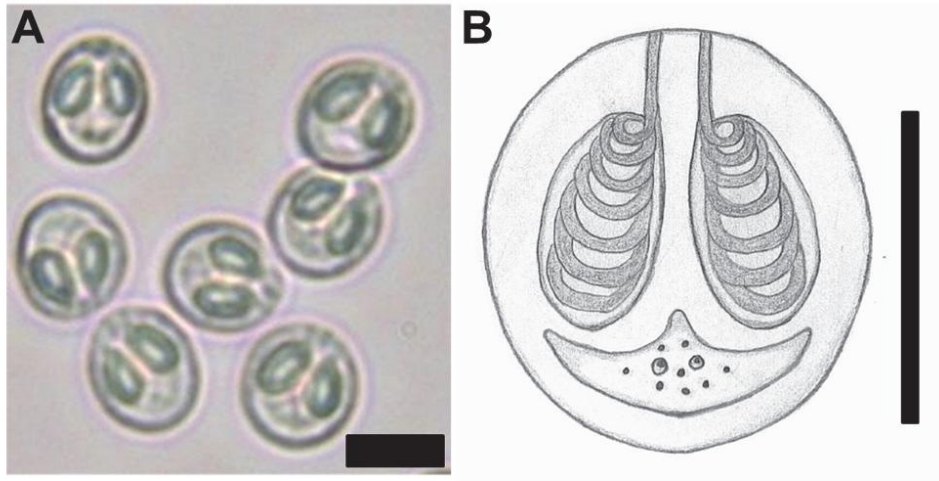


Fig. 7. *Myxobolus* sp. n. 4 parasite of kidney of *Brycon orthotaenia*. A: photomicrograph of mature fresh spores in frontal view. Scale bar = 10  $\mu$ m. B: schematic representation of the mature spore. Scale bar = 10  $\mu$ m



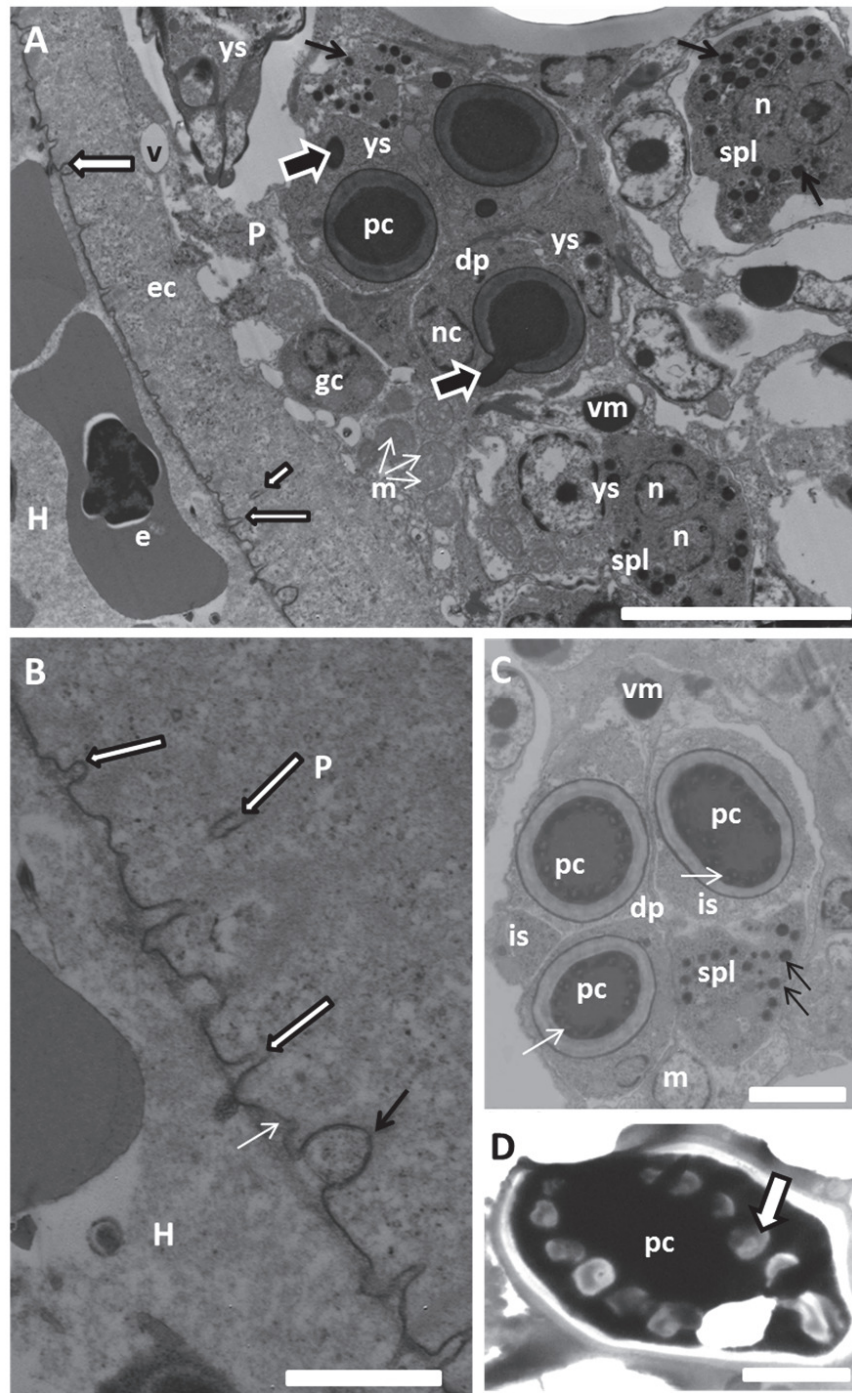


Fig. 8. Electron micrograph of kidney of *Brycon orthotaenia* infected by *Myxobolus* sp. n.  
4. A: Plasmodium (P) with plasmodial wall containing few pinocytotic channels (thick white



arrows) in the ectoplasm (ec). Below of the ectoplasm layer, may be observed numerous mitochondria (m), generative cells (gc) and disporic pansporoblasts (dp) with young spores (ys) in different section levels. Note polar capsules (pc) with polar filaments still not internalized (thick black arrows), sporoplasms (spl) binucleate (n), sporoplasmosomes (thin black arrow). Scale bar: 5  $\mu$ m. B: amplified area of A showing details of interface host-plasmodium. Note the single plasmodial membrane (thin white arrow) in direct contact to host cells, invaginations (thin black arrow) and pinocytic channels (thick white arrow). Scale bar: 1  $\mu$ m. C: disporic pansporoblast (dp) with two immature spores (is). Note polar capsules (pc) with their polar filaments (white arrows) and sporoplasm (spl) with sporoplasmosomes (black arrows) and mitochondria (m). Scale bar: 2  $\mu$ m. D: Polar capsule (pc) of a mature spore showing polar filaments (arrow). Scale bar: 1  $\mu$ m. H: host; P: plasmodium; vm: valve-forming material; e: erythrocyte.

Phylogenetic analysis shows South American *Myxobolus/Henneguya* species forming two distinct clades (A and B). Clade A was composed by species parasites of characiforms, mainly byconid hosts, and had *Myxobolus cordeiroi* Adriano et al., 2009, a parasite of siliriform of the family Pimelodidae, as basal species. In this clade, *Myxobolus* sp. n. 1, *Myxobolus* sp. n. 2, *Myxobolus* sp. n. 3 and *Myxobolus* sp. n. 4 appeared in a subclade containing four other species parasites of host of the family Bryconidae. Analysis of the genetic similarity of the clade A shows *Myxobolus* sp. n. 1 closely related with *M. macropasmodialis* (only 1.3% of distance); *Myxobolus* sp. n. 2 with *M. aureus* (2.0% of distance); *Myxobolus* sp. n. 3 and *Myxobolus* sp. n. 4 were closely related one to another (1.5% distance) and with *M. umidus* (respectively 1.5% and 1.9% of distance) (Table II). The clade B had *Henneguya piaractus* Martins & Souza, 1997, as basal branch and divided further into two sub clades, one composed by species parasitizing pimelodids and another one parasitizing characiform, bryconids, serrassalmids and anastomids (Fig. 9).

The lowest prevalence found in this study was found in *Myxobolus* sp. n. 2, (52.3%) and the largest one in *Myxobolus* sp. n. 1, (76.2%). For *Myxobolus* sp. n. 4, the prevalence was 60% and for *Myxobolus* sp. n. 3 66.7%. These prevalences did not vary significantly among the species ( $\chi^2 = 5.67$ ; df = 3).

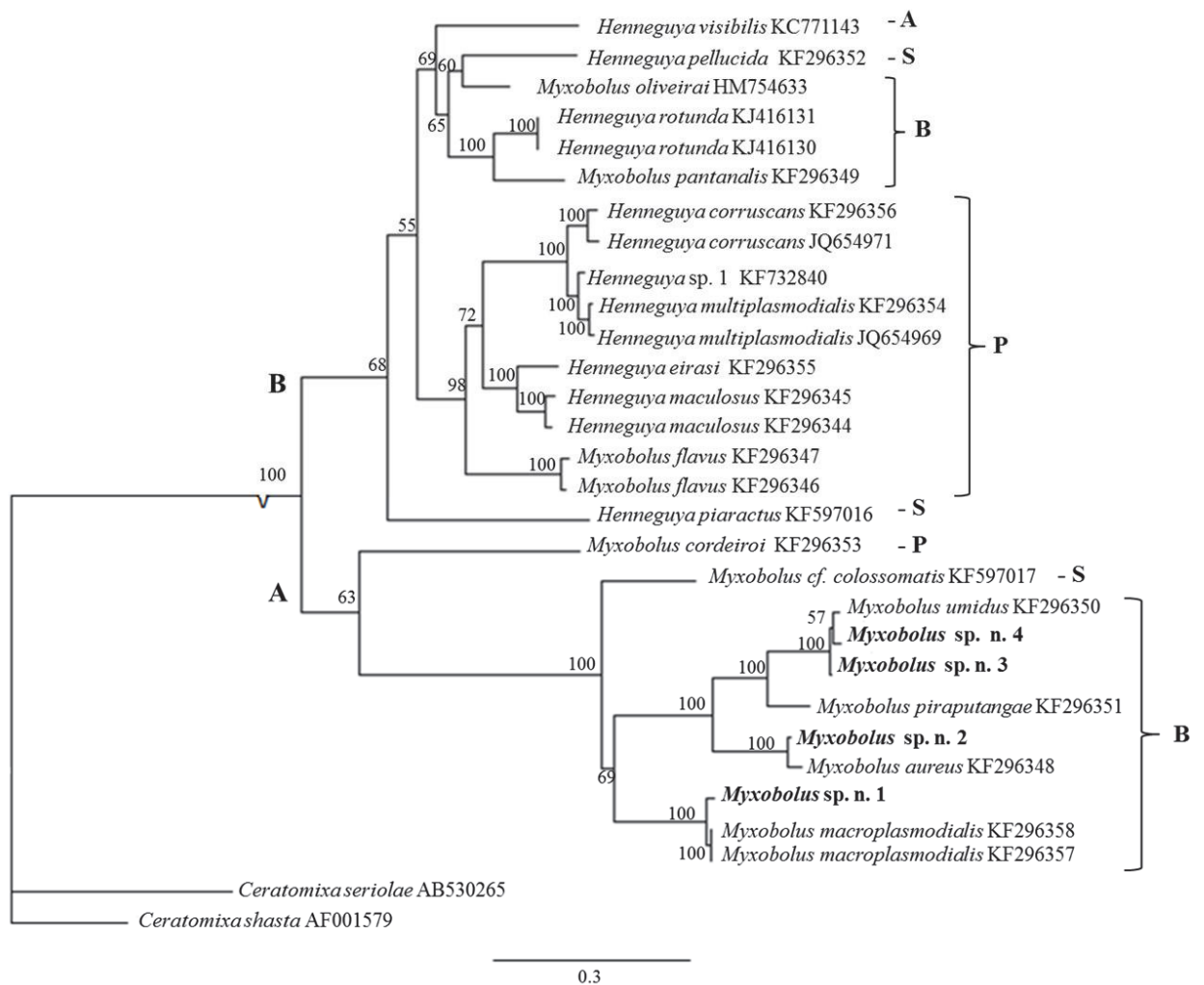


Fig. 9. Maximum-Likelihood tree showing relationship between the four new species *Myxobolus* parasites of bryconids hosts and other *Henneguya*/*Myxobolus* species parasites of South American fishes. Numbers above nodes indicate bootstrap confidence levels. A: Anostomidae; S: Serrasalminae; B: Bryconidae; P: Pimelodidae.

Table I. Comparative data of *Myxobolus* sp. n. 1; *Myxobolus* sp. n. 2; *Myxobolus* sp. n. 3 and *Myxobolus* sp. n. 4 with others *Myxobolus* species parasites of South American fishes. Spore dimensions, sites of infection and site of caught. LPC = length of the polar capsules; WPC = width of the polar capsules; NCF = number of coils of the polar filaments. (-): no data

| Species                          | Spore length     | Spore width     | Thickness     | LPC                            | WPC                             | NCF  | Site of infection | Host  | Locality                    |
|----------------------------------|------------------|-----------------|---------------|--------------------------------|---------------------------------|------|-------------------|---|-----------------------------|
| <i>Myxobolus</i> sp. n. 1        | 10.7 ± 0.4       | 8.1 ± 0.5       | 5.4 ± 0.1     | 4.7 ± 0.3                      | 2.3 ± 0.3                       | 9    | fins              | <i>Salminus franciscanus</i>                        | São Francisco river, Brazil |
| <i>Myxobolus</i> sp. n. 2        | 7.6 ± 0.4        | 4.8 ± 0.5       | —             | 3.9 ± 0.4                      | 1.6 ± 0.1                       | 9    | liver             | <i>Salminus franciscanus</i>                        | São Francisco river, Brazil |
| <i>Myxobolus</i> sp. n. 3        | 12.0 ± 0.8       | 8.3 ± 0.6       | 7.0 ± 0.8     | 4.6 ± 0.3                      | 2.8 ± 0.3                       | 6    | Spleen            | <i>Brycon orthotaenia</i>                           | São Francisco river, Brazil |
| <i>Myxobolus</i> sp. n. 4        | 10.5 ± 0.5       | 9.2 ± 0.7       | -             | 4.9 ± 0.4                      | 2.9 ± 0.2                       | 7    | kidney            | <i>Brycon orthotaenia</i>                           | São Francisco river, Brazil |
| <i>Myxobolus aureus</i>          | 12.6 ± 0.5       | 8.3 ± 0.3       | 5.5 ± 0.3     | 5.7 ± 0.3                      | 2.9 ± 0.2                       | 7–8  | liver             | <i>Salminus brasiliensis</i>                        | Pantanal wetland, Brazil    |
| <i>Myxobolus pantanalis</i>      | 9.3 ± 0.4        | 6.5 ± 0.4       | —             | 4.2 ± 0.5                      | 2.0 ± 0.1                       | 4–5  | Gill filaments    | <i>Salminus brasiliensis</i>                        | Pantanal wetland, Brazil    |
| <i>Myxobolus salminus</i>        | 10.1 ± 0.4       | 6.1 ± 0.4       | 5.0 ± 0.6     | 4.6 ± 0.2                      | 1.7 ± 0.1                       | 7–8  | gill              | <i>Salminus brasiliensis</i>                        | Pantanal, Brazil            |
| <i>Myxobolus macroplasmoidal</i> | 11 (10.5–12)     | 8.5 (8–9)       | 5.2 (5–5.5)   | 4.5 (4–5)                      | 2.8 (2–3)                       | 6    | Abdominal cavity  | <i>Salminus maxillosus</i> = <i>S. brasiliensis</i> | Mogi river, Brazil          |
| <i>Myxobolus paranensis</i>      | 12–15            | 7–8             |               | 6–7                            | 2.5                             |      | Testes, ovary     | <i>Salminus maxillosus</i> = <i>S. brasiliensis</i> | Argentina                   |
| <i>Myxobolus umidus</i>          | 13.5 ± 0.7       | 7.8 ± 0.4       | 7.7 ± 0.1     | 5.1 ± 0.4                      | 2.7 ± 0.3                       | 4–5  | Spleen            | <i>Brycon hilaarii</i>                              | Pantanal wetland, Brazil    |
| <i>Myxobolus piraputangae</i>    | 10.1 ± 0.5       | 8.7 ± 0.5       | 6.7 ± 0.3     | 5.2 ± 0.4                      | 3.0 ± 0.3                       | 4–5  | Kidney            | <i>Brycon hilaarii</i>                              | Pantanal wetland, Brazil    |
| <i>Myxobolus oliveirai</i>       | 11.2 ± 0.4       | 7.4 ± 0.5       | 4.6 ± 0.6     | 5.6 ± 0.2                      | 2.3 ± 0.2                       | 6–8  | gill              | <i>Brycon hilaarii</i>                              | Pantanal wetland, Brazil    |
| <i>Myxobolus brycon</i>          | 6.9 (6.5–7.2)    | 4.2 (3.9–4.8)   | 2.5 (1.9–2.8) | 4.2 (3.8–4.7)                  | 1.9 (1.7–2.5)                   | 8–9  | gill              | <i>Brycon hilaarii</i>                              | Pantanal, Brazil            |
| <i>Myxobolus franciscoi</i>      | 6.4 (6.0–6.9)    | 6.0 (5.8–6.4)   | 3.2           | 2.0                            | 1.5                             | 3    | fins              | <i>Prochilodus argenteu</i>                         | São Francisco river, Brazil |
| <i>Myxobolus porofilus</i>       | 5.7 ± 0.3        | 4.8 ± 0.2       |               | 1.6 ± 0.1                      | 1.1 ± 0.1                       | 3    | Visceral cavity   | <i>Prochilodus lineatus</i>                         | Mogi river, Brazil          |
| <i>Myxobolus lomi</i>            | 14.2 (11.8–15.8) | 11.1 (8.7–12.5) |               | 6.4 (5.2–.9);<br>6.0 (4.7–7.4) | 3.1 (2.3–4.0);<br>2.9 (2.2–4.2) | 8–11 | Gill filaments    | <i>Prochilodus lineatus</i>                         | Peixes river, Brazil        |
| <i>Myxobolus associatus</i>      | 15               | 10              |               | 7                              |                                 |      | Kidney            | <i>Leporinus mormyrops</i>                          | Brazil                      |

|                                |                  |                  |               |                  |               |       |                         |  |                      |
|--------------------------------|------------------|------------------|---------------|------------------|---------------|-------|-------------------------|--|----------------------|
| <i>Myxobolus colossomatis</i>  | 11.8 (11.4-11.2) | 6.9 (6.6-7.2)    | 3.7 (3.5-4.0) | 6.0 (5.8-6.6)    | 2.1 (1.8-2.5) | 7-8   | Connective tissue       | <i>Colossoma macropomum</i>                                | Brazil               |
| <i>Myxobolus cuneus</i>        | 10 ± 0.6         | 5.7 ± 0.3        |               | 5.7 ± 0.3        | 1.7 ± 0.2     | 8-9   | Connective tissue       | <i>Piaractus mesopotamicus</i>                             | São Paulo, Brazil    |
| <i>Myxobolus serrasalmi</i>    | 14.4 (12.5-18.0) | 8.6 (7.0-10.0)   |               | 7.7 (6.0-9.0)    | 3.1 (2.5-4.0) |       | Spleen, kidney, liver   | <i>Serrasalmus rhombeus</i>                                | Brazil               |
| <i>Myxobolus pygocentrus</i>   | 15-16            | 9-11             |               | 9-11             | 3-4           |       | Intestinal content      | <i>Pygocentrus piraya</i>                                  | Brazil               |
| <i>Myxobolus cunhai</i>        | 9-11             | 4-6              |               |                  |               |       | Intestinal content      | <i>Pygocentrus piraya</i> = <i>Pimelodus clarias</i>       | Brazil               |
| <i>Myxobolus noguchii</i>      | 13.6             | 8.5              |               | 6.8              | 2.2           |       | Gills (blood smear)     | <i>Serrasalmus spilopleura</i>                             | Brazil               |
| <i>Myxobolus myleus</i>        | 19.3             | 9.1              | 4.0           | 13.2             | 3.0           | 19-21 | Bile                    | <i>Myleus rubripinnis</i>                                  | Pará, Brazil         |
| <i>Myxobolus braziliensis</i>  | 10.1 (9.4-10.9)  | 5.3 (4.7-5.9)    | 3.6 (3.2-4.0) | 5.3 (5.0-5.4)    | 1.4 (1.4-1.4) | 9-11  | Gills (interlamellar)   | <i>Bunocephalus coracoideus</i>                            | Brazil               |
| <i>Myxobolus chondrophilus</i> | 6                | 4.5              |               | 3                |               |       | Gills                   | <i>Sardinella anchovina</i> = <i>S. aurita</i>             | Brazil               |
| <i>Myxobolus desaequalis</i>   | 18.3 (17.6-19.1) | 11.2 (10.6-11.9) | 4.4 (4.0-5.0) | 11.2 (10.7-11.9) | 4.9 (4.5-5.2) | 11-12 | Gill lamellae           | <i>Apteronotus albifrons</i>                               | Amazon, Brazil       |
| <i>Myxobolus galaxii</i>       | 13-15            | 8.8-10           |               |                  |               |       | All organs except gills | <i>Galaxias maculatus</i>                                  | Argentina            |
| <i>Myxobolus inaequus</i>      | 19.8 (15.6-22)   | 8.6 (7.8-9.3)    | 8.0 (7.7-8.5) | 11.8 (9.4-13)    | 3.6 (3.1-3.9) |       | Brain                   | <i>Eigenmannia virescens</i>                               | Brazil               |
| <i>Myxobolus insignis</i>      | 14.5 (14-15)     | 11.3 (11-12)     | 7.8 (7-8)     | 7.6 (7-8)        | 4.2 (3-5)     | 6     | Gills (intralamellar)   | <i>Semaprochilodus insignis</i>                            | Amazon river, Brazil |
| <i>Myxobolus kudoii</i>        | 8.5 - 8.9        | 6.5 - 7.3        |               | 3.5 - 4.2        | 1.3 - 2.0     |       | Integument              | <i>Nemathognata</i> sp.                                    | Brazil               |
| <i>Myxobolus lutzi</i>         | 10               | 7                |               |                  |               |       | Testis                  | <i>Girardinus januaris</i> = <i>Phalloptychus januaris</i> | Brazil               |
| <i>Myxobolus maculatus</i>     | 21.0 (19.7-23.0) | 8.9 (7.9-9.5)    | 7.5 (7.2-7.9) | 12.7 (11.8-13.8) | 3.2 (3.0-3.6) | 14-15 | Kidney                  | <i>Metynnis maculatus</i>                                  | Amazon river, Brazil |
| <i>Myxobolus magellanicus</i>  | 10-13            | 8.1-8.8          |               | 3                |               |       | Gills                   | <i>Galaxias maculatus</i>                                  | Argentina            |

|                               |                  |                  |               |                  |               |       |                                      |   |                          |
|-------------------------------|------------------|------------------|---------------|------------------|---------------|-------|--------------------------------------|---|--------------------------|
| <i>Myxobolus metynnis</i>     | 13.1 (12.9-13.5) | 7.8 (7.5-8.3)    | 3.9 (3.4-4.5) | 5.2 (5.0-5.5)    | 3.2 (3.0-3.6) | 8-9   | Connective subcutaneous tissue       | <i>Metynnis argenteus</i>                                     | Brazil                   |
| <i>Myxobolus peculiaris</i>   | 23.2 (23.0-23.2) | 14.8 (14.4-15.2) |               | 10.7 (10.5-10.9) | 4.4 (4.0-4.8) | 4 - 5 | Gills (smears)                       | <i>Cyphocharax nagelli</i>                                    | Brazil                   |
| <i>Myxobolus platanus</i>     | 10.7 (10-11)     | 10.8 (10-11)     | 5.0           | 7.7 (7-8)        | 3.8 (3.5-4)   | 5-6   | Spleen                               | <i>Mugil platanus</i>   | RS, Brazil               |
| <i>Myxobolus testicularis</i> | 8.6 (8.2-9.1)    | 7.2 (6.7-7.5)    | 2.7 (2.4-3.0) | 3.5 (3.3-3.8)    | 1.7 (1.3-2.0) | 5-6   | Testis                               | <i>Hemiodopsis microlepis</i> =<br><i>Hemiodus microlepis</i> | NE, Brazil               |
| <i>Myxobolus flavus</i>       | 9.2±0.2          | 6.5±0.3          | 4.2±0.2       | 4.5±0.2          | 1.6±0.1       | 4-5   | Gill arch                            | <i>Pseudoplatystoma corruscans</i>                            | Pantanal wetland, Brazil |
| <i>Myxobolus flavus</i>       | 9.3±0.3          | 6.6±0.3          | 4.0±0.2       | 4.5±0.2          | 1.8±0.1       | 4-5   | Gill arch                            | <i>Pseudoplatystoma reticulatum</i>                           | Pantanal wetland, Brazil |
| <i>Myxobolus absonus</i>      | 15.7 ± 1.5       | 10.2 ± 0.7       |               | 6.4 ± 0.7        | 3.6 ± 0.5     | 5     | Opercular cavity                     | <i>Pimelodus maculatus</i>                                    | Piracicaba river, Brazil |
| <i>Myxobolus cordeiroi</i>    | 10.8 ± 0.5       | 7.1 ± 0.2        | 5.2 ± 0.3     | 5.2 ± 0.3        | 1.4 ± 0.1     | 5-6   | Skin, gill arch, eyes, urin. bladder | <i>Zungaro jahu</i>   | Pantanal, Brazil         |
| <i>Myxobolus stokesi</i>      | 8.5              | 5.3              |               | 3.1              | 1.7           |       | Nose integument                      | <i>Pimelodella</i> (?) sp.                                    | Brazil                   |
| <i>Myxobolus sciades</i>      | 9.15             | 4.36             | 2.61          | 4.44             | 1.63          | 9-10  | Gill                                 | <i>Sciades herzbergii</i>                                     | Brazil                   |

Table II: Similarity matrix for the 18S rDNA sequences from *Henneguya* and *Myxobolus* species from Clade A of maximum-likelihood tree. The lower oblique shows the differences in terms of percentage of nucleotides, while the upper oblique shows the actual differences.

| Species                               | 1    | 2    | 3    | 4    | 5    | 6    | 7    | 8    | 9   |
|---------------------------------------|------|------|------|------|------|------|------|------|-----|
| 1 – <i>Myxobolus</i> sp. n. 1         | –    | 227  | 243  | 242  | 235  | 226  | 18   | 188  | 329 |
| 2 – <i>Myxobolus</i> sp. n. 2         | 14.4 | –    | 203  | 201  | 31   | 200  | 196  | 193  | 345 |
| 3- <i>Myxobolus</i> sp. n. 3          | 15.4 | 12.9 | –    | 27   | 252  | 19   | 250  | 207  | 351 |
| 4- <i>Myxobolus</i> sp. n. 4          | 15.3 | 12.8 | 1.5  | –    | 248  | 25   | 254  | 202  | 358 |
| 5 – <i>Myxobolus aureus</i>           | 15.2 | 2.0  | 14.4 | 14.2 | –    | 202  | 251  | 179  | 381 |
| 6 – <i>Myxobolus umidus</i>           | 17.3 | 15.3 | 1.5  | 1.9  | 15.5 | –    | 195  | 204  | 295 |
| 7- <i>Myxobolus macroplasmoidal</i>   | 1.3  | 14.6 | 16.6 | 16.9 | 16.7 | 17.7 | –    | 189  | 329 |
| 8 – <i>Myxobolus cf. colossomatis</i> | 14.2 | 14.5 | 15.6 | 15.2 | 13.5 | 18.7 | 14.3 | –    | 310 |
| 9 – <i>Myxobolus cordeiroi</i>        | 23.6 | 24.9 | 23.8 | 24.2 | 25.8 | 25.6 | 22.9 | 23.3 | –   |

## Discussion

In this study, based on morphology, 18S rDNA gene sequencing and ultrastructure, four novel species of *Myxobolus* were described infecting bryconid hosts from São Francisco basin. *Myxobolus* sp. n. 1 and *Myxobolus* sp. n. 2 were parasite *S. franciscanus* and *Myxobolus* sp. n. 3 and *Myxobolus* sp. n. 4 parasite *B. orthotaenia*. This was the first report of myxozoans infecting these fish species, which are endemic to this watershed.

The study of the host-parasite interaction through ultrastructural analyses revealed that of the four species here studied, only the plasmodia of *Myxobolus* sp. n. 1 were surrounded by connective capsule, which was composed by a single layer of fibroblasts. For the others three species, the plasmodial walls were in direct contact with the membrane of the host cells. The presence of connective capsule surrounding the plasmodium is a picture commonly observed in myxosporean infections, which would be a host reaction to isolate the plasmodium and preventing its dispersal to adjacent tissues (Sitjà-Bobadilla 2008). On the other hand, the presence of direct contact between plasmodial wall and host cells has also been largely documented in myxosporeans (Current 1979, El-Mansy &

Bashtar 2002, Matos et al. 2005, Adriano et al. 2005a, 2009, Abdel-Ghaffar et al. 2008, Naldoni et al. 2009) and according to Current et al. (1979), may play an important role in pathogeny. The plasmodia wall of all new species was formed by a single membrane, and had pinocytotic canals connecting the outside of the plasmodia to the ectoplasm zone, as seen in some other myxosporeans species (Current et al. 1979, Azevedo & Matos 2002, 2003, Adriano et al. 2005b). In *Myxobolus* sp. n. 3 and *Myxobolus* sp. n. 4 the wall plasmodia presented recesses and projections towards the host tissue, increasing the surface contact, a mechanism related to be nutritional activity, as also observed by Naldoni et al. (2009) and El-Mansy & Bashtar (2002).

The sporogenesis process of the four *Myxobolus* species here studied follows the pattern of the other *Myxobolus* species, wherein there generative cells and young developmental stage spores in the periphery of the plasmodium and immature and mature spores in toward center (Hallet & Diamant 2001, Casal et al. 2002, Adriano et al. 2005a, 2005b, 2006).

Phylogenetic analysis shows South American *Myxobolus/Henneguya* species forming two clades. In the clade A, *M. cordeiroi*, parasite of a pimelodid host, appears as basal species. *Myxobolus* cf. *colossomatis*, parasites of characiforms of the family Serrasalminidae, appears as a sister branch of the subclade formed exclusively by *Myxobolus* spp. parasites of characiforms of the family bryconid, including *Myxobolus* sp. n. 1 and *Myxobolus* sp. n. 2, parasites of *S. franciscanus* and *Myxobolus* sp. n. 3 and *Myxobolus* sp. n. 4, parasites of the *B. orthotaenia*. Four others species parasites of bryconid clustered in a subclade composed by species parasites of characiforms in the clade B, pointing the poliphyletic origem of the Myxobolids parasites of fishes of the family Bryconids, as suggested by Moreira et al. (2014b).

Eszterbauer (2004) suggested that the site of development plays an important role in phylogeny of the myxosporean species. In this context, *Myxobolus* sp. n. 1, which infects connective tissue of fin, appears as a sister species of *M. macroplasmodialis*, presumably parasite of serous membrane (connective tissue) of the abdominal organs or wall of *S. brasiliensis* (Molnár et al. 1998), another species of the genus *Salminus*. *Myxobolus* sp. n.

2, parasite of liver, grouped as sister species of *M. aureus*, a parasite of liver, also of *S. brasileinsis*. *Myxobolus* sp. n. 3 parasite of spleen and *Myxobolus* sp. n. sp. 4, parasite of kidney, both parasites of *B. orthotaenia*, grouped as sister species of *M. umidus*, a parasite of spleen of *B. hilaarii*. This picture shows the effects of host specificity and organs/tissue affinity as evolutionary signs to *Myxobolus/Henneguya* species, as suggested Eszterbauer (2004) and Carriero et al. (2013).

Our results showed that the prevalences of the four *Myxobolus* spp. here described was always above 50%, ranging from 52.3% to 76.3% and no significant difference was found among the species. In this same watershed, also observed high prevalence (80%) for *Henneguya* sp. n. 1, parasite of *Pseudoplatystoma corruncans* Spix & Agassiz 1829, but in other hand, Eiras et al. (2010), observed only 10% of infection of *M. franciscoi* in *P. argenteus*. In La plata basin, in fishes caught from natural environment, the prevalence has been lower than that found here, ranged of 2.6% to 38% (Adriano et al. 2009, Naldoni et al. 2011, Adriano et al. 2012, Carriero et al. 2013). In Amazon basin however, the prevalence has also been high, ranging of 26 to 40% (Azevedo et al. 2002, 2010, 2011, Casal et al. 2006). From others regions, the prevalence ranged from 13.5 to 20.2% in two tilapia species from Lake Nokoué (Bénin, West Africa) (Gbankoto et al. 2001) and Cech et al. (2012) observed prevalence ranging from 5% to 47% in infections of cyprinid fishes from river Danube, Hungary.

In this study, each fish species examined were infected by two *Myxobolus* species, pointing out the great diversity of myxosporeans yet unknown in the South America, as discussed by Naldoni et al. (2011). These findings reinforce the need for further studies in South American myxosporeans diversity, since there is the most diverse fresh water fish fauna of the planet, with many fish species with potential for cultivation.

### Literature Cited

Abdel-Ghaffar F, Abdel-Baki AS, Bayoumy EM, Bashtar AR and others (2008) Light and electron microscopic study on *Henneguya suprabranchiae* Landsberg, 1987 (Myxozoa:



- Myxosporea) infecting *Oreochromis niloticus*, a new host record. Parasitol Res 103: 609–617
- Adriano EA, Arana S, Cordeiro NS (2005a) Histology, ultrastructure and prevalence of *Henneguya piaractus* (Myxosporea) infecting the gills of *Piaractus mesopotamicus* (Characidae) cultivated in Brazil. Dis of Aquat Org 64: 229-235
- Adriano EA, Arana S, Cordeiro NS (2005b) An ultrastructural and histopathological study of *Henneguya pellucida* n. sp. (Myxosporea: Myxobolidae) infecting *Piaractus mesopotamicus* (Characidae) cultivated in Brazil. Parasite 12: 221-227
- Adriano EA, Arana S, Cordeiro NS (2006) *Myxobolus cuneus* n. sp. (Myxosporea) infecting the connective tissue of *Piaractus mesopotamicus* (Pisces: Characidae) in Brazil: histopathology and ultrastructural. Parasite 13: 137–142
- Adriano EA, Arana S, Carriero MM, Naldoni J, Ceccarelli PS, Maia AAM (2009) Light, electron microscopy and histopathology of *Myxobolus salminus* n. sp., a parasite of *Salminus brasiliensis* from the Brazilian Pantanal. Vet Parasitol 165: 25-29
- Adriano EA, Carriero MM, Maia AAM, Silva MRM, Naldoni J, Ceccarelli OS, Arana S (2012) Phylogenetic and host–parasite relationship analysis of *Henneguya multiplasmodialis* n. sp. infecting *Pseudoplatystoma* spp. in Brazilian Pantanal wetland. Vet Parasitol 185: 110–120
- Altschul SF, Madden TL, Schaffer AA, Zhang J, Zhang Z, Miller W, Lipman DJ (1997) Gapped BLASTn and PSI-BLAST: A new generation of protein database search programs. Nucleic Acids Res 25: 3389-3402
- Azevedo C, Matos E (2002) Fine structure of the myxosporean, *Henneguya curimata* n. sp., parasite of the Amazonian fish, *Curimata inornata* (Teleostei, Curimatidae). Jour Eukaryot Microbiol 49: 197-200
- Azevedo C, Matos E (2003) Fine structure of *Henneguya pilosa* sp. n. (Myxozoa: Myxosporea), parasite of *Serrasalmus altuvei* (Characidae), in Brazil. Folia Parasitol 50: 37–42

- Azevedo C, Casal G, Matos P, Alves A, Matos E (2011) *Henneguya torpedo* sp. nov. (Myxozoa), a parasite from the nervous system of the Amazonian teleost *Brachyhypopomus pinnicaudatus* (Hypopomidae). Dis Aquat Org 93: 235–242
- Barta JR, Martin DS, Liberato PA, Dashkevich M, Anderson JW, Feighner SD, Elbrecht A, Perkins-Barrow A, Jenkins MC, Danforth HD, Ruff MD, Profous-Juchelka H (1997) Phylogenetic relationships among eight *Eimeria* species infecting domestic fowl inferred using complete small subunit ribosomal DNA sequences. J Parasitol 83: 262–271
- Bartošova-Sojkova P, Hrabcova M, Peckova H, Patra S, Kodadkova A, Jurajda P, Tylm T, Holzer AS (2014) Hidden diversity and evolutionary trends in malacosporean parasites (Cnidaria: Myxozoa) identified using molecular phylogenetics. Int Jour Parasitol 44: 565–577
- Brasil-Sato MC (2003) Parasitos de Peixes da Bacia do São Francisco In: GODINHO, H.P., GODINHO A.L. (Ed.). Águas, Peixes e Pescadores do São Francisco das Minas Gerais. Belo Horizonte: Puc minas, p. 149-165
- Carriero MM, Adriano EA, Silva MRM, Ceccarelli PA, Maia AAM (2013) Molecular phylogeny of the *Myxobolus* and *Henneguya* genera with several new South American species. PLoS One 8:e73713
- Casal G, Matos E, Azevedo C (2002) Ultrastructural data on the spore of *Myxobolus maculatus* n. sp. (phylum Myxozoa), parasite from the Amazonian fish *Metynnis maculatus* (Teleostei). Dis Aquat Organ 51: 107–112
- Casal G, Matos E, Azevedo C (2006) A new myxozoan parasite from the amazonian fish *Metynnis argenteus* (Teleostei, Characidae): light and electron microscope observations. J Parasitol 92: 817–821
- Cech G, Molnár K and Székely C (2012) Molecular genetic studies on morphologically indistinguishable *Myxobolus* spp. infecting cyprinid fishes, with the description of three

- new species, *M. alvarezae* sp. nov., *M. sitjae* sp. nov. and *M. eirasianus* sp. nov. Act Parasitol 57(4): 354–366
- Current WL, Janovy JRJ, Knight SA (1979) *Myxosoma funduli* Kudo (Myxosporida) in *Fundulus kansae*: ultrastructure of the plasmodium wall and of sporogenesis. J Protozool 26: 574–583
- Diamant A, Whipps CM, Kent ML (2004) A new species of *Sphaeromyxa* (Myxosporidia: Sphaeromyxina: Sphaeromyxidae) in devil firefish, *Pterois miles* (Scorpaenidae), from the northern Red Sea: morphology, ultrastructure, and phylogeny. J Parasitol 90: 1434–1442
- Eiras JC, Molnár K, Luy S (2005) Synopsis of the species of *Myxobolus* Butschli, 1882 (Myxozoa: Myxosporidia: Myxobolidae). Syst Parasitol 61: 1–46
- Eiras JC, Monteiro CM, Brasil-Sato MC (2010) *Myxobolus franciscoi* sp. nov. (Myxozoa: Myxosporidia: Myxobolidae), a parasite of *Prochilodus argenteus* (Actinopterygii: Prochilodontidae) from upper São Francisco River, Brazil, with a revision of *Myxobolus* spp. from South America. Zoo 27 (1): 131–137
- Eiras JC, Zhang J, Molnár K (2014) Synopsis of the species of *Myxobolus* Bütschli, 1882 (Myxozoa: Myxosporidia: Myxobolidae) described between 2005 and 2013. Syst Parasitol 88:11–36
- El-Mansy A, Bashtar AR (2002) Histopathological and ultrastructural studies of *Henneguya suprabranchiae* Landsberg 1987 (Myxosporidia; Myxobolidae) parasitizing the suprabranchial organ of the freshwater catfish *Clarias gariepinus* Burchell 1822 in Egypt Parasitol Res 88: 617–626
- Eszterbauer E (2004) Genetic relationship among gill-infecting *Myxobolus* species (Myxosporidia) of cyprinids: molecular evidence of importance of tissue-specificity. Dis Aquatic Org 58:35–40

- Feist SW, Longshaw M (2006) *Phylum myxozoa*. In PTK Woo (ed.), *Fish diseases and disorders. Protozoan and metazoan infections*. Vol. 1, 2nd ed., CAB International. Oxfordshire 230-296
- Froese R, Pauly D (Eds.) (2013) FishBase. World Wide Web electronic publication, [www.fishbase.org](http://www.fishbase.org), 12/2013
- Gbankoto A, Pampouli C, Marques A, Sakiti GN (2001) Occurrence of myxosporean parasites in the gills of two tilapia species from Lake Nokoué (Bénin, West Africa): effect of host size and sex, and seasonal pattern of infection. *Dis Aquat Org* 44: 217-222
- Gómez D, Bartholomew J, Sunyer JO (2014) Biology and mucosal immunity to myxozoans, *Developmental and Comparative Immunology* 43: 243–256
- Guindon S, Gascuel O (2003) A simple, fast and accurate algorithm to estimate large phylogenies by maximum likelihood. *Syst Biol* 52: 696–704
- Hall TA (1999) BioEdit: A user-friendly biological sequence alignment editor and analysis program for Windows 95/98/NT. *Nucl. Acids Symp Ser* 41: 95–98
- Hallett SL, Diamant A (2001) Ultrastructure and small-subunit ribosomal DNA sequence of *Henneguya lesteri* n. sp (Myxosporea), a parasite of sand whiting *Sillago analis* (Sillaginidae) from the coast of Queensland, Australia. *Dis Aquat Organ* 46: 197–212
- Lom J, Dyková I (2006) Myxozoan genera: definition and notes on taxonomy, life-cycle terminology and pathogenic species. *Folia Parasitol* 53: 1–36
- Luque JL (2004) Biologia, epidemiologia e controle de parasitos de peixes. *Revta Bras. Parasitol Vet* 13(1):161-165
- Matos E, Tajdari J, Azevedo C (2005) Ultrastructural studies of *Henneguya rhamdia* n. sp. (Myxozoa) a parasite from the Amazon teleost fish, *Rhamdia quelen* (Pimelodidae). *J Eukaryot Microbiol* 52: 532–537

- Milanin T, Eiras JC, Arana S, Maia AAM, Alves AL, Silva MRM, Carriero MM, Ceccarelli PS, Adriano EA (2010) Phylogeny, ultrastructure, histopathology and prevalence of *Myxobolus oliverai* sp. nov., a parasite of *Brycon hilarii* (Characidae) in the Pantanal wetland, Brazil. Mem Inst Oswaldo Cruz 105: 762–769
- Moreira GSA, Adriano EA, Silva MRM, Ceccarelli PS, Maia AAM (2014a) Morphology and 18S rDNA sequencing identifies *Henneguya visibilis* n. sp., a parasite of *Leporinus obtusidens* from Mogi Guaçu River, Brazil. Parasitol Res 113: 81–90
- Moreira GSA, Adriano EA, Silva MRM, Ceccarelli PS, Maia AAM (2014b) The morphological and molecular characterization of *Henneguya rotunda* n. sp., a parasite of the gill arch and fins of *Salminus brasiliensis* from the Mogi Guaçu River, Brazil. Parasitol Res 113: 1703–1711
- Naldoni J, Arana S, Maia AAM, Ceccarelli PS, Tavares LER, Borges FA, Pozo CF, Adriano EA (2009) *Henneguya pseudoplatystoma* n. sp. causing reduction in epithelial area of gills in the farmed pintado, a South American catfish: Histopathology and Ultrastructure. Vet Parasitol 166: 52–59
- Naldoni J, Arana S, Maia AAM, Silva MRM, Carriero MM, Ceccarelli PS, Tavares LER, Adriano EA (2011) Host–parasite–environment relationship, morphology and molecular analyses of *Henneguya eirasi* n. sp. parasite of two wild *Pseudoplatystoma* spp. in Pantanal Wetland, Brazil. Vet Parasitol 177: 247–255
- Posada D (2008) jModelTest: phylogenetic model averaging. Mol Biol Evol 25: 1253–1256
- Rambaut A (2008) FigTree v1.1.1: Tree figure drawing tool. <http://tree.bio.ed.ac.uk/software/figtree/> (accessed: 16 Mar 2014).
- Sato Y, Fenerich-Verani, Godinho HP (2003) Reprodução induzida de peixes da bacia do São Francisco, p.275-289. In: Godinho H.P., Godinho A.L. (Eds). Águas, peixes e pescadores do São Francisco das Minas Gerais. Belo Horizonte, PUC Minas, 468

- Sato Y & Godinho H P (2003) Migratory fishes of the São Francisco River. Pp. 195-232. In: J. Carosfeld, B. Harvey, C. Ross & A. Baer (Eds.). Migratory fishes of South America: biology, fisheries and conservation status. World Fisheries Trust/The World Bank/International Development Research Centre, Ottawa, 372
- Sato Y & Godinho HP (1999) Peixes da bacia do rio São Francisco, p. 401-413. In: R. H. Lowe-McConnell. (1999). *Estudos ecológicos de comunidades de peixes tropicais*. São Paulo: Edusp, 534
- Sitja-Bobadilla A (2008) Fish immune response to myxozoan parasites. *Parasite* 15: 420–425
- Welcomme RL (1985) River fisheries. *FAO Fish. Tech Pap* 262:1-330

## 7. CONSIDERAÇÕES GERAIS

Os resultados obtidos durante os estudos realizados para o desenvolvimento desta tese permitiram concluir que espécimes de *P. corruscans*, *S. franciscanus* e *B. orthotaenia*, da bacia do rio São Francisco apresentaram infecção por espécies de mixosporídeos que ainda não haviam sido descritas na literatura. Exemplares de *P. corruscans* foram encontrados albergando uma espécie do gênero *Henneguya* (*Henneguya* sp. n. 1) nas brânquias, enquanto *S. franciscanus* e *B. orthotaenia* albergaram espécies do gênero *Myxobolus*, sendo que as espécies *Myxobolus* sp. n. 1 e *Myxobolus* sp. n. 2 foram encontradas respectivamente nas nadadeiras e fígado de *S. franciscanus* e *Myxobolus* sp. n. 3 e *Myxobolus* sp. n. 4 encontradas respectivamente no baço e rim de *B. orthotaenia*.

Por meio da análise ultraestrutural, foi possível concluir que em *Henneguya* sp. n. 1 a parede do plasmódio apresentou intensa atividade pinocítica. Uma camada de material finamente granular, observada em *Henneguya* sp. n. 1, e uma camada de tecido conjuntivo, observada em *Myxobolus* sp. n. 1, atuam impedindo o contato direto da parede do plasmódio com os tecidos hospedeiros. Os plasmódios de *Myxobolus* sp. n. 2, *Myxobolus* sp. n. 3 e *Myxobolus* sp. n. 4 tiveram contato direto com os tecidos de seus hospedeiros.

Com base no sequenciamento do 18S rDNA, foi possível concluir que as novas espécies aqui descritas agruparam em subclados formados por mixosporídeos que parasitam as mesmas famílias de hospedeiros e em segundo plano há um agrupamento de acordo com o sítio de infecção.



A diversidade de mixosporídeos encontrada nas espécies de peixes alvos deste estudo, as quais apresentam importância tanto para a pesca extrativista como para piscicultura, evidenciam a necessidade de se intensificar o estudo da diversidade e do potencial patogênico de mixosporídeos parasitos da ictiofauna brasileira.





## 8. ANEXOS

### 8.1 - Certificado da Comissão de Ética no uso de Animais CEUA/Unicamp.

---

CEUA/Unicamp

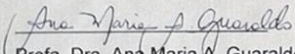
Comissão de Ética no Uso de Animais  
CEUA/Unicamp

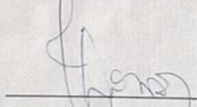
CERTIFICADO

Certificamos que o projeto "Mixosporídeos parasitos de *Pseudoplatystoma corruscans* (pintado), *Salminus franciscanus* (dourado), *Prochilodus spp* (curimbatá) e *Brycon orthotanea* (matrinchã) oriundos da Bacia do Rio São Francisco, MG" (protocolo nº 2334-1), sob a responsabilidade de Prof. Dr. Edson Aparecido Adriano / Juliana Naldoni, está de acordo com os Princípios Éticos na Experimentação Animal adotados pela Sociedade Brasileira de Ciência em Animais de Laboratório (SBCAL) e com a legislação vigente, LEI Nº 11.794, DE 8 DE OUTUBRO DE 2008, que estabelece procedimentos para o uso científico de animais, e o DECRETO Nº 6.899, DE 15 DE JULHO DE 2009.

O projeto foi aprovado pela Comissão de Ética no Uso de Animais da Universidade Estadual de Campinas - CEUA/UNICAMP - em 14 de março de 2011.

Campinas, 14 de março de 2011.

  
Profa. Dra. Ana Maria A. Guaraldo  
Presidente

  
Fátima Alonso  
Secretária Executiva

CEUA/UNICAMP  
Caixa Postal 6109  
13083-970 Campinas, SP - Brasil

Telefone: (19) 3521-6359  
E-mail: [comisib@unicamp.br](mailto:comisib@unicamp.br)  
<http://www.ib.unicamp.br/ceea/>

## 8.2 - Declaração da Comissão de Ética no uso de Animais CEUA/Unicamp.

**DECLARAÇÃO**

Declaro para os devidos fins que o conteúdo de minha tese de Doutorado intitulada **MYXOZOA PARASITOS DE *Pseudoplattystoma corruscans* (PINTADO), *Salminus franciscanus* (DOURADO) E *Brycon orthotacenia* (MATRINHÁ) ORIUNDOS DA BACIA DO RIO SÃO FRANCISCO, MG:**

( ) não se enquadra no § 4º do Artigo 1º da Informação CCPG 002/13, referente a biotecnologia e biossegurança.


Tem autorização da(s) seguinte(s) Comissão(ões):


( ) CIBio – Comissão Interna de Biossegurança, projeto No. \_\_\_\_\_, Instituição: \_\_\_\_\_

( X ) CEUA – Comissão de Ética no Uso de Animais, projeto No. 2334-1, Instituição: UNICAMP, Instituto de Biologia.


( ) CEP – Comissão de Ética em Pesquisa, protocolo No. \_\_\_\_\_, Instituição: \_\_\_\_\_

\* Caso a Comissão seja externa ao UNICAMP, anexar o comprovante de autorização dada ao trabalho. Se a autorização não tiver sido dada diretamente ao trabalho de tese ou dissertação, deverá ser anexado também um comprovante do vínculo do trabalho do aluno com o que constar no documento de autorização apresentada.

  
Aluna: Juliana Naldoni

  
Orientador: Edson Aparecido Adriano

Para uso da Comissão ou Comitê pertinente:  
(X) Deferido ( ) Indeferido

Carimbo e assinatura   
Prof. Dr. ALEQUANDRE RODRIGUES DE OLIVEIRA  
Presidente da Comissão de Ética no Uso de Animais CEUA/UNICAMP

Para uso da Comissão ou Comitê pertinente:  
( ) Deferido ( ) Indeferido

Carimbo e assinatura \_\_\_\_\_

b7c-25620-42560-4102-280-01-440106/31/3/2013/2013